

Friday

104th Scientific Assembly and Annual Meeting November 25-30 | McCormick Place, Chicago





Education Outcomes Research

Friday, Nov. 30 8:30AM - 10:00AM Room: E261





AMA PRA Category 1 Credits ™: 1.50 ARRT Category A+ Credit: 1.75

Participants

Pina C. Sanelli, MD, Manhasset, NY (Moderator) Research funded, Siemens AG;

Sub-Events

RC802A Education Outcomes Research: What Is It and How to Get Started

Participants

Pina C. Sanelli, MD, Manhasset, NY (Presenter) Research funded, Siemens AG;

LEARNING OBJECTIVES

1) Understand the components of education outcomes research. 2) Describe common methodology employed in education based research. 3) Maximize mentoring relationships from a mentor and mentee persepctive.

ABSTRACT

The learner will achieve the following objectives: 1. Understand the components of education outcomes research. 2. Describe common methodology employed in education based research. 3. Maximize mentoring relationships from a mentor and mentee persepctive.

RC802B Education Outcomes Research: Methods

Participants

Aine M. Kelly, MD, Ann Arbor, MI (Presenter) Nothing to Disclose

For information about this presentation, contact:

ainemariekelly@hotmail.com

LEARNING OBJECTIVES

1) Describe the scope of educational outcomes research. 2) Appraise published educational outcomes research. 3) Identify the most appropriate educational research method to answer your research question. 4) Define meaningful educational research outcomes

Active Handout: Aine Marie Kelly

http://abstract.rsna.org/uploads/2018/18001091/Educational Outcomes Research Methods RC802B.pdf

RC802C Mentoring from the Mentor Point-of-View

Participants

Christopher M. Straus, MD, Chicago, IL (Presenter) Nothing to Disclose

For information about this presentation, contact:

cstraus@uchicago.edu

LEARNING OBJECTIVES

1) The participant will be able to assemble and specify key elements pertaining to a high quality successful mentor. 2) Describe the characteristics of the current learner and what creates a successful mentor experience. 3) Mentors will be able to differentiate which of their skill set are pertinent in current educational forums.

RC802D Mentoring from the Mentee Point-of-View

Participants

Jordana Phillips, MD, Boston, MA (Presenter) Research Grant, General Electric Company; Consultant, General Electric Company

For information about this presentation, contact:

jphilli2@bidmc.harvard.edue

LEARNING OBJECTIVES

1) Define what is research. 2) Review different types of research projects. 3) Explore factors to consider when choosing a research project. 4) Emphasize the value of high-quality mentorship. 5) Identify opportunities to advance as a clinical researcher.



MR Imaging in the Thorax

Friday, Nov. 30 8:30AM - 10:00AM Room: E353C









AMA PRA Category 1 Credits ™: 1.50 ARRT Category A+ Credit: 1.75

FDA

Discussions may include off-label uses.

Sub-Events

RC803A MR Imaging of Mediastinal Masses

Participants

Jeanne B. Ackman, MD, Boston, MA (*Presenter*) Spouse, Stockholder, Everest Digital Medicine; Spouse, Consultant, Everest Digital Medicine; Spouse, Stockholder, Cynvenio Biosystems, Inc; Spouse, Scientific Advisory Board, Cynvenio Biosystems, Inc; Spouse, Consultant, PAREXEL International Corporation

LEARNING OBJECTIVES

1) Comprehend value of Thoracic MRI as a problem solver in the mediastinum 2) Understand how MR assists with tissue diagnosis 3) Learn how MR can add diagnostic specificity beyond that of CT

RC803B MR Imaging of the Lung: A Practical Clinical Approach

Participants

Juergen Biederer, MD, Heidelberg, Germany (Presenter) Nothing to Disclose

For information about this presentation, contact:

biederer@radiologie-darmstadt.de

LEARNING OBJECTIVES

1) To give an overview over appropriate indications for lung MRI. 2) To suggest a practical approach for the selection of suitable standard imaging protocols. 3) To discuss, how to adjust the standard examination for specific questions. 4) To make familiar with general aspects of lung MR image interpretation and the diagnostic scope of the technique.

Active Handout:Juergen Biederer

RC803C MR Imaging of Cardiac Masses

Participants

Phillip M. Young, MD, Rochester, MN (*Presenter*) Consultant, Arterys Inc

For information about this presentation, contact:

young.phillip@mayo.edu

RC803D MR Imaging of Aortopathies

Participants

Cristina Fuss, MD, Portland, OR (Presenter) Spouse, Officer, ViewRay, Inc

For information about this presentation, contact:

fussc@ohsu.edu

LEARNING OBJECTIVES

1) To familiarize the learner with the most common familiar aortopathies, their clinical background, imaging appearance on MRI and specific considerations for MR acquisition planning.

ABSTRACT

Familial aortopahties comprise a grounp of inherited disorders of aortic aneurysms and/or dissection including. These include Thoracic Aortic Aneurysms and Aortic Dissections (TAAD), Marfan syndrome, Loeys-Dietz syndrome, and Ehlers-Danlos syndrome, only to name the most common ones.



Ligamentous Injuries of the Knee: Mechanistic Approach with Emphasis on MR Imaging

Friday, Nov. 30 8:30AM - 10:00AM Room: E451A





AMA PRA Category 1 Credits ™: 1.50 ARRT Category A+ Credit: 1.75

Participants

Brady K. Huang, MD, San Diego, CA (*Director*) Nothing to Disclose Tetyana A. Gorbachova, MD, Huntingdon Vy, PA (*Presenter*) Nothing to Disclose Robert D. Boutin, MD, Davis, CA (*Presenter*) Nothing to Disclose Brady K. Huang, MD, San Diego, CA (*Presenter*) Nothing to Disclose

For information about this presentation, contact:

llenchik@wakehealth.edu

LEARNING OBJECTIVES

1) To delineate the MR imaging features typical of a variety of ligamentous injuries of the knee. 2) To illustrate how MR imaging findings, including those related to abnormalities in the subchondral bone of the femur, tibia, and/or patella, provide critical clues to the specific mechanism involved in these ligamentous injuries. 3) To define the characteristic MR imaging features associated with translational, angular, and rotational mechanisms that lead to injury of the anterior and posterior cruciate ligaments and the medial and lateral supporting structures of the knee.

ABSTRACT

This course will emphasize a mechanistic approach to ligamentous injuries of the knee, emphasizing MR imaging. Individual speakers will use this approach in their discussions of such injuries with attention focused on the anterior cruciate and posterior cruciate ligaments and the medial and lateral supporting structures. The importance of the distribution and pattern of bone injury, especially that in the subchondral region of the femur, tibia, and/or patella, will be illustrated with analysis of hyperextension, hyperflexion, and translational, angular, and rotational injuries, among others.

Active Handout: Brady Kirk Huang

http://abstract.rsna.org/uploads/2018/17000347/RC804.FRIDAY.HUANG.ACL RC804.pdf



Getting Through the Tough Spots in Neuro: Head & Neck (Interactive Session)

Friday, Nov. 30 8:30AM - 10:00AM Room: E450B



AMA PRA Category 1 Credits ™: 1.50 ARRT Category A+ Credit: 1.75

Participants

Deborah R. Shatzkes, MD, New York, NY (*Moderator*) Nothing to Disclose Christopher P. Hess, MD, PhD, Mill Valley, CA (*Moderator*) Nothing to Disclose

For information about this presentation, contact:

shatzkes@hotmail.com

Sub-Events

RC805A Jugular Foramen

Participants

Mark D. Mamlouk, MD, Santa Clara, CA (Presenter) Nothing to Disclose

For information about this presentation, contact:

mark.d.mamlouk@kp.org

LEARNING OBJECTIVES

1) Identify jugular foramen anatomy and help identify important landmarks. 2) Differentiate various lesions and mimics that can occur within the jugular foramen. 3) Recognize key features to include in the radiology report to aid surgical planning.

RC805B Orbital Apex

Participants

Stephen F. Kralik, MD, Indianapolis, IN (Presenter) Nothing to Disclose

LEARNING OBJECTIVES

1) Identify the normal anatomic structures that constitute the orbital apex and their relationships to adjacent spaces. 2) Determine the most appropriate imaging techniques for the evaluation of orbital apex pathology. 3) Develop an appropriate imaging differential diagnosis for orbital apex pathology.

RC805C Cavernous Sinus

Participants

Reza Forghani, MD,PhD, Cote-saint-Luc, QC (*Presenter*) Stockholder, Real-Time Medical, Inc; Founder, 4 Intel Inc; Stockholder, 4 Intel Inc; Consultant, General Electric Company; Speaker, General Electric Company

For information about this presentation, contact:

reza.forghani@mcgill.ca

LEARNING OBJECTIVES

1) Identify the normal anatomic structures that constitute the cavernous sinus and their relationship to adjacent spaces. 2) Apply the most appropriate imaging exam for the evaluation of the cavernous sinus. 3) Develop an approach for diagnostic evaluation of cavernous sinus pathology. 4) Assess and differentiate different pathologic entities affecting the cavernous sinus.

RC805D Pterygopalatine Fossa

Participants

Bruno A. Policeni, MD, Iowa City, IA (Presenter) Nothing to Disclose

For information about this presentation, contact:

bruno-policeni@uiowa.edu

LEARNING OBJECTIVES

1) Identify the normal anatomic landmarks in the Pterygopalatine Fossa and relationships to adjacent spaces. 2) Review the most appropriate imaging techniques for the evaluation of the Pterygopalatine Fossa pathology. 3) Develop an appropriate differential diagnosis for Pterygopalatine Fossa lesions.



Review of Pediatric Nuclear Medicine

Friday, Nov. 30 8:30AM - 10:00AM Room: E263











AMA PRA Category 1 Credits ™: 1.50 ARRT Category A+ Credit: <u>1</u>.75

LEARNING OBJECTIVES

1) Review of Pediatric Nuclear medicine, particularly for radiologists and nuclear medicine physicians who may not specialize in pediatric patients, and for resident and fellow trainees.

Sub-Events

RC811A Pediatric Gastrointestinal

Participants

Helen R. Nadel, MD, Palo Alto, CA (Presenter) Nothing to Disclose

For information about this presentation, contact:

hnadel@stanford.edu

LEARNING OBJECTIVES

1) Be able to list indications for GI scintigraphy in children. 2) Be able to describe scintigraphic patterns of disease on GI examinations in children.

RC811B Pediatric Genitourinary

Participants

Neha S. Kwatra, MBBS, MD, Boston, MA (Presenter) Nothing to Disclose

LEARNING OBJECTIVES

1) Describe pediatric renal diseases highlighting the complementary role of scintigraphy and other imaging modalities. 2) Explain pediatric-specific imaging considerations. 3) Identify important normal variants/pitfalls in interpretation.

RC811C Pediatric Musculoskeletal

Participants

Susan E. Sharp, MD, Cincinnati, OH (Presenter) Nothing to Disclose

For information about this presentation, contact:

susan.sharp@cchmc.org

LEARNING OBJECTIVES

1) Be able to describe the utilization and performance of nuclear medicine imaging for musculoskeletal indications in pediatric patients. 2) Be able to identify musculoskeletal findings on Tc-99m-MDP and F-18-FDG scans.

RC811D Case Presentation/Panel Discussion

Participants

Neha S. Kwatra, MBBS, MD, Boston, MA (Presenter) Nothing to Disclose



Pediatric Sonography (Interactive Session)

Friday, Nov. 30 8:30AM - 10:00AM Room: E353B





AMA PRA Category 1 Credits ™: 1.50 ARRT Category A+ Credit: 1.75

FDA Discussions may include off-label uses.

GENERAL INFORMATION

This interactive session will use RSNA Diagnosis Live™. Please bring your charged mobile wireless device (phone, tablet or laptop) to participate.

Sub-Events

RC813A **Imaging of Pediatric Breast Masses**

Participants

Teresa Chapman, MD, MA, Seattle, WA (Presenter) Nothing to Disclose

For information about this presentation, contact:

teresa.chapman@seattlechildrens.org

LEARNING OBJECTIVES

1) Recognize normal glandular tissue of the pediatric patient. 2) Apply appropriate management recommendations to breast ultrasound findings of a girl with a palpable abnormality. 3) Provide an appropriate differential diagnosis for a solid tissue finding in the pediatric breast.

Active Handout:Teresa Chapman

http://abstract.rsna.org/uploads/2018/18000657/Peds Breast Ultrasound_Chapman_RSNA2018 RC813A.pdf

RC813B **Sonography of Vascular Malformations**

Participants

Harriet J. Paltiel, MD, Boston, MA (Presenter) Nothing to Disclose

LEARNING OBJECTIVES

1) Discuss the ISSVA classification of vascular anomalies and US imaging features of a number of common pediatric vascular tumors and malformations.

RC813C Sonography of the Pediatric Neck

Participants

Susan J. Back, MD, Philadelphia, PA (Presenter) Consultant, Bracco Group; Grant, Bracco Group

For information about this presentation, contact:

backs@email.chop.edu

LEARNING OBJECTIVES

1) Describe the approach to ultrasound of the pediatric neck. 2) Recognize the sonographic appearance of common pediatric neck masses. 3) Develop an understanding of when other imaging modalities are needed to assess pediatric neck masses.



Interventional Series: Reproductive Health Interventions

Friday, Nov. 30 8:30AM - 12:00PM Room: E451B



AMA PRA Category 1 Credits ™: 3.25 ARRT Category A+ Credits: 3.75

FDA Discussions may include off-label uses.

Participants

Charles E. Ray JR, MD, PhD, Chicago, IL (Moderator) Nothing to Disclose

Sub-Events

RC814-01 Prostate Embolization: Technical Considerations

Friday, Nov. 30 8:30AM - 8:45AM Room: E451B

Participants

Jafar Golzarian, MD, Minneapolis, MN (Presenter) Officer, EmboMedics Inc; Consultant, Boston Scientific Corporation; Consultant, Medtronic plc; Consultant, Penumbra, Inc

LEARNING OBJECTIVES

- 1) To discuss the rationale for Prostate artery embolization. 2) To review the technique and challenges to perform the procedure.
- 3) To select best candidates for the PAE.

RC814-02 Prostate Embolization: Outcomes

Friday, Nov. 30 8:45AM - 9:00AM Room: E451B

Participants

Jafar Golzarian, MD, Minneapolis, MN (Presenter) Officer, EmboMedics Inc; Consultant, Boston Scientific Corporation; Consultant, Medtronic plc; Consultant, Penumbra, Inc

LEARNING OBJECTIVES

1) Understand indications and contraindications to prostatic artery embolization. 2) Understand the selection of patients who are ideally suited for prostatic artery embolization. 3) Become familiar with embolic materials used in PAE. 4) Identify and anticipate complications related to PAE. 5) Understand and interpret the existing literature on PAE and how this would translate into setting expectations for the procedure in a clinical setting. 6) Become familiar with the basic techniques of PAE.

RC814-03 PAE versus TURP: An Evidence-Based Comparison of Efficacy and Economic Cost in Current **Literature Using the GRADE System**

Friday, Nov. 30 9:00AM - 9:10AM Room: E451B

Awards

Trainee Research Prize - Medical Student

Participants

Patsy Lee, BSC, Hamilton, ON (Presenter) Nothing to Disclose Oleg Mironov, MD, Hamilton, ON (Abstract Co-Author) Nothing to Disclose Michael J. Connolly, MD, Hamilton, ON (Abstract Co-Author) Nothing to Disclose Martin E. Simons, MD, Toronto, ON (Abstract Co-Author) Nothing to Disclose Colm E. Boylan, MBBCh, FRCR, Hamilton, ON (Abstract Co-Author) Nothing to Disclose

For information about this presentation, contact:

patsywplee@gmail.com

PURPOSE

The purpose of this review is to use evidence-based evaluation to compare Prostatic Artery Embolization (PAE) with the goldstandard treatment for benign prostatic hypertrophy (BPH), transurethral resection of the prostate (TURP).

METHOD AND MATERIALS

We systematically reviewed evidence comparing TURP against the more recently-developed PAE. The key terms "BPH", "TURP", "PAE", "Quality of life" (QoL), and "International Prostate Symptoms Score" (IPSS) were used to identify 17 articles. Systematic reviews, literature reviews and protocols were excluded, leaving 8 articles which were evaluated using the GRADE system.

RESULTS

Moderate-level GRADE evidence on 45 patients and high-level GRADE evidence on 114 patients indicates equivalence in efficacy

between PAE and TURP at 12-month follow-up as evaluated by IPSS and QoL. Further, high-level GRADE evidence indicates equivalence through post-void residual volume and peak urinary flow at the 12-month follow-up. This equivalence in IPSS, QoL, post-void residual volume and peak urinary flow persists through to the 24-month follow-up. Moderate-level evidence indicates that there are no major complications associated with PAE. However, the same evidence demonstrates that 100% of patients undergoing TURP experience retrograde ejaculation, 26.7% experience urinary incontinence, and 2.9% require transfusion. In terms of minor complications, the same evidence indicates that all patients treated with TURP experience minor complications including hematuria, dysuria and pollakuria. Conversely, after PAE, patients experience self-limited post-embolization syndrome that does not require extended in-patient stay. Moderate-level evidence demonstrates that the in-hospital cost, out-of-hospital cost, and productivity-related cost due to absence from work are significantly less in PAE compared to TURP.

CONCLUSION

TURP and PAE are equivalent in efficacy at 12 and 24-months. TURP is associated with major complications such as retrograde ejaculation, urinary incontinence and transfusions. PAE is associated with only minor complications and lower cost.

CLINICAL RELEVANCE/APPLICATION

This article provides an evidence-based approach to support the treatment of BPH using PAE. BPH affects at least 50% of men by the age of 60 and increases in prevalence with age. Annual USA-wide expenditures are reported to total approximately \$6 billion.

RC814-04 Comprehensive Assessment of Imaging Outcomes Following Prostate Artery Embolization (PAE) for Benign Prostatic Hyperplasia

Friday, Nov. 30 9:10AM - 9:20AM Room: E451B

Participants

Rehan Ali, MBBS, Forest Park, IL (*Presenter*) Nothing to Disclose
Ahmed Gabr, MD, MBBCh, Chicago, IL (*Abstract Co-Author*) Nothing to Disclose
Samdeep Mouli, MD, Chicago, IL (*Abstract Co-Author*) Nothing to Disclose
Ronald A. Mora, MD, Chicago, IL (*Abstract Co-Author*) Nothing to Disclose
Nabeel Hamoui, MD, Chicago, IL (*Abstract Co-Author*) Nothing to Disclose
Joseph R. Kallini, MD, Los Angeles, CA (*Abstract Co-Author*) Nothing to Disclose
Ahsun Riaz, MD, Chicago, IL (*Abstract Co-Author*) Nothing to Disclose

Robert J. Lewandowski, MD, Chicago, IL (Abstract Co-Author) Consultant, BTG International Ltd; Advisory Board, Boston Scientific Corporation; Consultant, Cook Group Incorporated; Advisory Board, ABK Biomedical Inc; Advisory Board, Accurate Medical; Consultant, C. R. Bard, Inc;

Frank H. Miller, MD, Chicago, IL (Abstract Co-Author) Research Grant, Siemens AG

Riad Salem, MD, MBA, Chicago, ÌL (Abstract Co-Author) Research Consultant, BTG International Ltd; Research Grant, BTG International Ltd; Consultant, Eisai Co, Ltd; Consultant, Exelixis, Inc; Consultant, Bristol-Myers Squibb Company; Consultant, Dove;

PURPOSE

To assess the change in volume of prostate and imaging findings following prostate artery embolization (PAE) for benign prostate hyperplasia (BPH).

METHOD AND MATERIALS

With IRB approval, we analyzed prospectively acquired MR data of PAE patients at baseline and 6-month following treatment from 2015-17. We reviewed prostate MRs looking for sequelae of embolization [changes in signal intensity and/or enhancement, infection/inflammation, infarction, edema, and change in intravesical prostatic protrusion (IPP)]. We calculated the total volume (TV) and central gland volumes (CGV) using DynaCAD® and measured change in volumes. Analyses were performed using SPSS with P<0.05 considered significant.

RESULTS

Forty-three patients (n=43) met our inclusion criteria. 93% (30/43) and 100% (43/43) showed a decrease in TV and CGV at 6-months respectively. At baseline, median TV was 86 cc (range: 29.4-232) and median CGV was 54.4 cc (range: 12.9-165.5). Median decrease in TV was 18.2% (CI: 13.3-27.2) (p=0.0001) and median decrease in CGV was 26.7% (CI: 20.4-35.9) (p=0.0001). Thirty seven percent (16/43) of patients had IPP at baseline; 100% showed a decrease in size of median lobe at follow-up. At 6-month follow-up, 33% (14/43) showed imaging features of infarction, 79% (34/43) had decrease in T2-signal intensity, and 51% (22/43) showed a decrease in enhancement. None had edema, periprostatic fat changes or infection/inflammation.

CONCLUSION

PAE produces significant changes in both the TV and CGV of the prostate on MR imaging. These changes are most significant in patients with prostates > 80 cc in volume. Future studies will correlate changes in MR findings with clinical outcomes following PAE.

CLINICAL RELEVANCE/APPLICATION

Infarction is not significant finding in patients receiving PAE unlike fibroid embolization. PAE response can be assessed by measuring change in prostate volume and/or IPP change.

Honored Educators

Presenters or authors on this event have been recognized as RSNA Honored Educators for participating in multiple qualifying educational activities. Honored Educators are invested in furthering the profession of radiology by delivering high-quality educational content in their field of study. Learn how you can become an honored educator by visiting the website at: https://www.rsna.org/Honored-Educator-Award/ Frank H. Miller, MD - 2012 Honored EducatorFrank H. Miller, MD - 2014 Honored EducatorFrank H. Miller, MD - 2017 Honored EducatorFrank H. Miller, MD - 2018 Honored Educator

RC814-05 Uterine Fibroid Embolization: Techniques

Friday, Nov. 30 9:20AM - 9:35AM Room: E451B

Maureen P. Kohi, MD, San Francisco, CA (*Presenter*) Research Grant, Boston Scientific Corporation; Consultant, LaForce; Advisory Board, Boston Scientific Corporation; Advisory Board, AbbVie Inc

LEARNING OBJECTIVES

1) Understand the indications/contraindications to UAE. 2) Discuss procedural steps involved in simple and complex UAE. 3) Comprehend the periprocedural care of patients undergoing UAE.

RC814-06 Comparison of Reproductive Outcomes Following Uterine Fibroid Embolization (UFE) and Robotic-Assisted Laparoscopic Myomectomy in Patients with Symptomatic Uterine Fibroids and Correlation of MRI Characteristics with Pregnancy Outcomes after UFE

Friday, Nov. 30 9:35AM - 9:45AM Room: E451B

Participants

Maria A. Kotarska, PhD, Chicago, IL (Presenter) Nothing to Disclose

For information about this presentation, contact:

majakotarska@me.com

PURPOSE

To analyze and compare differences in reproductive outcomes following uterine fibroid embolization (UFE) and robotic-assisted laparoscopic myomectomy in patients with symptomatic uterine fibroids and to correlate MRI characteristics with pregnancy outcomes after UFE.

METHOD AND MATERIALS

Forty patients undergoing fertility-sparing treatment for symptomatic uterine fibroids between 2006 and 2016 who achieved any subsequent pregnancy at the same institution were analyzed. In the UFE group pre and post procedure MRI imaging data was correlated with pregnancy outcomes. MRI was analyzed in the UFE patient group for uterine volume, number , size and location of fibroids, submucosal grade and cavity distortion.

RESULTS

Patients who underwent UFE were more likely to have bulk symptoms as their presenting fibroid symptom (p=0.001), and to have intramural fibroid location (p=0.043). Patients with pregnancy after UFE had a smaller average diameter of the dominant fibroid at the time of treatment (5.2cm vs 7.4cm; p=0.0306), but uterine volume at the time of treatment was similar for both groups. Rates of post-procedure spontaneous abortion, preterm cesarean delivery, term cesarean delivery, and vaginal delivery did not differ between the two groups. The rate of composite adverse pregnancy outcomes for deliveries over 24 weeks, including uterine rupture, postpartum hemorrhage, abruption, and intrauterine growth restriction, did not differ significantly between the UFE and laparoscopic myomectomy groups (36% vs 28%; p=0.728). In patients who had positive pregnancy outcomes after UFE were associated on MRI with greater uterine volume reduction and lesser cavity distortion post procedure. Pre-procedure uterine volume, number of uterine incisions at myomectomy, predominant fibroid location, and time from procedure to pregnancy event were not associated with the risk of adverse pregnancy outcomes.

CONCLUSION

UFE and robotic-assisted laparoscopic myomectomy have equivalent reproductive outcomes and comparable rates of adverse pregnancy outcomes. Positive pregnancy outcomes post UFE were positively correlated on MRI with absence of cavity distortion and uterine volume reduction post embolization.

CLINICAL RELEVANCE/APPLICATION

The study impacts all female patients with symptomatic fibroids who desire to preserve their fertility and provides evidence based framework for decision making between treatment options.

RC814-07 Uterine Fibroid Embolization: Outcomes

Friday, Nov. 30 9:45AM - 10:00AM Room: E451B

Participants

James B. Spies, MD, Washington, DC (Presenter) Nothing to Disclose

LEARNING OBJECTIVES

1) Understand the symptomatic improvement that typically occurs as a result of uterine embolization. 2) Understand the recurrence rate that might be anticipated after uterine embolization. 3) Understand the reproductive outcomes from uterine embolization. 4) Understand the factors that might impact outcome from the procedure.

RC814-08 High-intensity Focused Ultrasound in the Treatment of Uterine Fibroids

Friday, Nov. 30 10:00AM - 10:15AM Room: E451B

Participants

Maureen P. Kohi, MD, San Francisco, CA (*Presenter*) Research Grant, Boston Scientific Corporation; Consultant, LaForce; Advisory Board, Boston Scientific Corporation; Advisory Board, AbbVie Inc

LEARNING OBJECTIVES

1) Understand indications/contraindications to HIFU for symptomatic uterine fibroids. 2) Comprehend periprocedural patient care and procedural steps. 3) Learn procedural outcomes and how they compare to UAE.

RC814-09 Pelvic Congestion Syndrome

Friday, Nov. 30 10:30AM - 10:45AM Room: E451B

Participants

Gordon McLennan, MD, Chagrin Falls, OH (*Presenter*) Grant, Siemens AG; Grant, Surefire Medical, Inc; Speakers Bureau, Medtronic plc; Speakers Bureau, General Electric Company; Speakers Bureau, Stryker Corporation; Advisory Board, Siemens AG; Advisory Board, Surefire Medical, Inc; Advisory Board, Stealth Medical; Advisory Board, Rene Medical, Inc; Advisory Board, F. Hoffmann-La Roche Ltd; Advisory Board, Bristol-Myers Squibb Company; Advisory Board, B. Braun Melsungen AG; Advisory Board, General Electric Company;

For information about this presentation, contact:

mclenng@ccf.org

LEARNING OBJECTIVES

1) Describe the different causes of chronic pelvic pain in women. 2) Describe the literature evidence that supports the diagnosis of pelvic congestion syndrome and the embolization of ovarian veins. 3) Describe the technical approaches to embolization of the ovarian vein and abnormal varicose veins from the internal iliac vein.

ABSTRACT

Pelvic Congestion Syndrome is defined as chronic pelvic pain associated with ovarian vein reflux. In some patients, it is associated with internal iliac vein reflux and varicose veins of the legs. The management of chronic pelvic pain is best achieved with a multidisciplinary approach that inovives gynecology, pain management, physical therapy, psychological therapy, and interventional radiology. We will review the literature supporting the diagnosis & treatment of this condition, highlight the differential diagnosis and other therapies that are often required and describe the technical approaches to ovarian vein embolization, internal iliac vein embolization and pudendal nerve block.

RC814-10 Efficacy of MR guided focused Ultrasound Surgery (MRgFUS) In Adenomyosis: A Study of 113 Symptomatic Adenomyosis in 92 Indian Patients

Friday, Nov. 30 10:45AM - 10:55AM Room: E451B

Participants

Ritu M. Kakkar, MBBS, DMRD, Mumbai, India (*Abstract Co-Author*) Nothing to Disclose Shrinivas B. Desai, MD, Mumbai, India (*Presenter*) Nothing to Disclose

For information about this presentation, contact:

riturupesh@gmail.com

PURPOSE

To assess the efficacy of MR guided focused ultrasound surgery (MRGFUS) in treating adenomyosis by evaluation of non-perfused volumes (NPV) and symptom severity score (SSS).

METHOD AND MATERIALS

92 Indian women with 113 significant symptomatic adenomyosis (SSS > 21) were selected after approval from ethics committee. Adenomyosis with definable treatable areas(>2cm) were included. Patients with SSS <21 and non definable treatable areas were excluded. Pre treatment raw and transformed SSS were calculated. Treatment was performed on a 1.5-T whole-body system (Signa; GE Healthcare) in the ExAblate 2000 (InSightec) device. During treatment the patient lies prone and a gel pad couples the patients abdomen to a phased array coil in a sealed water bath in the treatment table. The system generates a high intensity acoustic beam that is focused on target , leading to tissue necrosis . Post treatment results were evaluated by assessing non perfused areas on contrast enhanced scans. Patients were called for follow up at 6 months .SSS was enquired and MRI pelvis with contrast was performed to calculate the non-perfused volume.

RESULTS

74% of our patients had significant reduction in symptom severity score following treatment. The reduction in mean raw and transformed SSS pre and 6 months post treatment was statistically significant . The mean volume of adenomyosis prior to treatment was 139.47 ± 102.497 SD, while non perfused volumes 6 months after treatment were 71.26 ± 51.15 SD. This difference was found to be statically significant (0.000134). We used Non-perfused Volume (NPV) and its percentage of the total adenomyotic volume before the treatment (NPV%) and correlated these with the Reduction in the Symptom Severity Score at 6 months and found the correlation strong and positively linear (Pearsons correlation of .644 and .928 with NPV and NPV %).

CONCLUSION

MRgFUS is able to achieve NPV values that will result in clinically significant reduction in symptoms. The reduction in the SSS and percentage of adenomyosis reduction follows the NPV very closely and linearly, which means that achieving greater NPV will essentially result in significant symptom reduction.

CLINICAL RELEVANCE/APPLICATION

MRgFUS is a non invasive ,safe and effective modality for the treatment of Adenomyosis providing good symptomatic relief and long term results

RC814-11 Efficacy of MR Guided Focused Ultrasound Surgery in Treatment of Uterine Fibroids: A Study of 1214 Fibroids-Indian Experience

Friday, Nov. 30 10:55AM - 11:05AM Room: E451B

Participants

Ritu M. Kakkar, MBBS, DMRD, Mumbai, India (*Abstract Co-Author*) Nothing to Disclose Shrinivas B. Desai, MD, Mumbai, India (*Presenter*) Nothing to Disclose

For information about this presentation, contact:

PURPOSE

To evaluate the role of MRgFUS in management of Uterine Fibroids in terms of clinical improvement in symptoms as suggested by decrease in Symptom Severity Score (SSS) and reduction in Non perfused volume ,and to access early and late adverse effects of treatment.

METHOD AND MATERIALS

• 1214 symptomatic fibroids in 717 Indian women were selected. Patients with uterine fibroids showing enhancement on screening MRI were recruited for the study. Patients with non enhancing /calcified fibroids were excluded. Pretreatment raw and transformed symptom severity score was was calculated. Treatment was performed on a 1.5-T whole-body system (Signa; GE Healthcare) in the ExAblate 2000 (InSightec) device. During treatment the patient lies prone and a gel pad couples the patients abdomen to a phased array coil in a sealed water bath. The system generates a high intensity acoustic beam that is focused on target, leading to tissue necrosis. Post treatment results were evaluated by assessing non perfused volume on contrast enhanced scans. All patients were followed up at 6 months with post contrast MR pelvis Symptom severity score and Non perfused volume was calculated ,delayed adverse events were enquired.

RESULTS

The reduction in both mean raw and transformed SSS before and 6 months post treatment was statistically significant (p=0.0001). The mean volume of fibroids before treatment was 145.76 cc with SD 81.22 cc .At 6 months follow up there was statistically significant reduction in the volume of fibroids with mean being 105.75 cc and SD 59.95 cc (p value 0.0001). The Non Perfused Volume (NPV) achieved after the procedure was 88.21% with a SD of 7.60%. And this has transformed into greater reduction of fibroid volume at 6 months.65% patients had no adverse effects following treatment .Leg pain was seen in 15% patients immediately after treatment and 2% continued having mild leg pain after 6 months .2 patients (0.2%) had intestinal perforation.

CONCLUSION

MRgFUS provides statistically significant reduction in symptom severity index and fibroid volumes at 6 month follow up The adverse effect profile is acceptable with major events occurring in a very small percentage of patients

CLINICAL RELEVANCE/APPLICATION

MRgFUS is a good ,safe, non invasive replacement to conventional invasive therapies like hysterectomy and myomectomy for uterine fibroids with comparable success rates and lower side effect profile .

RC814-12 Contraceptive Implant Migration and Removal

Friday, Nov. 30 11:05AM - 11:20AM Room: E451B

Participants

Paul J. Rochon, MD, Aurora, CO (*Presenter*) Moderator and Speaker, Penumbra, Inc; Speakers Bureau, C. R. Bard, Inc; Speaker, Cook

LEARNING OBJECTIVES

1) Understand the types of subcutaneous hormonal contraceptive implants. 2) Understand the risks factors and complications associated with placing these implants. 3) Understand methods used in interventional radiology to remove complex contraceptive implants.

RC814-13 Post-partum Hemorrhage

Friday, Nov. 30 11:20AM - 11:35AM Room: E451B

Participants

Matthew A. Brown, MD, Aurora, CO (Presenter) Nothing to Disclose

LEARNING OBJECTIVES

1) Review risk factors for postpartum hemorrhage. 2) Describe treatment options for postpartum hemorrhage and role of transcatheter embolization. 3) Discuss procedural technique and challenges of pelvic artery embolization for postpartum hemorrhage.

RC814-14 Uterine Artery Embolization to Reduce Operative Blood Loss and Transfusion Requirements during Cesarean-Hysterectomy in Patients with Invasive Placenta

Friday, Nov. 30 11:35AM - 11:45AM Room: E451B

Awards

Student Travel Stipend Award

Participants

Melinda Wang, New York, NY (Presenter) Nothing to Disclose

Alana Wade, MD, Tacoma, WA (Abstract Co-Author) Nothing to Disclose

Deddeh M. Ballah, MD, San Francisco, CA (Abstract Co-Author) Nothing to Disclose

Maureen P. Kohi, MD, San Francisco, CA (*Abstract Co-Author*) Research Grant, Boston Scientific Corporation; Consultant, LaForce; Advisory Board, Boston Scientific Corporation; Advisory Board, AbbVie Inc

PURPOSE

Invasive placenta (IP) is a life-threatening pathology with maternal mortality as high as 7%. With an increasing number of IP diagnoses in the US, advance planning allows for the use of prophylactic measures to decrease morbidity and mortality. This study aims to evaluate the efficacy of uterine artery embolization (UAE) after cesarean delivery and prior to hysterectomy in patients with IP for decreasing blood loss and transfusion requirements when compared to either Cesarean-hysterectomy (C-hyst) alone or C-hyst with uterine artery ligation (UAL).

METHOD AND MATERIALS

This is a retrospective observational study including patients with IP treated with C-hyst at our institution from 5/2014-10/2017. Patients included were divided into three groups depending on procedure received (UAE, UAL, or C-hyst alone). Emergent cases, patients who did not undergo hysterectomy, and patients without pathologic diagnosis of IP were excluded. Primary outcomes were estimated blood loss (EBL) and blood transfusion requirements.

RESULTS

A total of 33 patients were included in the study (UAE group: n=6; UAL group: n=7; control group: n=20). Mean EBL in the UAE group was 1233 mL (SD: ± 605 mL) compared to 3120 mL (SD: ± 1722 mL) in the control group (p=0.03) and 2700 mL (SD: ± 1095 mL) in the UAL group (p=0.06). Mean transfusion requirement, including pRBC and Cell Saver, in the UAE group was 258 mL (SD: ± 325 mL) compared to 1210 mL (SD: ± 1441 mL) in the control group (p=0.18) and 1481 mL (SD: ± 1174 mL) in the UAL group (p=0.27). No differences were seen between the UAL and control groups in EBL (p=0.89) or transfusion requirements (p=0.89). There were no substantial differences in length of postpartum stay, surgical complication rates, or ICU admission rates.

CONCLUSION

C-hyst is the current standard of management in IP but itself carries significant mortality and morbidity. In our study, prophylactic UAE significantly decreases intraoperative blood loss when compared to C-hyst alone and marginally decreases EBL when compared to C-hyst with UAL. Decreased transfusion requirements in cases with UAE were not statistically significant but may be clinically significant. UAE appears to be a feasible and potentially advantageous option within a multidisciplinary approach to IP.

CLINICAL RELEVANCE/APPLICATION

In patients with invasive placenta, UAE prior to hysterectomy may offer a multidisciplinary option to decrease blood loss compared to hysterectomy alone.

RC814-15 Gender Differences in Peripheral Vascular Disease

Friday, Nov. 30 11:45AM - 12:00PM Room: E451B

Participants

Kristofer M. Schramm, MD, Aurora, CO (Presenter) Nothing to Disclose

LEARNING OBJECTIVES

Learning Objectives: To describe trends in female vascular diseaseTo review barriers to female access to care and treatment of vascular diseaseTo establish differences in outcomes in open and endovascular repair of female vascular disease

LEARNING OBJECTIVES

1) To highlight differences in the risk factors for, presentation of, and sequelae of peripheral artery disease in men and women. 2) To highlight treatment related differences in peripheral artery disease in men and women. 3) To review the existing data regarding endovascular management of peripheral artery disease in women.

ABSTRACT

In the last 20 years, peripheral artery disease (PAD) has been increasingly recognized as a significant cause of morbidity and mortality in the United States. PAD has traditionally been identified as a male dominant disease; however, recent population trends and studies in PAD suggest that women are affected at least as often as men. Women comprise a larger population of the elderly than men, as well as an increasing proportion of patients with PAD. Much of the existing research on PAD has focused on whole populations, and gender specific data on PAD is sparse. This review focuses on gender specific differences in presentation, management, and outcomes of PAD intervention that are important considerations for the interventional radiologist.



Radiologist's Value in the Multidisciplinary Team

Friday, Nov. 30 8:30AM - 10:00AM Room: E350



AMA PRA Category 1 Credits ™: 1.50 ARRT Category A+ Credit: 1.75

Participants

Cherie M. Kuzmiak, DO, Chapel Hill, NC (Moderator) Research Grant, Delphinus Medical Technologies, Inc

LEARNING OBJECTIVES

1) Define high-risk lesions. 2) Review radiologic-pathologic features and characteristics of high-risk lesions. 3) Discuss approaches to high-risk lesions with attention to management considerations and controversies. 4) Describe and discuss the imaging features of the major subtypes of invasive breast cancer with integration of pathology. 5) Understand the molecular classification of breast cancer and its impact on patient prognosis. 6) Describe patients' perspectives of breast imaging experiences with a focus on pain, anxiety, and emotional distress relating to abnormal results and biopsy procedures. 7) Define interventions for reducing patients' negative experiences related to abnormal results and biopsy procedures.

Sub-Events

RC815A Management of High Risk Lesions

Participants

Samantha L. Heller, MD, PhD, New York, NY (Presenter) Nothing to Disclose

For information about this presentation, contact:

Samantha. Heller@nyumc.org

LEARNING OBJECTIVES

1) Define high-risk lesions. 2) Review radiologic-pathologic features and characteristics of high-risk lesions. 3) Discuss approaches to high-risk lesions with attention to management considerations and controversies.

RC815B Imaging Appearance of Cancer Subtypes

Participants

Cherie M. Kuzmiak, DO, Chapel Hill, NC (Presenter) Research Grant, Delphinus Medical Technologies, Inc

LEARNING OBJECTIVES

1) Describe and discuss the imaging features of the major subtypes of invasive breast cancer with integration of pathology. 2) Understand the molecular classification of breast cancer and its impact on patient prognosis.

RC815C Improving the Patient's Experience

Participants

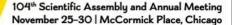
Mary S. Soo, MD, Durham, NC (Presenter) Nothing to Disclose

For information about this presentation, contact:

mary.soo@duke.edu

LEARNING OBJECTIVES

1) Describe patients' perspectives of breast imaging experiences with a focus on pain, anxiety, and emotional distress relating to abnormal results and biopsy procedures. 2) Define interventions for reducing patients' negative experiences related to abnormal results and biopsy procedures.





Interacting Effectively with Referring Physicians in the Digital Age (Sponsored by RSNA Public Information Committee)

Friday, Nov. 30 8:30AM - 10:00AM Room: E352



AMA PRA Category 1 Credits ™: 1.50 ARRT Category A+ Credit: 0

Participants

Max Wintermark, MD, Lausanne, Switzerland (*Moderator*) Advisory Board, General Electric Company; Consultant, More Health; Consultant, Magnetic Insight; Consultant, Icometrix; Consultant, Nines; Annette J. Johnson, MD, Augusta, GA (*Presenter*) Nothing to Disclose Andrew B. Rosenkrantz, MD, New York, NY (*Presenter*) Nothing to Disclose Tarik K. Alkasab, MD, PhD, Boston, MA (*Presenter*) Nothing to Disclose

For information about this presentation, contact:

max.wintermark@gmail.com

LEARNING OBJECTIVES

1) Discern what referring physicians want and need from radiologists in the digital age. 2) Better implement virtual radiology rounds and other digital tools. 3) Leverage enterprise IT to improve radiology communication and collaboration.

ABSTRACT

In transitioning to a value-based practice in the digital age, it is imperative that the radiologist learn to interact efficiently and effectively with other members of the patient's healthcare team. In this course, attendees will learn how to harness the growing number of digital tools and reporting capabilities to improve their interactions with referring clinicians.



CT Radiation Dose Reduction: Techniques and Clinical Implementation

Friday, Nov. 30 8:30AM - 10:00AM Room: E253CD







AMA PRA Category 1 Credits ™: 1.50 ARRT Category A+ Credit: 1.75

Participants

Lifeng Yu, PhD, Chicago, IL (Coordinator) Nothing to Disclose

For information about this presentation, contact:

yu.lifeng@mayo.edu

LEARNING OBJECTIVES

1) Review techniques that are currently available for radiation dose reduction. 2) Understand general dose management and optimization strategies and how they are implemented in adult CT. 3) Understand strategies to optimize scanning protocols in pediatric CT.

ABSTRACT

This course will provide an overview of techniques and clincial implementations of radiation dose reduction in CT.

Sub-Events

RC823A Overview of Technology for Radiation Dose Reduction

Participants

Joseph W. Stayman, PhD, Baltimore, MD (*Presenter*) Research Grant, Canon Medical Systems Corporation; Research Grant, Carestream Health, Inc; Research Grant, Elekta AB; Research collaboration, Fischer Medical; Research Grant, Medtronic plc; Research collaboration, Koninklijke Philips NV; Research Grant, Siemens AG

LEARNING OBJECTIVES

1) Identify targets for radiation dose reductions in x-ray CT. 2) Gain an understanding of dose reduction strategies based on innovations in hardware design and development. 3) Gain an understanding of dose reduction strategies based on data processing chain improvements including iterative reconstruction methods. 4) Understand some of the trade-offs in dose reduction as well as limitations on dose reduction.

RC823B Dose Optimization Strategy and Clinical Implementation in Adult CT

Participants

Lifeng Yu, PhD, Chicago, IL (Presenter) Nothing to Disclose

For information about this presentation, contact:

yu.lifeng@mayo.edu

LEARNING OBJECTIVES

1) Introduce dose management and optimization strategies in adult CT. 2) Describe how dose reduction techniques are clinical implemented in adult CT, including neuro, chest, abdominal, cardiovascular, and MSK.

RC823C Dose Reduction and Protocol Optimization in Pediatric CT

Participants

Robert MacDougall, MSc, Boston, MA (Presenter) Nothing to Disclose

For information about this presentation, contact:

robert.d.macdougall@childrens.harvard.edu

LEARNING OBJECTIVES

1) Recognize the important of clinical indication on CT protocol design. 2) Describe the different commercial implementations of kV and mA modulation algorithms and understand methods of standardizing image quality across platforms. 3) Understand the effect of reconstruction algorithms on acquisition parameter selection in pediatric CT.



Six Common Difficult Problems in GI and GU MRI: The Experts' Approach

Friday, Nov. 30 8:30AM - 10:00AM Room: E351



GU

MR

AMA PRA Category 1 Credits ™: 1.50 ARRT Category A+ Credit: 1.75

Participants

Hero K. Hussain, MD, Ann Arbor, MI (Moderator) Nothing to Disclose

Sub-Events

RC829A The CT Indeterminate Lesion in the Non-Cirrhotic Liver: Extracellular or Hepatobiliary Contrast-

Enhanced MRI

Participants

Hero K. Hussain, MD, Ann Arbor, MI (Presenter) Nothing to Disclose

For information about this presentation, contact:

hh141@aub.edu.lb

LEARNING OBJECTIVES

1) Describe the difference between extracellular and hepatobiliary contrast with regard to the mechanism of action and effect on post contrast phases. 2) Explain the types of liver lesions seen on CT that may benefit from imaging with hepatobiliary contrast.

RC829B Is MRI Needed to Further Evaluate a CT Indeterminate Renal Mass?

Participants

Hersh Chandarana, MD, New York, NY (*Presenter*) Equipment support, Siemens AG; Software support, Siemens AG; Advisory Board, Siemens AG; Speaker, Bayer AG;

For information about this presentation, contact:

hersh.chandarana@nyumc.org

LEARNING OBJECTIVES

1) Limitation of CT imaging in characterization of small renal masses (with focus on discriminating benign/indolent renal tumors from aggressive renal cancer). 2) Role of MRI as a problem solving tool in characterizing cystic and solid renal masses. 3) Evolving role of MRI in renal mass (histologic) subtyping and assessment of renal tumor aggressiveness.

RC829C Perianal Fistulae: What Does the Surgeon Want to Know?

Participants

Mahmoud M. Al-Hawary, MD, Ann Arbor, MI (Presenter) Nothing to Disclose

LEARNING OBJECTIVES

1) Review normal anatomy of the anal sphincter complex and surrounding pelvic structures. 2) Discuss etiology, pathophysiology and classification of perianal fistulas. 3) Correlate implication of imaging findings on disease management.

RC829D How Do I Perform and Interpret MRI of Pelvic Floor Weakness?

Participants

Victoria Chernyak, MD, MS, Bronx, NY (Presenter) Nothing to Disclose

For information about this presentation, contact:

vichka17@hotmail.com

LEARNING OBJECTIVES

1) Familiarize themselves with MR protocol for assessment of pelvic floor dysfunction. 2) Learn techniques for improving patient cooperation for dynamic images. 3) Identify normal anatomy of anterior, middle and posterior compartments. 3) Apply reference lines and angles used in assessment of pelvic floor dysfunction. 4) Identify and grade the severity of pelvic floor relaxation. 5) Identify and grade the severity of pelvic organ prolapse.

RC829E Is MRI the Next Step After US to Evaluate Non-Obstetric Pelvic Pain in Pregnancy?

Participants

Reena C. Jha, MD, Washington, DC (Presenter) Nothing to Disclose

1) Review the common causes of non obstetric pelvic pain in pregnancy. 2) Recognize the unique diagnostic and therapeutic challenges in the pregnant patient with pelvic pain. 3) Discuss the safety considerations of imaging in pregnancy. 4) Review the evolving imaging and clinical literature on appropriate investigation of acute pelvic pain pregnancy. 5) Discuss the utility of MRI as a supplement to US in the pregnant patient.

RC829F How Do I Perform a Diagnostic MRI in a Non-Cooperative Patient?

Participants

Mustafa R. Bashir, MD, Cary, NC (*Presenter*) Research Grant, Siemens AG; Research Grant, General Electric Company; Research Grant, NGM Biopharmaceuticals, Inc; Research Grant, TaiwanJ Pharmaceuticals Co, Ltd; Research Grant, Madrigal Pharmaceuticals, Inc; Research Consultant, RadMD

For information about this presentation, contact:

mustafa.bashir@duke.edu

LEARNING OBJECTIVES

1) Describe patient and technical factors that may contribute to suboptimal or nondiagnostic body MRI examinations.2) Discuss methods for reducing the impact of the above factors using clinically-available MRI techniques.

ABSTRACT

Patient motion is a major issue in abdominal MRI. Not only are some patients unable to sustain a breath-hold, but breathing motion can be unpredictable. In this talk we will discuss a variety of techniques for combating motion, including fast imaging, special k-space filling trajectories, and respiratory gating using extrinsic and intrinsic signals.



Radiology Compensation and Finance

Friday, Nov. 30 8:30AM - 10:00AM Room: E353A





AMA PRA Category 1 Credits ™: 1.50 ARRT Category A+ Credit: 1.75

Participants

Vincent P. Mathews, MD, Hartland, WI (Moderator) Nothing to Disclose

For information about this presentation, contact:

vmathews@mcw.edu

LEARNING OBJECTIVES

See subsection Objectives.

Sub-Events

RC832A Health Care Reform and Radiology Reimbursement

Participants

Robert J. Witte, MD, Rochester, MN (Presenter) Nothing to Disclose

For information about this presentation, contact:

witte.robert@mayo.edu

LEARNING OBJECTIVES

1) Provide a history of important legislation and policies that have had a significant impact on health care reform. 2) Review recent transformative health care legislation and policies impacting radiology reimbursement.

RC832B The Financial Impact of Accountable Care Organization on Radiology

Participants

Suresh K. Mukherji, MD, Northville, MI (Presenter) Nothing to Disclose

LEARNING OBJECTIVES

1) Review that impact of ACO's on Radiologist's compensation.

RC832C Radiology Compensation Benchmarks

Participants

Vincent P. Mathews, MD, Hartland, WI (Presenter) Nothing to Disclose

For information about this presentation, contact:

vmathews@mcw.edu

LEARNING OBJECTIVES

1) To learn about the implementation of fair market values compensation plans. 2) To understand the importance of utilizing appropriate benchmarks for clinical productivity measures.

RC832D Testifying as an Expert Witness: Rules, Compensation and other Rewards, and Penalties

Participants

Leonard Berlin, MD, Wilmette, IL (Presenter) Nothing to Disclose

For information about this presentation, contact:

lberlin@live.com

LEARNING OBJECTIVES

1) Understand the need for and the purpose of requiring expert witnesses to be presenting and give testimony in medical malpractice courtroom trials. 2) Recognize the positions taken by the ACR and state medical licensing boards regarding expert witness testimony. 3) Learn what is expected of expert witnesses regarding their testimony - specifically what they can say and cannot say - when testifying under oath in a court of law.



Breast Elastography (Hands-on)

Friday, Nov. 30 8:30AM - 10:00AM Room: E264





AMA PRA Category 1 Credits ™: 1.50 ARRT Category A+ Credit: 0

Participants

Richard G. Barr, MD, PhD, Campbell, OH (*Presenter*) Consultant, Siemens AG; Consultant, Koninklijke Philips NV; Research Grant, Siemens AG; Research Grant, SuperSonic Imagine; Speakers Bureau, Koninklijke Philips NV; Research Grant, Bracco Group; Speakers Bureau, Siemens AG; Consultant, Canon Medical Systems Corporation; Research Grant, Esaote SpA; Research Grant, BK Ultrasound; Research Grant, Hitachi, Ltd

Stamatia V. Destounis, MD, Scottsville, NY (*Presenter*) Research Grant, Hologic, Inc; Research Grant, Delphinus Medical Technologies, Inc

Rajas N. Chaubal, MBBS, MD, Thane, India (Presenter) Nothing to Disclose

Nitin G. Chaubal, MD, MBBS, Mumbai, India (Presenter) Nothing to Disclose

Chander Lulla, MBBS, Mumbai, India (Presenter) Nothing to Disclose

Vito Cantisani, MD, Rome, Italy (*Presenter*) Speaker, Canon Medical Systems Corporation; Speaker, Bracco Group; Speaker, Samsung Electronics Co, Ltd;

Maija Radzina, MD, PhD, Riga, Latvia (Presenter) Nothing to Disclose

Phan T. Huynh, MD, Houston, TX (Presenter) Nothing to Disclose

Paula B. Gordon, MD, Vancouver, BC (*Presenter*) Stockholder, OncoGenex Pharmaceuticals, Inc; Stockholder, Volpara Health Technologies Limited; Scientific Advisory Board, Real Imaging Ltd; Scientific Advisory Board, DenseBreast-info, Inc;

Tanya W. Moseley, MD, Houston, TX (Presenter) Nothing to Disclose

Catherine W. Piccoli, MD, Voorhees, NJ (Presenter) Stockholder, Qualgenix LLC;

Gary J. Whitman, MD, Houston, TX (Presenter) Nothing to Disclose

Anna I. Holbrook, MD, Atlanta, GA (Presenter) Nothing to Disclose

Rachna Dutta, MD, Cleveland, OH (*Presenter*) Nothing to Disclose

Valerio Forte, MD, Rome, Italy (Presenter) Nothing to Disclose

Daniele Fresilli, Roma, Italy (*Presenter*) Nothing to Disclose

Giuseppe Schillizzi, Roma, Italy (*Presenter*) Nothing to Disclose

Gregorio Alagna, Rome, Italy (*Presenter*) Nothing to Disclose

Valeria de Soccio, JD, Rome, Italy (Presenter) Nothing to Disclose

For information about this presentation, contact:

riaclinic@gmail.com

nitin.chaubal@gmail.com

rajas.chaubal@gmail.com

sdestounis@ewbc.com

rdutta@metrohealth.org

LEARNING OBJECTIVES

1) To explain the difference between strain and shear wave elastography. 2) To review how to characterize breast lesions as benign or malignant on elastography. 3) To demonstrate how to perform both strain and shear wave elastography for breast imaging.

Honored Educators

Presenters or authors on this event have been recognized as RSNA Honored Educators for participating in multiple qualifying educational activities. Honored Educators are invested in furthering the profession of radiology by delivering high-quality educational content in their field of study. Learn how you can become an honored educator by visiting the website at: https://www.rsna.org/Honored-Educator-Award/ Richard G. Barr, MD, PhD - 2017 Honored Educator



Want to Learn More About Imaging Informatics? Education, Resources and Certifications

Friday, Nov. 30 8:30AM - 10:00AM Room: E260





AMA PRA Category 1 Credits ™: 1.50 ARRT Category A+ Credit: 1.75

Participants

Christopher J. Roth, MD, Raleigh, NC (Moderator) Nothing to Disclose

LEARNING OBJECTIVES

1) Summarize the forces driving physician adoption and leadership in local and national informatics initiatives. 2) Outline freely available educational resources to expand imaging informatics understanding. 3) Describe available imaging informatics courses and fellowships. 4) Detail common certifications available to imaging and non-imaging informatics leaders to demonstrate their knowledge. 5) Know the current imaging informatics 'hot topics.'

Sub-Events

RC854A Landscape of Online Resources for Informatics Self-Study

Participants

Marc D. Kohli, MD, San Francisco, CA (Presenter) Nothing to Disclose

LEARNING OBJECTIVES

1) Identify online sources of content for didactic informatics self-study. 2) Identify online resources for hands-on study of database and programming concepts.

RC854B Formal Opportunities and Resources for Imaging Informatics Training

Participants

Tessa S. Cook, MD, PhD, Philadelphia, PA (Presenter) Royalties, Osler Institute

For information about this presentation, contact:

tessa.cook@uphs.upenn.edu

LEARNING OBJECTIVES

1) Discuss currently available options for basic and advanced training in imaging informatics available to radiologists at all levels of training and career stage.

RC854C Imaging and Nonimaging Informatics Society Certifications: What is Out There and is it Valuable?

Participants

Christopher J. Roth, MD, Raleigh, NC (Presenter) Nothing to Disclose

LEARNING OBJECTIVES

1) Describe the value of obtaining certifications as an informatics leader. 2) Compare available opportunities for pursuing three common informatics certifications relevant to RSNA members and attendees: American Board of Imaging Informatics Certified Imaging Informatics Professional (ABII CIIP) certification, the American Board of Preventative Medicine Clinical Informatics (ABPM CI) ABMS board certification, and Healthcare Information and Management Systems Society Certified Professional in Health Information & Management System (HIMSS CPHIMS).



SPIS61

International Symposium in Musculoskeletal Radiology (In Conjunction with Asian Musculoskeletal Society (AMS), European Society of Musculoskeletal Radiology (ESSR), German Society of Musculoskeletal Radiology (DGMSR), International Skeletal Society (ISS), Korean Society of Musculoskeletal Radiology (KSMR) and Society of Skeletal Radiology (SSR))







AMA PRA Category 1 Credits ™: 3.00 ARRT Category A+ Credits: 3.50

FDA Discussions may include off-label uses.

Sub-Events

SPIS61A Top Tips in MSK Radiology: MSK Techniques

Friday, Nov. 30 9:30AM - 10:30AM Room: E450A

Participants

Laura W. Bancroft, MD, Orlando, FL (Moderator) Author with royalties, Wolters Kluwer nv; Speaker, World Class CME; Editor, Thieme Medical Publishers, Inc; Travel support, Thieme Medical Publishers, Inc; ;;

For information about this presentation, contact:

laura.bancroft.md@flhosp.org

LEARNING OBJECTIVES

1) Review the salient imaging features of some of the most commonly encountered musculoskeletal diagnoses.

SPIS61B **Top Tips to Reduce Artifacts in MSK MRI**

Friday, Nov. 30 9:30AM - 9:45AM Room: E450A

Participants

David A. Rubin, MD, Saint Louis, MO (Presenter) Nothing to Disclose

For information about this presentation, contact:

rubinda@wustl.edu

LEARNING OBJECTIVES

1) Recognize the source of common artifacts on MSK MIR images. 2) Anticipate artifacts before they occur. 3) Devise simple interventions to reduce or eliminate artifacts without sacrificing time or SNR. 4) Communicate with their technologists regarding MRI techniques.

SPIS61C Top Tips for Functional MRI

Friday, Nov. 30 9:45AM - 10:00AM Room: E450A

Participants

Won-Hee Jee, MD, Seoul, Korea, Republic Of (Presenter) Research Grant, Bayer AG;

For information about this presentation, contact:

whjee12@gmail.com

LEARNING OBJECTIVES

1) Describe the role of functional MRI in MSK imaging. 2) Apply functional MRI to MSK imaging in clinical practice. 3) List the top benefits of functional MRI in MSK imaging.

SPIS61D Top Tips for MR/CT Arthrography

Friday, Nov. 30 10:00AM - 10:15AM Room: E450A

Participants

Reto Sutter, MD, Zurich, Switzerland (Presenter) Nothing to Disclose

LEARNING OBJECTIVES

1) Know and assess indications of MR and CT arthrography for different joints. 2) Identify the classic approaches for joint injections. 3) Compare the benefits of MR and CT arthrograms versus non-contrast MR and CT imaging. 4) Recognize diagnostic pitfalls of MR and CT arthrography.

SPIS61E Discussion

Friday, Nov. 30 10:15AM - 10:30AM Room: E450A

SPIS61F Top Tips in MSK Radiology: MSK Pitfalls

Friday, Nov. 30 10:30AM - 11:30AM Room: E450A

Participants

Jung-Ah Choi, MD, Seoul, Korea, Republic Of (*Moderator*) Research Grant, Bracco Group; Andrew J. Grainger, MRCP, FRCR, Leeds, United Kingdom (*Moderator*) Consultant, Levicept Ltd; Director, The LivingCare Group;

For information about this presentation, contact:

andrewgrainger@nhs.net

LEARNING OBJECTIVES

1) Review the imaging characteristics of commonly encountered musculoskeletal entities with similar or overlapping features.

SPIS61G Top Pitfalls in Fracture Diagnosis

Friday, Nov. 30 10:30AM - 10:45AM Room: E450A

Participants

Mini N. Pathria, MD, San Diego, CA (Presenter) Nothing to Disclose

LEARNING OBJECTIVES

1) Develop a systematic approach to evaluating radiographs in the injured patient, focusing on soft tissue indicators of injury, articular alignment, and assessment of the bone cortex. 2) Detect patient characteristics (such as advanced age etc) and imaging limitations (poor positioning etc) that lead to interpretation errors. 3) Identify radiographic imaging findings that indicate underlying musculoskeletal injury and the need for further imaging.

Active Handout: Mini Nutan Pathria

http://abstract.rsna.org/uploads/2018/18003680/Pitfalls Fracture Diagnosis RSNA 2018 SPIS61I.pdf

SPIS61H Top Pitfalls in Groin Pain

Friday, Nov. 30 10:45AM - 11:00AM Room: E450A

Participants

Philip Robinson, MBChB, Leeds, United Kingdom (Presenter) Director, The LivingCare Group

For information about this presentation, contact:

philip.robinson10@nhs.net

LEARNING OBJECTIVES

1) Explain the biomechanics and functional anatomy of the anterior pelvis (groin) in relation to athletes. 2) Compare the theories and nomenclature for the pathogenesis of chronic groin pain in athletes. 3) Contrast the Imaging findings in symptomatic and asymptomatic athletes focusing on MR imaging. 4) Critique the interpretation of these findings and what research shows they relate to in terms of diagnosis, prognosis and decision making for treatment.

ABSTRACT

Groin pain in the athlete is a complex process with different surgical and radiological researchers focusing on different structures in the hope of identifying the primary cause for chronic groin pain. There is a resulting confusion over terminology with, for example, osteitis pubis, adductor pain and sportsman's hernia encompassing many different potential conditions for different clinicians. In reality there is a lot of crossover with many or all of the anatomical region thought to be involved by chronic shearing forces acting through the symphysis pubis and surrounding soft tissues contributing to the development of groin pain. Research is also now increasingly showing that previous imaging findings thought to be pathognomonic for groin pain are found in asymptomatic kicking athletes. This talk will review such potential pitfalls and offer a reporting strategy.

SPIS61I Top Pitfalls of Osteoporosis

Friday, Nov. 30 11:00AM - 11:15AM Room: E450A

Participants

James F. Griffith, MD, Shatin, Hong Kong (Presenter) Nothing to Disclose

SPIS61J Discussion

Friday, Nov. 30 11:15AM - 11:30AM Room: E450A

SPIS61K Top Tips in MSK Radiology: MSK Research Trends

Friday, Nov. 30 11:30AM - 12:30PM Room: E450A

Participants

James F. Griffith, MD, Shatin, Hong Kong (*Moderator*) Nothing to Disclose Lawrence M. White, MD, FRCPC, Toronto, ON (*Moderator*) Nothing to Disclose

For information about this presentation, contact:

LEARNING OBJECTIVES

1) Review some of the common musculoskeletal research trends with current clinical applications in patient care.

SPIS61L Top Trends in Tumor Imaging

Friday, Nov. 30 11:30AM - 11:45AM Room: E450A

Participants

Takatoshi Aoki, MD, PhD, Kitakyusyu, Japan (Presenter) Nothing to Disclose

LEARNING OBJECTIVES

- 1) Review the advanced techniques in musculoskeletal oncology. 2) Describe the radiomics for bone and soft tissue tumor imaging.
- 3) List the newly updated entities of bone and soft tissue tumors.

SPIS61M Top Trends in Marrow Imaging

Friday, Nov. 30 11:45AM - 12:00PM Room: E450A

Participants

Frederic E. Lecouvet, MD, Brussels, Belgium (Presenter) Nothing to Disclose

LEARNING OBJECTIVES

1) Identify achievements, indications and future developments of whole skeleton MRI in oncology. Know new treatment paradigms and expectations from imaging in oncology. 2) Understand the growing importance of multiparametric approaches and radiomics in oncologic marrow imaging. 3) Differentiate various spontaneaous epiphyseal lesions sharing bone marrow edema at MRI as common feature. 4) Understand the prognostic role of MRI. 5) Identify the upcoming technical developments and new indications of MRI and dual energy CT in bone marrow pathology.

SPIS61N Top Trends in Extremity Imaging

Friday, Nov. 30 12:00PM - 12:15PM Room: E450A

Participants

Christine B. Chung, MD, La Jolla, CA (Presenter) Nothing to Disclose

LEARNING OBJECTIVES

1) Identify current challenges and gaps in clinical practice for evaluation of musculoskeletal tumors, bone marrow and extremity pathology. 2) Apply novel imaging and post-processing techniques that improve diagnosis and characterization of musculoskeletal tumors, bone marrow and extremity pathology.

SPIS610 Discussion

Friday, Nov. 30 12:15PM - 12:30PM Room: E450A



SST01

Breast Imaging (Multimodality Breast Imaging)

Friday, Nov. 30 10:30AM - 12:00PM Room: E353B

BR

AMA PRA Category 1 Credits ™: 1.50 ARRT Category A+ Credit: 1.75

FDA

Discussions may include off-label uses.

Participants

Colleen H. Neal, MD, Ann Arbor, MI (*Moderator*) Nothing to Disclose Debra S. Copit, MD, Wynnewood, PA (*Moderator*) Research funded, Hologic, Inc

Sub-Events

SST01-01 Comparative the Average Glandular Dose between Digital Breast Tomosynthesis (DBT) and Full-Field Digital Mammography (FFDM): Correlation with Breast Thickness and Density

Friday, Nov. 30 10:30AM - 10:40AM Room: E353B

Participants

Chanjuan Wen, Guangzhou, China (*Presenter*) Nothing to Disclose Weimin Xu, Guangzhou, China (*Abstract Co-Author*) Nothing to Disclose Hui Zeng, Guangzhou, China (*Abstract Co-Author*) Nothing to Disclose Zilong He, Guangzhou, China (*Abstract Co-Author*) Nothing to Disclose Weiquo Chen, Guangzhou, China (*Abstract Co-Author*) Nothing to Disclose

For information about this presentation, contact:

182389433@qq.com

PURPOSE

To compare the average glandular dose (AGD) between single-view digital breast tomosynthesis (DBT) and single-view full-field digital mammography (FFDM), and to evaluate the correlation of AGD with breast thickness and density.

METHOD AND MATERIALS

A total of 318 female patients who underwent both DBT and FFDM (DBT and FFDM were performed in the same compression thickness in each breast) were included. 636 DBT images of unilateral breast mediolateral oblique (MLO) view and 636 FFDM images of unilateral breast mediolateral oblique (MLO) view were analyzed. Mammographic breast density was determined according to BI-RADS breast density grading, and breast thickness and AGD per exposure in MLO views retrieved from DICOM headers were recorded. Breast thickness were divided into the following four groups: <= 30cm, 31 \sim 45cm, 46 \sim 60cm and > 60cm. The statistical analyses used variance analysis and Pearson's correlation for parametric tests.

RESULTS

(1) The AGD of DBT had a weak negative correlation with breast density (correlation coefficient =-0.305, P<0.001), decreased as the breast density increased. The AGD of FFDM did not change significantly with breast density increased (correlation coefficient =-0.027, P=0.501). (2) Breast thickness was significantly associated with AGDs, and both AGDs of FFDM and DBT increased with increased breast thickness (correlation coefficient =0.771 and 0.935, respectively, all P<0.001). (3) When breast density was >75% and breast thickness was >60cm, the AGD of DBT was lower than that of FFDM, and the difference was statistical significant (P = 0.031).

CONCLUSION

The AGD of DBT increased with breast thickness increased and decreased with breast density. For thick and dense breast, the radiation dose of DBT was lower than that of FFDM.

CLINICAL RELEVANCE/APPLICATION

In this study, we evaluated the AGD of MLO FFDM and DBT according to breast density and thickness.

SST01-02 Accuracy of Molecular Breast Imaging in Patients with Suspicious Calcifications

Friday, Nov. 30 10:40AM - 10:50AM Room: E353B

Participants

Carrie B. Hruska, PhD, Rochester, MN (*Abstract Co-Author*) Institutional license agreement, CMR Naviscan Corporation Katie N. Hunt, MD, Rochester, MN (*Presenter*) Nothing to Disclose Matthew Johnson, Rochester, MN (*Abstract Co-Author*) Nothing to Disclose Amy Lynn Conners, MD, Rochester, MN (*Abstract Co-Author*) Nothing to Disclose Michael K. O'Connor, PhD, Rochester, MN (*Abstract Co-Author*) Royalties, Gamma Medica, Inc Deborah J. Rhodes, MD, Rochester, MN (*Abstract Co-Author*) Nothing to Disclose

Dietlind Wahner-Roedler, MD, Rochester, MN (Abstract Co-Author) Nothing to Disclose

PURPOSE

Molecular breast imaging (MBI), which shows uptake of Tc-99m sestamibi in metabolically-active tissue, has been proposed as a tool for determining whether biopsy of mammographically-detected lesions is necessary. Here, our goal was to evaluate the diagnostic accuracy of MBI in patients with suspicious calcifications on mammography.

METHOD AND MATERIALS

Women scheduled to undergo stereotactic biopsy of calcifications detected on 2D mammography were prospectively enrolled to undergo MBI prior to biopsy. MBI was performed with injection of Tc-99m sestamibi and a dedicated gamma camera. A breast radiologist interpreted MBI in conjunction with mammography.

RESULTS

In 71 women studied, 76 discrete areas of calcifications were identified for biopsy, of which pre-biopsy MBI was positive in 17/76 (22%). Of 76 calcification lesions, 24 (32%) were malignant, including 20 DCIS and 4 invasive ductal cancer; MBI was positive in 10/20 (50%) DCIS and 2/4 (50%) invasive cancers. In 21 cancers with calcification morphology of amorphous, coarse heterogeneous, or fine pleomorphic (BI-RADS 4B), MBI was positive in 12/21 (57%), while in three cancers with fine linear or fine linear branching calcifications (BI-RADS 4C), MBI was negative in all 3 (p=0.06). Calcification distribution was more varied for the MBI-positive cancers (0 regional, 7 grouped, 1 linear, 4 segmental) than for the MBI-negative cancers (1 regional, 10 grouped, 1 linear, 0 segmental) (p=0.14). The median pathologic size for MBI-positive cancers was 1.5 cm (range=0.5-3.2 cm) compared to 0.9 cm (range=0.1-2.0 cm) for MBI-negative cancers (p=0.09). Beyond calcification lesions, detection of non-mass focal areas of uptake on MBI led to additional biopsies of 6 sites, of which 2 were malignant (DCIS). The overall positive and negative predictive values of MBI were 61% (14/23) and 81% (48/59), respectively.

CONCLUSION

MBI has insufficient negative predictive value to be used for identifying calcifications in which biopsy could be avoided. However, MBI can reveal additional sites of mammographically-occult disease.

CLINICAL RELEVANCE/APPLICATION

Negative findings on MBI should not be used to avoid biopsy of suspicious calcifications on mammography.

SST01-03 Staging Early Breast Cancer with Simultaneous PET/ MRI: Impact on Management

Friday, Nov. 30 10:50AM - 11:00AM Room: E353B

Participants

Sangeeta Taneja, MD, New Delhi, India (*Presenter*) Nothing to Disclose Ramesh Sarin, MS, New Delhi, India (*Abstract Co-Author*) Nothing to Disclose Amarnath Jena, MD, New Delhi, India (*Abstract Co-Author*) Nothing to Disclose Aru Singh, PhD, New Delhi, India (*Abstract Co-Author*) Nothing to Disclose

For information about this presentation, contact:

s_tanejaa@yahoo.com

PURPOSE

Breast cancer is a biologically heterogenous disease with certain clinical subtypes having a greater propensity to develop metastasis even at an early stage. In its present state, NCCN recommends 18-F FDG PET CT in patients above clinical stage III disease. There have been reports on PET CT in altering clinical stage in early breast cancer. DCE (Dynamic Contrast-Enhanced) MRI has been shown to detect additional disease in the ipsilateral & contralateral breast. Simultaneous PET/MRI combines 18F-FDG PET & MRI of the whole body & DCE-MRI of the breast in a single examination. This retrospective study evaluates the impact of simultaneous 18F-FDG PET/MRI in pretreatment staging of early breast cancer (Stage I-IIIA).

METHOD AND MATERIALS

The study was approved by institutional ethics committee. 101 patients with histologically proven breast cancer (clinical stage I, IIA, IIB, IIIA) who underwent simultaneous PET/MRI (including DCE MRI breast) were included. Breast lesions, nodes & metastases were evaluated on PET, MRI & PET-MRI for lesion count & diagnostic confidence (DC).

RESULTS

101 index breast lesions were identified on MRI, PET/MRI (Mean DC 4.96) & 99 on PET (Mean DC >=4). MRI detected multifocality in 15 (14.8%), multicentricity in 10 (9.90%) & contralateral unsuspected cancer in 2 patients. PET detected axillary nodal metastases in 12/18 (DC>=4), MRI in 15/18 (DC>=4) and PET/MRI in 15/18 patients. Distant metastases were found in 18 /101 (18 %) on PET (Mean DC score 4.1), MRI (Mean DC score=3.7) & PET/MRI (Mean DC score =4.7) with bone (n =11), lymph nodes (mediastinal; n=2), liver (n=4), brain (n=1) & lung (n=5). The mean metastatic lesion size on MRI was 1.52 ± 0.25 cm (Range: 0.5-5.7cm). PET MRI changed the overall stage in 66 patients (65%, upstaging: 62, downstaging:4) & overall change in management in 29 % of early stage breast cancer patients including 18 patients who were upstaged to stage IV.

CONCLUSION

Simultaneous18F-FDG PET/MRI has the potential to impact the initial staging in early breast cancer for an overall improved patient management.

CLINICAL RELEVANCE/APPLICATION

Simultaneous PET/MRI has the potential to alter the stage and hence the clinical management in patients with early breast cancer thus reducing the morbidity and cost due to inappropriate therapies.

SST01-04 The Gambler's Fallacy in Screening Mammography

Participants

Andrew L. Callen, MD, San Francisco, CA (*Presenter*) Nothing to Disclose Omar Mesina, San Francisco, CA (*Abstract Co-Author*) Nothing to Disclose Sivan G. Marcus, BS, San Francisco, CA (*Abstract Co-Author*) Nothing to Disclose Iryna Lobach, San Francisco, CA (*Abstract Co-Author*) Nothing to Disclose Bonnie N. Joe, MD, PhD, San Francisco, CA (*Abstract Co-Author*) Nothing to Disclose Edward A. Sickles, MD, San Francisco, CA (*Abstract Co-Author*) Nothing to Disclose Heather I. Greenwood, MD, San Francisco, CA (*Abstract Co-Author*) Nothing to Disclose

For information about this presentation, contact:

andrew.callen@ucsf.edu

PURPOSE

It has been documented in multiple settings that the sequence of decisions already made affects future decision-making. One component of this phenomenon is known as the gambler's fallacy: the tendency to underestimate the likelihood of 'streaks' (successive identical decisions) occurring by chance. The purpose of this study was to determine if the gambler's fallacy affects radiologists interpreting screening mammography.

METHOD AND MATERIALS

This was a retrospective, HIPPA compliant IRB approved study. Patients who underwent routine screening mammography in 2014 at our institution were included, with 8,543 total exams, which was sufficient to detect a 1% change in recall rate based on an 80% power calculation with a two-sided 0.05 significance level, for our recall rate of 7%. Data were collected from log books containing the BI-RADS assessments of routine screening mammograms, the order in which the examinations were interpreted, and the number of preceding BI-RADS 0 and BI-RADS 1 or 2 assessments for each exam. If recalled (BI-RADS-0), subsequent diagnostic exam BI-RADS assessment also was recorded. Analysis was performed using Fishers exact test to evaluate whether an increasing number of preceding decisions to not recall (BI-RADS-1 or 2) resulted in an increased number of recalls that did not lead to a cancer diagnosis. False positive was defined as a BI-RADS 0 assessment at screening, followed by a BI-RADS 1, 2 or 3 at diagnostic breast imaging. A true positive was defined as a BI-RADS 0 assessment at screening, followed by a BI-RADS 4 or 5 assessment at diagnostic breast imaging.

RESULTS

Data on 8,543 routine screening exams was collected for the year 2014. An average of 20.9 exams were batch read in each session. 700 exams (8%) were assessed as BI-RADS 0. Of those, 231 (33%) were assigned either BIRADS-4 or 5 at the time of diagnostic imaging. True and false positives were compared, stratified by the number of preceding BI-RADS 1 or 2 assessments in that batch-read session. Exams with a higher number of preceding negative assessments did not have a higher false positive rate.

CONCLUSION

At our academic institution, we did not observe a statistically significant effect of the gambler's fallacy in one year's worth of screening mammography.

CLINICAL RELEVANCE/APPLICATION

We did not detect an effect of the gambler's fallacy in one year's worth of screening mammography at an academic institution.

SST01-05 Outcomes of Ductal Carcinoma in Situ According to Detection Modality: A Multicenter Study Comparing Recurrences Between Mammography and Breast US

Friday, Nov. 30 11:10AM - 11:20AM Room: E353B

Participants

Jung Hyun Yoon, MD, Seoul, Korea, Republic Of (*Presenter*) Nothing to Disclose Kyunghwa Han, PhD, Seoul, Korea, Republic Of (*Abstract Co-Author*) Nothing to Disclose Jieun Koh, MD, Seongnam, Korea, Republic Of (*Abstract Co-Author*) Nothing to Disclose Ga Ram Kim, MD, Seoul, Korea, Republic Of (*Abstract Co-Author*) Nothing to Disclose Hye Jung Kim, Daegu, Korea, Republic Of (*Abstract Co-Author*) Nothing to Disclose Young Mi Park, MD, PhD, Busan, Korea, Republic Of (*Abstract Co-Author*) Nothing to Disclose Ji Hyun Youk, MD, Seoul, Korea, Republic Of (*Abstract Co-Author*) Nothing to Disclose Jin Chung, MD, Seoul, Korea, Republic Of (*Abstract Co-Author*) Nothing to Disclose In Hye Chae, Seoul, Korea, Republic Of (*Abstract Co-Author*) Nothing to Disclose Eun Jung Choi, MD, PhD, Jeonju, Korea, Republic Of (*Abstract Co-Author*) Nothing to Disclose Hee Jung Moon, MD, Seoul, Korea, Republic Of (*Abstract Co-Author*) Nothing to Disclose

For information about this presentation, contact:

lvjenny@yuhs.ac

PURPOSE

To determine whether if disease recurrence and intrinsic characteristics of ductal carcinoma in situ (DCIS) is associated to the imaging method of detection in asymptomatic women who are diagnosed with DCIS.

METHOD AND MATERIALS

This retrospective, multicenter study was conducted at 8 institutions including 844 women who were treated for asymptomatic, pure DCIS who had preoperative mammography and breast ultrasonography (US) available for review. Mean follow up interval after treatment of the 844 women was 91.2 months (standard deviation: 533.3, range: 6.4-180.9 months). Medical records and breast images were reviewed by 8 breast-imaging dedicated radiologists for clinicopathologic information and image analysis. Kaplan-Meier analysis and univariable/multivariable Cox proportion hazard model was used to analyze the recurrence-free survival rates and factors associated with recurrence after DCIS treatment.

RESULTS

Of the 844 women who were treated for DCIS, 25 (3.0%) had developed recurrences. Patients with US-detected DCIS had significantly lower 5- and 10-year recurrence-free survival rates compared to patients with mammography-detected ones (P=0.011). US-detected DCIS had significantly lower 5- and 10-year recurrence-free survival rates compared to mammography-detected ones in patients <50years or with mammographically-dense breasts (P=0.002, and 0.002, respectively). Multivariable analysis showed that US for detection modality (HR: 4.451, 95% CI: 1.530, 12.950, P=0.006) and HER2 positivity (HR: 4.036, 95% CI: 1.438, 11.330, P=0.008) showed significant association to recurrences.

CONCLUSION

US for detection modality and HER2 positivity were factors significantly associated to recurrences in patients treated for asymptomatic DCIS.

CLINICAL RELEVANCE/APPLICATION

Supplementary screening US may enable detection of clinically important DCIS, especially in younger women or mammographically-dense breasts in which mammography has suboptimal performances in detection of DCIS or small invasive cancers.

SST01-06 Do Triple Negative Breast Cancers Have Characteristic Imaging Features According to Androgen Receptor and Vimentin Status?

Friday, Nov. 30 11:20AM - 11:30AM Room: E353B

Participants

Rosalind P. Candelaria, MD, Houston, TX (Presenter) Nothing to Disclose

Beatriz E. Adrada, MD, Houston, TX (*Abstract Co-Author*) Nothing to Disclose Lumarie Santiago, MD, Houston, TX (*Abstract Co-Author*) Nothing to Disclose

Deanna L. Lane, MD, Houston, TX (Abstract Co-Author) Nothing to Disclose

Wei Wei, Houston, TX (Abstract Co-Author) Nothing to Disclose

Wei T. Yang, MD, Houston, TX (Abstract Co-Author) Consultant, General Electric Company; Medical Advisory Board, Seno Medical Instruments, Inc

Monica L. Huang, MD, Houston, TX (Abstract Co-Author) Nothing to Disclose

Elsa M. Arribas, MD, Houston, TX (Abstract Co-Author) Nothing to Disclose

Gaiane M. Rauch, MD, PhD, Houston, TX (Abstract Co-Author) Nothing to Disclose

Alastair Thompson, Houston, TX (Abstract Co-Author) Nothing to Disclose

Stacy Moulder, MD, Houston, TX (Abstract Co-Author) Research funded, AstraZeneca PLC; Research funded, F. Hoffmann-La Roche Ltd; Research funded, Oncothyreon; Research funded, Novartis AG; Research funded, Merck KGaA

For information about this presentation, contact:

rcandelaria@mdanderson.org

PURPOSE

Lehmann et al (Journal of Clinical Investigation, 2011) previously identified six molecular subtypes of triple negative breast cancer (TNBC) through analysis of gene expression profiles; the luminal androgen receptor (LAR) subtype has been shown to have a higher percentage of regional spread to lymph nodes and the mesenchymal (M) subtype, a lower percentage. The purpose of this study is to determine if TNBCs have characteristic imaging features based on androgen receptor (AR) and vimentin (VM) status, which are surrogate immunohistochemical markers for the LAR and M subtypes of TNBC, respectively.

METHOD AND MATERIALS

This study is part of a clinical trial of stage I-III TNBC patients, which is being conducted at a single quaternary care center. A total of 144 patients, who were randomized to the intervention arm of being informed of the results of their molecular characterization including androgen receptor and vimentin status prior to receiving neoadjuvant chemotherapy, were included in this interim imaging analysis. Androgen-receptor-positive tumors (AR+) were defined as having >=15% staining. Vimentin-positive (VM+) tumors were defined as having >=50% staining. Two experienced, fellowship-trained breast radiologists used BIRADS (Breast Imaging Reporting and Data System) lexicon to review and reach consensus on all imaging studies (i.e., mammogram, ultrasound, and breast magnetic resonance imaging) while blinded to the immunohistochemical results. Fisher's exact test was used to assess the association of AR or VM status with imaging features. P values less than 0.05 was considered statistically significant.

RESULTS

Androgen-receptor-positive TNBC was significantly associated with scattered and heterogeneous breast composition on mammography (p=0.04), presenting as a mass with calcifications on mammography (p=0.04), having an irregular shape on ultrasound (p=0.005), and having an irregular margin on MRI (p=0.04). However, vimentin expression in TNBC was not significantly associated with any specific imaging features.

CONCLUSION

TNBCs have characteristic imaging features based on androgen receptor status but not based on vimentin status.

CLINICAL RELEVANCE/APPLICATION

Multimodality breast imaging may help identify LAR TNBC, which has been shown to be a subtype with a higher rate of regional nodal disease and with decreased response to neoadjuvant chemotherapy.

Usefulness of Surveillance MR for Early and Late Recurrent Breast Cancer in Women after Breast-Conservation Therapy

Friday, Nov. 30 11:30AM - 11:40AM Room: E353B

Participants

Jeong Min Lee, Seoul, Korea, Republic Of (*Presenter*) Nothing to Disclose Bong Joo Kang, Seoul, Korea, Republic Of (*Abstract Co-Author*) Nothing to Disclose

Sung Hun Kim, Su Won, Korea, Republic Of (Abstract Co-Author) Nothing to Disclose

For information about this presentation, contact:

jmlee328@gmail.com

PURPOSE

To investigate the diagnostic performance of mammography, ultrasonography, and breast magnetic resonance imaging (MRI) for early and late recurrences in patients who underwent breast-conservation therapy (BCT) for breast cancer.

METHOD AND MATERIALS

This retrospective study was approved by our institutional review board. Between January 2014 and February 2018, 1312 women with 1951 surveillance breast MR examinations after BCT were studied. We assessed the cancer detection rate of each surveillance MR, mammography and ultrasound.

RESULTS

Of 1951 cases of surveillance postoperative MRI, 59 cases were confirmed as cancer recurrence through biopsy. Nineteen cases of recurrences within 12 months post-BCT were defined as early recurrences while other 40 cases of recurring after 13 months post-BCT were defined as late recurrences. There were no statistically significant differences in patients' demographics between two groups with p > 0.05; age at cancer diagnosis, age at recurrence, symptoms, laterality of recurred cancer and intense surveillance. Among 19 patients with early recurrence, 7 cases were detected on mammography (36.8%), 10 on ultrasound (52.6%), and 17 on MRI (89.5%). Of 40 patients with late recurrence, 24 were detected on mammography (60%), 29 on ultrasound (72.5%) and 39 on MRI (97.5%). In both groups, MRI showed significantly higher cancer detection rate than mammography or ultrasound (p < 0.01).

CONCLUSION

In breast cancer patients with BCT, regardless of early or late, postoperative MR surveillance showed a significantly higher detection rate for cancer recurrence than mammography or ultrasound.

CLINICAL RELEVANCE/APPLICATION

Postoperative surveillance MR is useful tool for screening early or late cancer recurrence in breast cancer patients with breast conserving therapy.

SST01-08 The Role of Digital Breast Tomosynthesis (DBT) versrus Automated Breast Ultrasound (ABUS) in the Detection and Characterization of the Different Breast Lesions

Friday, Nov. 30 11:40AM - 11:50AM Room: E353B

Participants

Maha H. Helal IV, MD, Cairo, Egypt (*Presenter*) Nothing to Disclose Sahar Mansour, MD, Cairo, Egypt (*Abstract Co-Author*) Nothing to Disclose Lamia Bassam, Cairo, Egypt (*Abstract Co-Author*) Nothing to Disclose Reham Hussein, Cairo, Egypt (*Abstract Co-Author*) Nothing to Disclose Emad Elgemeie, Cairo, Egypt (*Abstract Co-Author*) Nothing to Disclose

For information about this presentation, contact:

dr.mahahelal@yahoo.com

PURPOSE

DBT and ABUS are advanced applications of digital mammography and breast ultrasound respectively. We aimed to evaluate the role of DBT versus ABUS in the detection and characterization of breast lesions

METHOD AND MATERIALS

Institutional review board approval was obtained for this prospective study that included 80 patients with 87 breast lesions. Methods of evaluation were digital breast tomosynthesis and automated breast ultrasound. For mammogram acquisition the system acquires a traditional digital mammogram and a tomosynthesis scanning in the same compression in the MLO and CC views. 3D ABUS were done for anteroposterior; lateral and medial acquisitions. Included breast lesions were analyzed regarding size, shape, margin, extension, calcifications and multiplicity. Operative data was the gold standard reference

RESULTS

ABUS showed more accurate measurements of the size of the breast lesions as DBT overestimated 18.8% of masses, on the other hand ABUS over estimated 25% of masses. No size under estimation by both modalities. ABUS was superior to DBT in estimation of the shape of the lesions 87% versus 69.6% for DBT, but both displayed similar values in the evaluation of the margins (65.2%). Tomosynthesis was far better in the detection of calcification in 40 lesions; while automated ultrasound was able to detect calcifications in only 11 lesions of them. Multiplicity was better demonstrated by ABUS that showed an accuracy of 100% compared to 80% by DBT. We found out that the sensitivity of tomosynthesis in detection and characterization of breast masses was 100 %, the specificity was 81.25%, the positive predictive value was 87.5% and the negative predictive value was 100%. On the other hand the sensitivity of automated ultrasound was 100%, the specificity was 75%, the positive predictive value was 84% and the negative predictive value was 100%.

CONCLUSION

DBT and ABUS, both showed near estimation in the detection and characterization of breast lesions. DBT is the modality for calcifications and ABUS is more accurate in the detection of multiplicity.

CLINICAL RELEVANCE/APPLICATION

DBT is considered as an adjunct to digital mammogram to increase the conspicuity of the different breast lesions. ABUS is a revolution in the ultrasound scanning of the breast that can be used as a non-invasive, fast and easy tool of breast imaging in early detection (i.e. screening) and differentiation of breast lesions.

SST01-09 First Description of Molecular Imaging Heterogeneity Profiles for Breast Tumors and Its Clinical Utility

Friday, Nov. 30 11:50AM - 12:00PM Room: E353B

Participants

MIchel Herranz, Santiago de Compostela, Spain (*Presenter*) Nothing to Disclose
Lucia Grana Lopez, MD, Lugo, Spain (*Abstract Co-Author*) Nothing to Disclose
Ines Dominguez, Santiago de Compostela, Spain (*Abstract Co-Author*) Nothing to Disclose
Sonia Argibay, MD, PhD, Santiago de Compostela, Spain (*Abstract Co-Author*) Nothing to Disclose
Manuel Vazquez-Caruncho, MD, Lugo, Spain (*Abstract Co-Author*) Nothing to Disclose
Roberto Garcia Figueiras, MD, PhD, Santiago de Compostela, Spain (*Abstract Co-Author*) Nothing to Disclose
Alvaro Ruibal, MD, PhD, Santiago de Compostela, Spain (*Abstract Co-Author*) Nothing to Disclose

For information about this presentation, contact:

michel.herranz.carnero@sergas.es

PURPOSE

The concept of tumor heterogeneity, also called in Radiology as Tumor Texture, is based on the different areas of tumor uptake, which correspond to different levels of expression, cellularity, hypoxia or other parameters interested in being measured. We want to know if the description of the tumor heterogeneity uses in Radiology has its relation with PET parameters and if any biological characteristics of the breast tumors have a structure-function correlation.

METHOD AND MATERIALS

We have analyzed 1000 consecutive patients with breast cancer in a dedicated breast PET (dbPET). Different parameters have been defined that allow us to find a pattern of Texture and Heterogeneity (TeHe), for this, and following the rules of the radiological descriptions we defined a series of structural templates that cover practically all tumors, a mathematical formula has been defined for this correlation, and a assisted software for tumor shape description has been used to perform 3D categories.

RESULTS

7 different patterns divided into 5 groups for TeHe are described, and classified as: 1: Homogeneous-diffuse, 2: Lobular, 3: Annular and Spindle, 4: Eccentric and Focused; and 5: Speckled. A numerical value has been assigned between 1 and 5 for this classification with 1 being the most homogeneous and 5 being the most heterogeneous. This value is achieved through a mathematical relationship: medSUV/maxSUV: values close to 1 denote a high homogeneity and those close to 0 indicate a high heterogeneity. Process is complicated when tumor geometry becomes part of this heterogeneity. In those cases, some geometric patterns may explain similar values. We have analyzed the clinical utility of this classification and we have found two major uses: i) in the description of the efficiency of neoadjuvant therapy, where changes in TeHe pattern define responders of non-responders and ii) we have found, for the FIRST TIME, a correlation between TeHe patterns and the molecular subtype, crucial fact in the future of imaging based breast cancer diagnosis.

CONCLUSION

Studies of tumor heterogeneity based on metabolism show us different patterns that correlate with molecular subtypes and predict response to treatments.

CLINICAL RELEVANCE/APPLICATION

Tumor Texture and Heterogeneity are becoming, like in conventional radiology, in a new tool for prediction of response to the treatment and in molecular subtype characterization.



SST02

Chest (Thoracic Malignancy)

Friday, Nov. 30 10:30AM - 12:00PM Room: E350

CH |

СТ |

MR

NM

AMA PRA Category 1 Credits ™: 1.50 ARRT Category A+ Credit: 1.75

FDA

Discussions may include off-label uses.

Participants

Girish S. Shroff, MD, Houston, TX (Moderator) Nothing to Disclose Andrew J. Plodkowski, MD, Brookside, NJ (Moderator) Nothing to Disclose

Sub-Events

SST02-01 Radiologist Variability in the Determination of the T-Size Descriptor Cutpoints in the Eighth Edition of the TNM Classification of Lung Cancer (TNM8)

Friday, Nov. 30 10:30AM - 10:40AM Room: E350

Participants

Julia Hine, MBBS, London, United Kingdom (Presenter) Nothing to Disclose Anouchka Goldman, MBBS, London, United Kingdom (Abstract Co-Author) Nothing to Disclose Jie-Ying Kowa, MBBS, London, United Kingdom (Abstract Co-Author) Nothing to Disclose Sarah L. Sheard, MBBS, FRCR, London, United Kingdom (Abstract Co-Author) Nothing to Disclose Konstantinos Stefanidis, MD, PhD, London, United Kingdom (Abstract Co-Author) Nothing to Disclose Sisa Grubnic, MD, London, United Kingdom (Abstract Co-Author) Nothing to Disclose Joanna Moser, MBChB, FRCR, London, United Kingdom (Abstract Co-Author) Nothing to Disclose Ioannis Vlahos, MRCP, FRCR, London, United Kingdom (Abstract Co-Author) Research Consultant, Siemens AG Research Consultant, General Electric Company

PURPOSE

Based on pathological size TNM8 introduced additional T-descriptor size cutpoints at 1cm intervals impacting stage groups. Our aim was to determine whether radiological staging by different radiologists consistently classifies lesion size within this more detailed staging

METHOD AND MATERIALS

4 thoracic radiologists (4-17yr experience) staged 180 consecutive new lung cancers, recording multiple parameters blinded to the study aim. Readers were provided with axial 2.5mm, 1mm, coronal and sagittal 3mm images and asked to stage the primary as per clinical practice. Readers recorded the solid component for subsolid lesions. 2 observers covertly recorded the image series used for review and measurement. Inter-rater consistency of primary lesion size and T-size determination was evaluated. The impact of reader recorded lesion characteristics on consistency was assessed.

RESULTS

Readers recorded lesions as solid in 78-87% of cases, part-solid in 11-17% and pure ground glass in 1-2% with a moderate mean inter-rater kappa (0.71). 176 lesions were considered measurable by at least 3 readers (median 38mm, 7-113mm), 95% evaluated by all 4 readers. Readers varied widely in measurement plane (2.5mm:20-90%, 1mm:2-54%, coronal:7-24%, sagittal:0-26%) and mean number of planes reviewed (1.1-3.0). For lesions the mean range of measurement about the consensus median size was 31% (3-175%). Increased reader range of measurement about the median size was associated with part solid (mean 43% v 29% solid, p<0.01 Mann Whitney U) and cavitary lesions (32 v 19%, p<0.05). Atelectasis and spiculation were not significant. Using median size to determine T-descriptors, only 42% of cases had 100% reader concordance (74% concordance for at least 67% of readers). Complete concordance was significantly lower for groups T1c-T3 (20-35%) and higher in the remaining groups (42-67%). Mean inter-rater T assignment kappa was 0.57 (moderate), but higher with weighted kappa (0.80, good).

CONCLUSION

There is considerable variation in tumor size determination by thoracic radiologists, influenced by lesion perceived morphology, and measurement choices that result in lower inter-reader concordance for the narrower range TNM8 T-size criteria.

CLINICAL RELEVANCE/APPLICATION

Pathological size data informed increased numbers of cutpoints in TNM8 to better predict survival but increases radiological stage uncertainty and inter-reader variance in clinical practice.

Honored Educators

Presenters or authors on this event have been recognized as RSNA Honored Educators for participating in multiple qualifying educational activities. Honored Educators are invested in furthering the profession of radiology by delivering high-quality educational content in their field of study. Learn how you can become an honored educator by visiting the website at: https://www.rsna.org/Honored-Educator-Award/ Ioannis Vlahos, MRCP,FRCR - 2015 Honored Educator

SST02-02 A Novel Algorithm to Approach Multiple Lung Cancers with Multiple Pulmonary Sites of Involvement: Differentiation between Multiple Primary Lung Cancers and Intrapulmonary Metastasis

Friday, Nov. 30 10:40AM - 10:50AM Room: E350

Participants

Young Joo Suh, MD, Seoul, Korea, Republic Of (*Presenter*) Nothing to Disclose Hyun-Ju Lee, MD, PhD, Seoul, Korea, Republic Of (*Abstract Co-Author*) Nothing to Disclose Jiseon Oh, MD, Seoul, Korea, Republic Of (*Abstract Co-Author*) Nothing to Disclose Pamela K. Sung, MD, Seoul, Korea, Republic Of (*Abstract Co-Author*) Nothing to Disclose Heera Yoen, MD, Seoul, Korea, Republic Of (*Abstract Co-Author*) Nothing to Disclose Sewoo Kim, MD, Seoul, Korea, Republic Of (*Abstract Co-Author*) Nothing to Disclose Seungchul Han, MD, Seoul, Korea, Republic Of (*Abstract Co-Author*) Nothing to Disclose Sungeun Park, MD, Seoul, Korea, Republic Of (*Abstract Co-Author*) Nothing to Disclose Jung Hee Hong, Daegu, Korea, Republic Of (*Abstract Co-Author*) Nothing to Disclose Heekyung Kim, Seoul, Korea, Republic Of (*Abstract Co-Author*) Nothing to Disclose Jiyeon Lim, Seoul, Korea, Republic Of (*Abstract Co-Author*) Nothing to Disclose Soon Ho Yoon, MD, Seoul, Korea, Republic Of (*Abstract Co-Author*) Nothing to Disclose Young Tae Kim, MD, PhD, Seoul, Korea, Republic Of (*Abstract Co-Author*) Nothing to Disclose Yoon Kyung Jeon, Seoul, Korea, Republic Of (*Abstract Co-Author*) Nothing to Disclose

For information about this presentation, contact:

rongzusuh@gmail.com

PURPOSE

To develop an differentiation algorithm in patents with multiple lung cancers, using clinical and imaging variables.

METHOD AND MATERIALS

We retrospectively included 112 lesions in 55 patients (57 pairs) with multiple lung cancers who received at least two separate surgeries between January 2007 and December 2016. Each pair of multiple lung cancers was classified into two categories with histopathologic findings as the standard reference: multiple primary lung cancer (MPLC) and intrapulmonary metastasis (IPM). We established five serial questions for differentiation; 'Is either nodule pure ground-glass nodule on CT?' or 'Are both of the two lesions ground-glass dominant nodules?' (Step1), 'Does either nodule harbor air-bronchogram or irregular shape?' (Step2), 'Do both of the two nodules have the same or different grade of maximal standardized uptake values (SUVmax) on PET/CT?' (Step3), and 'Does either case harbor mediastinal LN or distant metastasis on preoperative work-up?' (Step4). The SUVmax values were classified into grade 1(<2.5), grade 2(2.5-5.0), and grade 3(>5.0). At each decision step, each pair was classified as MPLC or IPM. The sensitivity, specificity, and accuracy of the differentiation algorithm were analyzed.

RESULTS

Among 57 pairs, 36 pairs (63.2%) were classified as MPLCs, and the other 21 pairs (26.8%) as IPMs of standard reference. In step1, 14 pairs were classified as MPLC. In step2, 10 pairs with absence of air-bronchogram or irregular contour on both lesions were classified as IPM. In step3, 8 pairs showing two grades of separate SUV were classified as MPLC. In step4, 3 pairs with mediastinal LN or distant organ metastasis were classified as IPMs and 22 pairs were considered MPLC. The sensitivity for MPLC (specificity for IPM), specificity for MPLC (sensitivity for IPM), and accuracy were 94.4%, 52.4%, and 78.9%, respectively. Accuracy for each step was 100% for step 1, 90% for step 2, 62.5% for step 3 and 68% for step 4, respectively.

CONCLUSION

Approach algorithm using comprehensive information of clinical and imaging variables can allow differentiation between MPLCs and IPMs in a substantial number of cases of multiple lung cancers with multiple pulmonary sites of involvement.

CLINICAL RELEVANCE/APPLICATION

Our approach algorithm using clinical and imaging information can help differentiation between MPLCs and IPMs in multiple lung cancers.

SST02-03 Risk of Occult Mediastinal Disease in Non-Small Cell Lung Cancer Patients with Radiographic NO Disease according to Tumor Location

Friday, Nov. 30 10:50AM - 11:00AM Room: E350

Participants

Dongyoung Jeong, MD, Seoul, Korea, Republic Of (*Presenter*) Nothing to Disclose Sun Hye Shin, Seoul, Korea, Republic Of (*Abstract Co-Author*) Nothing to Disclose Yeonu Choi, Seoul, Korea, Republic Of (*Abstract Co-Author*) Nothing to Disclose Jiyeong Lee, MD, Seoul, Korea, Republic Of (*Abstract Co-Author*) Nothing to Disclose

For information about this presentation, contact:

dongyoung.jeong@samsung.com

PURPOSE

Lung cancer guidelines recommend invasive mediastinal staging for patients with centrally located tumors without evidence of nodal disease on imaging studies. However, there is no uniform definition of central tumor. This study aims to evaluate the risk of occult mediastinal disease in non-small cell lung cancer (NSCLC) patients with radiographic NO disease according using several different definitions for central tumor.

METHOD AND MATERIALS

Of the patients who underwent curative-intent surgical resection or endobronchial ultrasound-guided transbronchial needle

aspiration between January 2014 and December 2015, 1,337 consecutive patients with radiographic N0 disease were identified. Based on the most proximal part of the tumor in computed tomography (CT) image, tumors were categorized using five different definitions; contact with hilar structure, located within inner one-third or two-thirds of hemithorax according to concentric or sagittal lines.

RESULTS

About 7% (93/1337) of patients had occult N2 disease and they had significantly larger tumor size and more solid tumors in CT image. All but inner two-thirds of hemithorax by sagittal line were associated with N2 disease. However, only inner one-third of hemithorax by concentric line remained significant after adjustment for tumor size and density in CT (adjusted odds ratio [95% confidence interval], 2.29 [1.28-4.11]).

CONCLUSION

We suggest using inner one-third of hemithorax by concentric line as indication of EBUS-TBNA in NSCLC with radiographic N0 disease.

CLINICAL RELEVANCE/APPLICATION

Using inner one-third of hemithorax by concentric line as indication of EBUS-TBNA in NSCLC with radiographic N0 disease.

SST02-04 Comparison of Computed Tomography and Clinical Findings Between Immune-Related Pneumonitis and Pneumonia by Pathogen in Patients Treated with Anti-Programmed Death-1 (PD-1)/Programmed Death Ligand 1 (PD-L1) Therapy

Friday, Nov. 30 11:00AM - 11:10AM Room: E350

Participants

Cherry Kim, MD, Ansan, Korea, Republic Of (*Presenter*) Nothing to Disclose Mi Young Kim, MD, PhD, Seoul, Korea, Republic Of (*Abstract Co-Author*) Nothing to Disclose Chang-Min Choi, Seoul, Korea, Republic Of (*Abstract Co-Author*) Nothing to Disclose Yeon Joo Kim, Seoul, Korea, Republic Of (*Abstract Co-Author*) Nothing to Disclose

PURPOSE

Immune-related pneumonitis (IRP) is an uncommon but potentially fatal toxicity of anti-programmed death-1 (PD-1)/programmed death ligand 1 (PD-L1) therapy for intrathoracic malignancy including non-small cell lung cancer. The purpose of study was to compare CT and clinical findings between IRP and pneumonia by pathogen.

METHOD AND MATERIALS

A total of 154 patients who received anti-PD-1/PD-L1 therapy were identified from 2014 to 2017. Among these patients, IRP developed in 9 (5.8%) and pneumonia in 30 (19.5%), which were confirmed through multidisciplinary approach. CT findings (reticulation, consolidation, ground glass opacity [GGO], interlobular septal thickening, micro- [<10mm] and macro-nodules [>=10mm], bronchial wall thickening, bronchiectasis, pleural effusion, and lesion distribution/bilaterality) and clinical features (symptom, smoking history, cancer staging, laboratory findings, underlying disease, prior radiotherapy history) were compared between IRP and pneumonia. Grade and outcome of IRP were also investigated.

RESULTS

In chest CT, diffuse reticulation (44.4% vs.0%, P=0.02), patchy/diffuse GGO (100% vs. 50%, P=0.01), and interlobular septal thickening (66.7% vs. 10%, P=0.002) were significantly more frequent in IRP than in pneumonia, whereas macronodule (0 vs. 36.7%, P=0.033) was significantly more common in pneumonia than IRP. IRP significantly showed peripheral location (77.8% vs. 16.7%, P=0.001) and bilateral distribution (44.4% vs. 3.3%, P=0.007). However, there were no significant differences in clinical findings between IRP and pneumonia. Among the IRP patients, 66.7% (6 of 9) of cases were grade 3, and 66.7% improved with drug holding/steroid therapy. The median onset duration of IRP from the first prescription was 126 days (range, 40-669), the median time for improvement was 43 days (range, 21-45), and the median time to death due to IRP was 18 days (range, 11-55).

CONCLUSION

Several CT findings including diffuse reticulation, patchy/diffuse GGO, and interlobular septal thickening with bilateral and peripheral distribution were more frequent in IRP than pneumonia by pathogen. Clinical findings were overlapped.

CLINICAL RELEVANCE/APPLICATION

It is crucial to suspect IRP as opposed to pneumonia in routine practice. Radiologists should be familiar with those findings of IRP to avoid delayed diagnosis and serious drug related complication.

SST02-06 Growth Rates of Thymic Epithelial Tumor and Thymic Cyst: Is Differentiation Feasible?

Friday, Nov. 30 11:20AM - 11:30AM Room: E350

Participants

Hyungjin Kim, MD, Seoul, Korea, Republic Of (*Presenter*) Nothing to Disclose
Soon Ho Yoon, MD, Seoul, Korea, Republic Of (*Abstract Co-Author*) Nothing to Disclose
Jihang Kim, MD, Seongnam, Korea, Republic Of (*Abstract Co-Author*) Nothing to Disclose
Kyung Won Lee, MD, PhD, Seongnam, Korea, Republic Of (*Abstract Co-Author*) Nothing to Disclose
Ye Ra Choi, MD, Seoul, Korea, Republic Of (*Abstract Co-Author*) Nothing to Disclose
Hyoun Cho, MD, Seoul, Korea, Republic Of (*Abstract Co-Author*) Nothing to Disclose
Jin Mo Goo, MD, PhD, Seoul, Korea, Republic Of (*Abstract Co-Author*) Research Grant, Samsung Electronics Co, Ltd; Research
Grant, Lunit Inc

For information about this presentation, contact:

khj.snuh@gmail.com

To investigate the growth rate of thymic epithelial tumors (TETs) and thymic cysts to determine whether they can be differentiated, and to identify clinico-radiological predictors of interval growth and their differential implications.

METHOD AND MATERIALS

This retrospective study included 122 patients (male:female=64:58; mean age, 57.2 years) with pathologically proven thymic cysts (n=56) or TETs (n=66) who underwent 2 serial chest CT scans at least 8 weeks apart. Average diameters were measured, and volume-doubling times (VDTs) were calculated. Attenuation was also measured and clinical characteristics were recorded. VDTs were compared between the thymic cysts and TETs using the log-rank test. Predictors of growth were analyzed using the log-rank test and Cox regression analysis.

RESULTS

The frequency of growth did not significantly differ between TETs and thymic cysts (P=0.279). The VDT of the thymic cysts (median, 324 days) was not significantly different from that of the TETs (median, 475 days; P=0.808). Water attenuation (<=20 Hounsfield Unit) predicted growth in thymic cysts (P=0.016; HR, 13.2 [95% CI, 1.6-107.3]) and lesion size (>17.2 mm) predicted growth in TETs (P=0.008 for size and P=0.029 for size*time; HR=e^(-0.001 \times time+1.654)). Among the growing lesions, positive and negative predictive values of water attenuation for the thymic cysts was 93% and 80%, respectively.

CONCLUSION

The frequencies of interval growth and VDTs were indistinguishable between TETs and thymic cysts. Water attenuation and lesion size predicted growth in thymic cysts and TETs, respectively. Among the growing lesions, the water attenuation was a differential feature of thymic cysts.

CLINICAL RELEVANCE/APPLICATION

Water attenuation (<=20 HU) indicates thymic cysts for the growing thymic lesions. Thus, CT follow-up, instead of surgical resection, can be recommended for the obvious cysts even if they show interval growth.

SST02-07 Cut-Off Value of MR Enhancement for Differentiating Benign Cysts from Solid Anterior Mediastinal Lesion: A Preliminary Observation

Friday, Nov. 30 11:30AM - 11:40AM Room: E350

Participants

Eui Jin Hwang, Seoul, Korea, Republic Of (Presenter) Nothing to Disclose

Soon Ho Yoon, MD, Seoul, Korea, Republic Of (Abstract Co-Author) Nothing to Disclose

Jihang Kim, MD, Seongnam, Korea, Republic Of (Abstract Co-Author) Nothing to Disclose

Ho Yun Lee, MD, Seoul, Korea, Republic Of (Abstract Co-Author) Nothing to Disclose

Jin Mo Goo, MD, PhD, Seoul, Korea, Republic Of (Abstract Co-Author) Research Grant, Samsung Electronics Co, Ltd; Research Grant, Lunit Inc

Munyoung Paek, Seoul, Korea, Republic Of (Abstract Co-Author) Nothing to Disclose

Jeanne B. Ackman, MD, Boston, MA (*Abstract Co-Author*) Spouse, Stockholder, Everest Digital Medicine; Spouse, Consultant, Everest Digital Medicine; Spouse, Stockholder, Cynvenio Biosystems, Inc; Spouse, Scientific Advisory Board, Cynvenio Biosystems, Inc; Spouse, Consultant, PAREXEL International Corporation

For information about this presentation, contact:

ken921004@hotmail.com

PURPOSE

To determine the optimal cut-off value of MR enhancement for the differentiation of benign cysts from solid lesions in the anterior mediastinum.

METHOD AND MATERIALS

The derivation dataset consisted of 19 consecutive patients with pathologically proven benign cysts (n=7) and solid lesions (n=12) in the anterior mediastinum who underwent a diagnostic contrast-enhanced MR from two institutions. We measured maximum diameters, T1 and T2 signal intensities (SI), apparent diffusion coefficients (ADCs) from diffusion-weighted images, and relative enhancement ratios (RERs). T1 and T2 SIs were normalized by SI of cerebrospinal fluid. RERs were obtained from the subtraction of axial pre- and post-contrast T1-weighted fat-suppressed images after the precise non-rigid image registration of the two images using a dedicated WIP software (MRI Arithmetics, Siemens Healthcare, Erlangen, Germany). After comparison of image variables between cysts and solid masses, the cutoff value of the most differential MR variable was determined based on a receiver operating characteristic curve. For validation, two separate datasets were utilized: 1) 15 patients with 8 cysts and 7 solid lesions from another institution (validation dataset 1); 2) 11 patients with MR-proven stable benign cysts more than 2 years (validation dataset 2). Diagnostic accuracies were calculated from validation datasets.

RESULTS

Normalized T2 SI (0.21-0.92 vs. 0.12-0.58; P=.013), ADC (1.76-4.09 vs. 0.66-2.93 10-3 mm2/s; P=.013), and RER (0.41-24.1% vs. 28.1-771.7%; P<.001) significantly differed between cysts and solid masses. RER of 26% or less was determined as the cutoff value for differentiation of cysts from solid masses. In validation dataset 1, the cutoff value showed sensitivity of 87.5% and specificity of 100%, the sensitivity of 90.9% was observed in validation dataset 2.

CONCLUSION

The assessment of RER with the cutoff value of 26% can appropriately differentiate benign cysts from solid anterior mediastinal masses.

CLINICAL RELEVANCE/APPLICATION

The differentiation of benign cysts from solid anterior mediastinal masses can be supported by quantitative measurement of RER, potentially reducing a futile thymectomy.

Esophageal Squamous Cell Carcinoma

Friday, Nov. 30 11:40AM - 11:50AM Room: E350

Participants

Dongyoung Jeong, MD, Seoul, Korea, Republic Of (*Presenter*) Nothing to Disclose Kyung Soo Lee, Seoul, Korea, Republic Of (*Abstract Co-Author*) Nothing to Disclose Yeonu Choi, Seoul, Korea, Republic Of (*Abstract Co-Author*) Nothing to Disclose Sunggoo Park, MD,DVM, Seoul, Korea, Republic Of (*Abstract Co-Author*) Nothing to Disclose

For information about this presentation, contact:

dongyoung.jeong@samsung.com

PURPOSE

We have previously shown that initial PET-SUVmax(Standardized uptake value) of early esophageal cancer helps both discriminating T1a and T1b stage esophageal squamous cell carcinoma(eSCC) from other eSCCs. In this study, we analyze the impact of PET-SUVmax for patient's survival.

METHOD AND MATERIALS

This retrospective study was based on 435 patients with a surgically proven early T- (Tis or T1a [< T1a], T1b and T2) stage eSCC. We performed survival analysis by the Kaplan-Meier method and comparisons of survival using log-rank test.

RESULTS

131 < T1a, 234 T1b, and 70 T2 eSCCs were enrolled. Mean SUVmax value were 2.53 for < T1a eSCCs, 4.02 for T1b eSCCs and 9.69 for T2 eSCCs. With ROC curve analysis, cut off value of SUVmax 3.05 (AUC: 0.757; 95% CI, 0.710-0.803; P < .001) at PET provided sensitivity 74.8% (98/131), specificity 70.1% (213/304), respectively, for differentiating < T1a eSCCs from other cancers. Cut off value of SUVmax 5.65 (AUC: 0.897; 95% CI, 0.857-0.937; P < .001) provided sensitivity 77.1% (54/70), specificity 87.7% (320/365), respectively, for differentiating T1 (< T1b) eSCCs from T2 eSCCs. In multivariate analysis, both SUVmax and pathologic staging including tumor size and node involvement were significant predictors of survival (p < 0.01). Survival analysis and log-rank test showed significant difference for overall survival among groups based on proposed cut-off SUVmax values (p =0.008 for cut off value 3.05, p <0.001 for cut off value 5.65)

CONCLUSION

In early esophageal squamous cell carcinomas, SUVmax gives us powerful predictor of overall survival after resection.

CLINICAL RELEVANCE/APPLICATION

Pretreatment SUVmax of primary esophageal cancer shows powerful predictive values which can be comparable to pathologic T stage.

SST02-09 Surgically Resected T1- and T2-Stage Esophageal Squamous Cell Carcinoma: T and N Staging Performance of EUS- and PET/CT

Friday, Nov. 30 11:50AM - 12:00PM Room: E350

Participants

Dongyoung Jeong, MD, Seoul, Korea, Republic Of (*Presenter*) Nothing to Disclose
Kyung S. Lee, MD, PhD, Seoul, Korea, Republic Of (*Abstract Co-Author*) Nothing to Disclose
MinYeong Kim, MD, Seoul, Korea, Republic Of (*Abstract Co-Author*) Nothing to Disclose
Myung Jin Chung, MD, Seoul, Korea, Republic Of (*Abstract Co-Author*) Research Grant, General Electronic Company; Research
Grant, Samsung Electronics Co, Ltd; Research Grant, Lunit Inc
Joon Young Choi, MD, PhD, Seoul, Korea, Republic Of (*Abstract Co-Author*) Nothing to Disclose

For information about this presentation, contact:

dongyoung.jeong@samsung.com

PURPOSE

To demonstrate the frequency of nodal metastases and to disclose the diagnostic performance of endoscopic ultrasonography (EUS) and PET/CT in T and N staging in surgically resected early-stage esophageal squamous cell carcinomas (eSCCs).

METHOD AND MATERIALS

IRB approved this retrospective study with waiver of informed consent for reviewing medical record. We included 435 patients with an early T-stage (Tis or T1a [< T1a], T1b and T2) eSCC. The rates of metastatic lymphadenopathy were calculated. Then, the performance of EUS and PET/CT in subdividing T and N stages was assessed.

RESULTS

131 < T1a, 234 T1b, and 70 T2 eSCCs were identified. In discriminating < T1a from other cancers, the sensitivity, specificity and accuracy of EUS were 60.3% (79/131), 80.3% (244/304), and 74.3% (323/435), respectively. With ROC curve analysis, cutoff value of SUVmax 3.05 at PET provided sensitivity 73.3% (96/131), specificity 70.4% (214/304), and accuracy 71.3% (310/435) for differentiating < T1a eSCCs from others. Ten (7.6%) of 131 < T1a cancers had nodal metastasis. In discriminating N0 from nodepositive disease, sensitivity, specificity and accuracy of EUS were 89.6% (267/298), 41.6% (57/137) and 74.5% (324/435), respectively, whereas those of PET/CT were 88.9% (265/298), 38.7% (53/137), and 73.1% (318/435), respectively.

CONCLUSION

In > 70% of patients with < T1a eSCCs, the tumor stage can be discriminated from higher stage cancers by using EUS or PET/CT, and substantial percentage (7.6%) of < T1a eSCC patients have nodal metastases, but the nodes are missed in more than half of the patients in clinical staging.

CLINICAL RELEVANCE/APPLICATION

Substantial percentage (7.6%) of < T1a eSCC patients have nodal metastases, and nodal metastasis rates increase as T stage increases (T1b [37.6%] and T2 [55.7%]). Moreover, more than half of nodal metastases were missed on PET/CT or EUS. Thus, after endoscopic surgery or even after curative surgical resection of < T1a eSCCs, adjuvant therapy is needed for those having nodal metastasis.



SST03

Gastrointestinal (Advanced MRI Techniques)

Friday, Nov. 30 10:30AM - 12:00PM Room: E352



AMA PRA Category 1 Credits ™: 1.50 ARRT Category A+ Credit: 1.75

FDA

Discussions may include off-label uses.

Participants

Hersh Chandarana, MD, New York, NY (*Moderator*) Equipment support, Siemens AG; Software support, Siemens AG; Advisory Board, Siemens AG; Speaker, Bayer AG;

Myeong-Jin Kim, MD, PhD, Seoul, Korea, Republic Of (*Moderator*) Nothing to Disclose Frank H. Miller, MD, Chicago, IL (*Moderator*) Research Grant, Siemens AG

Sub-Events

SST03-01 Efficacy of Gadoxetic Acid-Enhanced MRI for Evaluating Biliary Anatomy in Living Donor Liver Transplantation

Friday, Nov. 30 10:30AM - 10:40AM Room: E352

Participants

Sang Hyun Choi, Seoul, Korea, Republic Of (*Presenter*) Nothing to Disclose Kyoung Won Kim, Seoul, Korea, Republic Of (*Abstract Co-Author*) Nothing to Disclose Jin Sil Kim, MD, Seoul, Korea, Republic Of (*Abstract Co-Author*) Nothing to Disclose Hye Young Jang, Daejeon, Korea, Republic Of (*Abstract Co-Author*) Nothing to Disclose

PURPOSE

To determine the added value of combined T2-magnetic resonance cholangiography (MRC) and hepatobiliary phase-MRC (T2+HBP-MRC) for evaluating the biliary anatomy in living liver donors by comparing it with T2-MRC alone, and evaluate the clinical usefulness of T2+HBP-MRC for surgical planning

METHOD AND MATERIALS

Our institutional review board approved this study and waived the requirement for informed consent. Between January and December 2016, we included 276 donors who underwent T2 and gadoxetic acid-enhanced MRI before right hemihepatectomy for living donor liver transplantation. Two reviewers evaluated the biliary anatomy classification using T2-MRC in the first session and T2+HBP-MRC in the second session. The sensitivity, specificity and confidence level (5-point scale) of T2-MRC and T2+HBP-MRC for variant biliary anatomy were evaluated using McNemar's test or paired t-test. The agreement rates of each biliary anatomy classification between MRC and operative cholangiography and the underestimated rates of multiple BDO for each MRC were evaluated using McNemar's test.

RESULTS

Of the 276 donors, variant biliary anatomy was observed in 36.2% (100/276). T2+HBP-MRC showed a significantly higher sensitivity for diagnosing variant biliary anatomy than T2-MRC alone (99.0% [99/100] vs. 89.0% [87/100], p = 0.006) with better confidence level (4.9 ± 0.3 vs. 4.6 ± 0.7 , p<0.001), and inter-observer agreement (kappa, 0.902 vs. 0.730). A significantly higher agreement of biliary anatomy classification with operative cholangiography (98.6% [272/276] vs. 89.9% [248/276], p<0.001) and a significantly decreased the underestimation rate of multiple BDO (5.8% [16/276] vs. 9.4% [26/276], p=0.002) were obtained by T2+HBP-MRC than T2-MRC alone.

CONCLUSION

T2+HBP-MRC can be more useful than T2-MRC alone by improving diagnostic performance of variant biliary anatomy and giving information to make accurate surgical plans.

CLINICAL RELEVANCE/APPLICATION

T2+HBP-MRC can be clinically more useful than T2-MRC alone for evaluating biliary anatomy in living donor liver transplantation.

SST03-02 In Vivo Imaging of Hepatocellular Carcinoma Using Hyperpolarized Water

Friday, Nov. 30 10:40AM - 10:50AM Room: E352

Participants

Sebastian Fischer, MD, Frankfurt, Germany (*Presenter*) Nothing to Disclose Richard D. Maeder, Frankfurt, Germany (*Abstract Co-Author*) Nothing to Disclose Vasyl Denysenkov, Frankfurt, Germany (*Abstract Co-Author*) Nothing to Disclose Stefan Zangos, MD, Frankfurt Am Main, Germany (*Abstract Co-Author*) Nothing to Disclose Thomas Prisner, Frankfurt, Germany (*Abstract Co-Author*) Nothing to Disclose Thomas J. Vogl, MD, PhD, Frankfurt, Germany (*Abstract Co-Author*) Nothing to Disclose

For information about this presentation, contact:

sebastian.fischer@kgu.de

PURPOSE

Besides the risk of allergic reactions and a nephrogenic systemic fibrosis, research showed remnants of Gadolinium based MR contrast agents (GBCA) in the brain - with unknown long-term effects. Purpose is to examine dynamic nuclear polarization (DNP) of water as a method to generate MR contrast and to prove it can be used for imaging of hepatocellular cancer (HCC) in vivo.

METHOD AND MATERIALS

Liquid-state Overhauser DNP hyperpolarizes water molecules by temporarily coupling their nuclear spin to the electron spin of irradiated radicals under resonance conditions. Microwave irradiation takes place in a resonator chamber containing immobilized TEMPO radicals, passed by a NaCl solution at a flow rate of 800µl/min within the bore of a 1.5T scanner. After catheterization of iliac vessels hyperpolarized water was administered directly at the celiac trunk of transgenic TGFa/c-myc mice that develop HCC. The aorta, its hepatic branches and the liver were visualized at 2 fps with dynamic GRE sequences (TR 6.4ms, TE 2.8ms, FoV 58x78x5mm, Matrix 128x77px) for 10 sec. Temporal DNP signal intensities, SNR and CNR values were measured in the aorta, hepatic artery, HCC and liver parenchyma. Anatomic sections und IHC staining confirmed the lesions as HCCs.

RESULTS

Magnitude imaging featured mainly a negative signal due to short relaxation time and fast signal decay during repetitive GRE pulses. In phase imaging signal intensities increased by factor 2.1 in the aorta, 1.6 in the hepatic artery and 1.2 in HCC and liver parenchyma. These changes were subsequently visible at the following periods after application: sec. 1-4 in the aorta, sec. 3-7 in the hepatic artery, sec. 4-8 in HCC and only slowly in the liver parenchyma, illustrating the HCC's typical early arterial enhancement. SNR increased up to 1.7 times and CNR up to 10.8 times. After stopping microwave power no contrast resides.

CONCLUSION

The in-bore DNP setup continuously creates hyperpolarized water, featuring high T1 signal enhancements in MR imaging and a short relaxation time. The strong contrast enhancement made a dynamic visualization of the supplying vessels and the typical contrast dynamics of HCCs possible - even using a standard clinical 1.5T scanner.

CLINICAL RELEVANCE/APPLICATION

Hyperpolarized water might be a promising future alternative to GBCA in MR angiographies and liver imaging without risking the potential adverse effects or intracorporal remnants.

SST03-03 Modified Breath-Hold Compressed-Sensing 3D Magnetic Resonance Cholangiopancreatograph: Clinical Feasibility in Biliary and Pancreatic Disorders

Friday, Nov. 30 10:50AM - 11:00AM Room: E352

Participants

Liang Zhu, MD, Beijing, China (Abstract Co-Author) Nothing to Disclose Huadan Xue, MD, Beijing, China (Presenter) Nothing to Disclose Zhao Yong Sun, Beijing, China (Abstract Co-Author) Nothing to Disclose Tianyi Qian, PhD, Beijing, China (Abstract Co-Author) Nothing to Disclose Tianyi Qian, PhD, Beijing, China (Abstract Co-Author) Nothing to Disclose Elisabeth Weiland, Erlangen, Germany (Abstract Co-Author) Employee, Siemens AG Bernd Kuehn, PhD, Erlangen, Germany (Abstract Co-Author) Employee, Siemens AG Patrick Asbach, MD, Berlin, Germany (Abstract Co-Author) Nothing to Disclose Zheng Yu Jin, MD, Beijing, China (Abstract Co-Author) Nothing to Disclose

For information about this presentation, contact:

zhuliang_pumc@163.com?bjdanna95@163.com

PURPOSE

To prospectively evaluate the clinical feasibility of a modified 3D breath-hold (BH) compressed-sensing (CS) MRCP prototype protocol with small field-of-view (FOV) and high spatial resolution (modified BH-CS-MRCP), and to compare its performance with respect to the original BH-CS-MRCP and navigator-triggered (NT)-CS-MRCP.

METHOD AND MATERIALS

In this prospective IRB approved study, a total of 82 patients (46 male, median age, 55 years, range, 16-79 years) underwent 3D CS-MRCP on a 3T MR scanner. Three protocols (modified BH-CS-MRCP, original BH-CS-MRCP and NT-CS-MRCP) were performed in random order. Acquisition time of each protocol was recorded. Image quality, background suppression, duct visibility and diagnostic confidence with duct anatomic variations and duct-related pathologies were rated on a 5-point scale by two blinded radiologists independently. The diagnostic performance of each protocol was calculated using receiver operating characteristic curves.

RESULTS

Acquisition time was 17 seconds for both BH-CS-MRCP protocols, and 127.5 ± 36.9 seconds for NT-CS-MRCP. In 75 cooperative patients, the incidence of major artifacts was low for all protocols (5.3%-8.0%). Background suppression was similar with the two BH-CS-MRCP protocols, both inferior to the NT-CS-MRCP protocol. Modified BH-CS-MRCP and NT-CS-MRCP depicted pancreatic duct and second-level branches of biliary duct better than original BH-CS-MRCP (all p<0.01). The diagnostic performance for detecting bile duct abnormalities was similar for all protocols(all p>0.05), whereas for detecting pancreatic duct abnormalities, modified BH-CS-MRCP and NT-CS-MRCP had significantly better performance(both p<0.01). In 7 non-cooperative patients, NT-CS-MRCP had superior image quality than both BH protocols (both p<0.01).

CONCLUSION

Modified BH-CS-MRCP is clinically feasible for pancreatic and biliary disorders. NT-CS-MRCP is useful in non-cooperative patients.

CLINICAL RELEVANCE/APPLICATION

The general image quality with CS-MRCP was reported to be similar or even superior compared to the conventional navigator-triggered (NT) protocol. However, according to previous reports, the visibility of the pancreatic duct with the original BH-CS-MRCPwas lower, and the diagnostic yield was lower. We found that the modified BH-CS-MRCP is feasible in clinical patients, with image quality and diagnostic performance equally good or better than NT-CS-MRCP.

SST03-04 Assessment of Liver Stiffness with Free-Breathing MR Elastography in Patients and Volunteers

Friday, Nov. 30 11:00AM - 11:10AM Room: E352

Participants

Jiahui Li, MD, Rochester, MN (Presenter) Nothing to Disclose

Ziying Yin, PhD, Rochester, MN (Abstract Co-Author) Nothing to Disclose

Bogdan Dzybak, Rochester, MN (Abstract Co-Author) Nothing to Disclose

Kevin J. Glaser, Rochester, MN (Abstract Co-Author) Intellectual property, Magnetic Resonance Elastography Technology; Stockholder, Resoundant, Inc

Yi Sui, Rochester, MN (Abstract Co-Author) Nothing to Disclose

Sudhakar K. Venkatesh, MD, FRCR, Rochester, MN (Abstract Co-Author) Nothing to Disclose

Armando Manduca, PhD, Rochester, MN (Abstract Co-Author) Royalties, General Electric Company

Richard L. Ehman, MD, Rochester, MN (Abstract Co-Author) CEO, Resoundant, Inc Stockholder, Resoundant, Inc

Meng Yin, PhD, Rochester, MN (Abstract Co-Author) Intellectual property, Magnetic Resonance Innovations, Inc; Stockholder, Resoundant, Inc

For information about this presentation, contact:

li.jiahui@mayo.edu

PURPOSE

Liver MR elastography (MRE), as a quantitative imaging biomarker for hepatic fibrosis, is often performed during breath hold at end-expiration to avoid the changes due to respiratory motion. However, some patients have limited ability to perform adequate breath holds (e.g., pediatric and sedated patients). Our study purpose is to evaluate the technical feasibility and measurement variation of a rapid, free-breathing MRE technology for assessing liver stiffness (LS) with a comparison of standard breath-held MRE.

METHOD AND MATERIALS

We have recruited 32 patients with chronic liver diseases, and 8 controls. A standard breath-held multi-slice 2D GRE-MRE was performed to calculate the baseline liver stiffness (LSB). A view-sharing based reconstruction strategy for a free-breathing single-shot multi-slice 2D EPI-MRE was performed to calculate median liver stiffness (LSM) within anatomically co-registered ROIs, and its temporal variation Δ LS (defined in FigB). We performed Bland-Altman and intraclass correlation (ICC) analyses to analyze variance statistics and method accuracy, and Spearman correlation analyses to evaluate the relationships between LSB, LSM and Δ LS in non-cirrhotic (LSB<5kPa) and cirrhotic (LSB>=5kPa) livers respectively, with a 0.05 significance level.

RESULTS

FigA shows two example LSB and LSM images of a healthy liver and a cirrhotic liver, respectively. FigB shows an example of dynamic liver stiffness measurement in free-breathing MRE. Bland-Altman analysis shows mean difference of -0.18kPa between LSB and LSM with ICC of 0.96. FigC illustrates that LSM excellently agrees with LSB in all subjects (R2=0.87, p<0.0001*), highly accurate in 33 non-cirrhotic livers (LSM=1.03×LSB, p<0.0001*), moderately underestimates LSB in 7 cirrhotic livers (LSM=0.79×LSB, p<0.0001*). Measurement variation (FigC, shown as bubble size) increases with disease severity(R2=0.40, p<0.0001).

CONCLUSION

Our preliminary results suggest that free-breathing MRE provides highly accurate liver stiffness value, especially for non-cirrhotic livers.

CLINICAL RELEVANCE/APPLICATION

The free-breathing MRE excellently agreeing to conventional breath-held liver stiffness will be beneficial for pediatric and sedated patients.

Honored Educators

Presenters or authors on this event have been recognized as RSNA Honored Educators for participating in multiple qualifying educational activities. Honored Educators are invested in furthering the profession of radiology by delivering high-quality educational content in their field of study. Learn how you can become an honored educator by visiting the website at: https://www.rsna.org/Honored-Educator-Award/ Richard L. Ehman, MD - 2016 Honored EducatorSudhakar K. Venkatesh, MD, FRCR - 2017 Honored Educator

SST03-05 Inter- and Intra-Reader Agreement of Different Parameters of Gadoxetic Acid Enhanced Hepatobiliary Phase Imaging in Patients with Chronic Liver Diseases: A Comparison Study

Friday, Nov. 30 11:10AM - 11:20AM Room: E352

Participants

Lucian Beer, MD,PhD, Vienna, Austria (*Presenter*) Nothing to Disclose

Nina Bastati, MD, Vienna, Austria (Abstract Co-Author) Nothing to Disclose

Sarah Poetter-Lang, Vienna, Austria (Abstract Co-Author) Nothing to Disclose

Dietmar Tamandl, MD, Vienna, Austria (Abstract Co-Author) Nothing to Disclose

Michael Elmer, Vienna, Austria (Abstract Co-Author) Nothing to Disclose

Claude B. Sirlin, MD, San Diego, CA (Abstract Co-Author) Research Grant, Gilead Sciences, Inc; Research Grant, General Electric Company; Research Grant, Siemens AG; Research Grant, Bayer AG; Research Grant, ACR Innovation; Research Grant, Koninklijke Philips NV; Research Grant, Celgene Corporation; Consultant, General Electric Company; Consultant, Bayer AG; Consultant, Boehringer Ingelheim GmbH; Consultant, AMRA AB; Consultant, Fulcrum Therapeutics; Consultant, IBM Corporation; Consultant,

Exact Sciences Corporation; Advisory Board, AMRA AB; Advisory Board, Guerbet SA; Advisory Board, VirtualScopics, Inc; Speakers Bureau, General Electric Company; Author, Medscape, LLC; Author, Resoundant, Inc; Lab service agreement, Gilead Sciences, Inc; Lab service agreement, ICON plc; Lab service agreement, Intercept Pharmaceuticals, Inc; Lab service agreement, Shire plc; Lab service agreement, Enanta; Lab service agreement, Virtualscopics, Inc; Lab service agreement, Alexion Pharmaceuticals, Inc; Lab service agreement, Takeda Pharmaceutical Company Limited; Lab service agreement, sanofi-aventis Group; Lab service agreement, Johnson & Johnson; Lab service agreement, NuSirt Biopharma, Inc; Contract, Epigenomics; Contract, Arterys Inc Ahmed Ba-Ssalamah, MD, Vienna, Austria (Abstract Co-Author) Consultant, Bayer AG; Speaker, Novartis AG; Speaker, Siemens AG; Speaker, Bayer AG;

PURPOSE

To examine inter- and intra-observer reliability between different hepatobiliary phase (HBP) image scores on gadoxetic-acid (GA)-enhanced MRI and their correlation with clinical parameters and liver function in patients with diffuse chronic liver disease.

METHOD AND MATERIALS

This retrospective IRB-approved study included 353 patients (224 male, 129 female, mean age 53.4 ±13.8 years) with chronic liver disease who had undergone GA-enhanced MRI of the liver between 2010-2015. Relative liver enhancement (RLE), contrast uptake index (CUI), hepatic uptake index (HUI), and liver to spleen contrast ratio (LSC) were calculated by two radiologist independently using unenhanced and GA-enhanced HPB images (obtained 20 minutes after GA administration); 50 image sets were reviewed twice to assess intra-observer reliability. Albumin-bilirubin (ALBI) grade, Child-Pugh score and Model of End Stage Liver Disease (MELD) were calculated as markers of disease severity. Associations between HPB and disease severity markers were assessed (Spearman 's correlation). Reader reliability was evaluated using intraclass correlation coefficient (ICC).

RESULTS

There was a significant correlation (p<0.001 for all) between five pairs of MR-derived parameters: RLE-CEI (R=0.947,), RLE-LSC (R=0.813,) RLE-HUI (R=0.767), CEI-LSC (R=0.818) and HUI-LSI (R=0.943). Depending on the MR parameter, MR-disease severity correlation coefficients ranged from 0.482-0.525 for ALBI-score, 0.371-0.430 for MELD, and 0.490-0.333 for Child-Pugh. Intra-observer ICCs ranged from 0.979 (0.963-0.989) for RLE to 0.816 (0.670-0.898) for LSI indicating excellent agreement. Inter-observer ICCs ranged from 0.979 (0.962.0.988) for RLE to 0.792 (0.629-833) for HUI.

CONCLUSION

Strong correlations were observed between different MR-derived HBP-based parameters with each other and between these parameters and disease severity markers. MR-derived parameters showed excellent inter- and intra-observer agreement.

CLINICAL RELEVANCE/APPLICATION

Qualitative MR-derived HBP imaging parameters have high observer releiability and show promise for evaluation of chronic liver disease severity.

SST03-06 Abbreviated Gadoxetic Acid-Enhanced MRI (AGAM) Including Second Shot Arterial Phase (SSAP) for Liver Metastasis Workup

Friday, Nov. 30 11:20AM - 11:30AM Room: E352

Participants

Jeong Woo Kim, MD, Seoul, Korea, Republic Of (*Presenter*) Nothing to Disclose Chang Hee Lee, MD, Seoul, Korea, Republic Of (*Abstract Co-Author*) Nothing to Disclose Yang Shin Park, MD, Seoul, Korea, Republic Of (*Abstract Co-Author*) Nothing to Disclose Hyunji Lee, Seoul, Korea, Republic Of (*Abstract Co-Author*) Nothing to Disclose Jongmee Lee, Seoul, Korea, Republic Of (*Abstract Co-Author*) Nothing to Disclose Jae Woong Choi, MD, Seoul, Korea, Republic Of (*Abstract Co-Author*) Nothing to Disclose Kyeong Ah Kim, MD, Seoul, Korea, Republic Of (*Abstract Co-Author*) Nothing to Disclose Cheol Min Park, MD, Seoul, Korea, Republic Of (*Abstract Co-Author*) Nothing to Disclose

For information about this presentation, contact:

chlee86@korea.ac.kr

PURPOSE

To evaluate feasibility of AGAM protocol including SSAP for liver metastasis workup

METHOD AND MATERIALS

This retrospective study was approved by our IRB and the requirement for informed consent was waived. 108 patients with hepatic metastasis who underwent gadoxetic acid-enhanced MRI using a modified injection protocol were included. Modified injection protocol included routine dynamic imaging after a first injection of 6-mL and SSAP after a second injection of 4-mL. Primary cancer sites consisted of colorectum (n=59), stomach (n=16), biliary trees (n=16), pancreas (n=7), and others (n=7). The image set 1 consisted of T2WI, chemical shift image, DWI, and T1-weighted dynamic image including hepatobiliary phase (HBP) [full original protocol]. The image set 2 consisted of T2WI, DWI, HBP, and SSAP [abbreviated protocol]. Acquisition time was measured in each image set. Visual assessment of vascularity was performed in the original arterial phase (AP), SSAP, and their subtraction images. After excluding patients with >=10 metastatic lesions, 149 lesions in 51 patients were included for detection and characterization analysis. The reference standard was a combination of pathologic result and follow-up image. Two radiologists independently reviewed two image sets regarding the presence and probability of liver metastasis with >6-week time interval. The diagnostic performance of each image set for each reader was compared by using a jackknife alternative free-response receiver operating characteristic (JAFROC) analysis. The sensitivity and positive predictive value (PPV) were also calculated.

RESULTS

Acquisition time was significantly shorter in img set 2 than in img set 1 (1118.3 ± 128.3 vs. 372.8 ± 30.5 sec, p<0.0001). Regarding the visual assessment of vascularity, 98.8% (85/86) hypervascular metastases (hyperintense on the original AP) showed hyperintensity on the SSAP and/or SS subtraction images. For both readers, average JAFROC figure-of-merit was not significantly different between img set 1 and 2 (0.998 vs. 0.997, p=0.210), and sensitivity and PPV did not show significant difference.

CONCLUSION

AGAM protocol including SSAP can provide faster image acquisition with preserving visual vascularity and diagnostic performance for liver metastasis workup.

CLINICAL RELEVANCE/APPLICATION

For liver metastasis workup, AGAM protocol can serve as a faster and more convenient alternative without compromising the diagnostic performance.

SST03-07 Magnetization Transfer Imaging Adds Information to Conventional MRIs to Differentiate Inflammatory and Fibrotic Intestinal Strictures in Crohn's Disease

Friday, Nov. 30 11:30AM - 11:40AM Room: E352

Participants

Zhuangnian Fang, Guangzhou, China (*Presenter*) Nothing to Disclose Xuehua Li II, Guangzhou, China (*Abstract Co-Author*) Nothing to Disclose Ren Mao, MD, Guang Zhou, China (*Abstract Co-Author*) Nothing to Disclose Canhui Sun, MD, PhD, Guangzhou, China (*Abstract Co-Author*) Nothing to Disclose Shiting Feng, MD, Guangzhou, China (*Abstract Co-Author*) Nothing to Disclose Ziping Li, MD, PhD, Guangzhou, China (*Abstract Co-Author*) Nothing to Disclose

PURPOSE

Identifying inflammation- or fibrosis-predominant strictures in patients with Crohn's disease (CD) is crucial for developing treatment strategies. We evaluated the value of magnetization transfer (MT) with conventional MRI in characterizing CD stricture types using surgical histopathology as a reference standard.

METHOD AND MATERIALS

Forty patients with CD who underwent MRI scanning before surgery were enrolled. MRI parameters included: T2WI hyperintensity, bowel wall thickness, enhancement pattern changes over time, enhancement pattern and gain ratio in dynamic contrast-enhanced image phases, and MT ratios. Group and logistic regression analyses were performed to identify MRI variables for predicting inflammation and fibrosis, respectively.

RESULTS

Significant correlations with histological inflammation scores were shown for wall thickness (r=0.361, P=0.001) and T2WI hyperintensity (r=0.396, P<0.001), whereas histological fibrosis scores were significantly correlated with MT ratio (r=0.681, P<0.001) and wall thickness (r=0.461, P<0.001). Using T2WI hyperintensity as a predictor, conventional MRI could differentiate mild and moderate-to-severe inflammation with a sensitivity of 0.871 and a specificity of 0.800. The MT ratio could discriminate mild and moderate-to-severe fibrosis with a sensitivity and a specificity of 0.913 and 0.923, respectively. Combining MT ratios and T2WI hyperintensity, the MRI classification moderately agreed with the pathological stricture classification (P<0.01, K=0.567). The diagnostic accuracy of T2WI hyperintensity and MT ratio were 84% and 87%, with a moderate agreement between the MRI and the pathological classification (P<0.01, K=0.576).

CONCLUSION

The MT ratio in addition to conventional MRI improves the differentiation of fibrotic from inflammatory components of a small bowel stricture in patients with CD.

CLINICAL RELEVANCE/APPLICATION

Measuring the degree of bowel inflammation and fibrosis help optimize management strategies.

SST03-08 Transient Severe Motion in Gadoxetate Disodium Enhanced Liver MRI: A Multi-Center and Multi-Reader Trial in 1789 Patients

Friday, Nov. 30 11:40AM - 11:50AM Room: E352

Participants

Guido M. Kukuk, MD, Bonn, Germany (*Presenter*) Nothing to Disclose
Kristina I. Ringe, MD, Hannover, Germany (*Abstract Co-Author*) Nothing to Disclose
Martin H. Maurer, MD, Bern, Switzerland (*Abstract Co-Author*) Nothing to Disclose
Peter Reimer, MD, Karlsruhe, Germany (*Abstract Co-Author*) Nothing to Disclose
Sabine Michalik, MD, Hamburg, Germany (*Abstract Co-Author*) Nothing to Disclose
Johannes Wessling, MD, Muenster, Germany (*Abstract Co-Author*) Nothing to Disclose
Rolf Fimmers, Bonn, Germany (*Abstract Co-Author*) Nothing to Disclose
Jonas Doerner, MD, Cologne, Germany (*Abstract Co-Author*) Nothing to Disclose
Claas P. Naehle, MD, Bonn, Germany (*Abstract Co-Author*) Nothing to Disclose
Winfried A. Willinek, MD, Bonn, Germany (*Abstract Co-Author*) Speakers Bureau, Bayer AG Speakers Bureau, Bracco Group Speakers
Bureau, General Electric Company Speakers Bureau, Koninklijke Philips NV Speakers Bureau, Sirtex Medical Ltd
Andreas G. Schreyer, MD, Regensburg, Germany (*Abstract Co-Author*) Nothing to Disclose

Julian A. Luetkens, MD, Bonn, Germany (Abstract Co-Author) Nothing to Disclose

For information about this presentation, contact:

Guido.Kukuk@ukbonn.de

PURPOSE

To determine the frequency of transient severe motion occurring in dynamic gadoxetate disodium enhanced liver MRI in a large multi-center setting.

METHOD AND MATERIALS

Institutional review board approval with a waiver for informed consent was obtained from all participating institutions from two different countries for this retrospective study. 1789 gadoxetate disodium enhanced liver MR examinations (1069 male and 720 female patients) acquired after intravenous administration of 5-20 ml gadoxetate disodium were included. 7156 dynamic data sets (pre-contrast, arterial phase, portal venous phase, late venous phase; each acquired during a single breath-hold) were reviewed by 10 radiologists with a minimum of 5 years after board certification. To determine interrater agreement and reliability all radiologists were obliged to review 40 selected additional data sets as a pre-requisite. Image evaluation was performed on a 5-point scale (1, no respiratory motion artifacts; 5, extensive respiratory motion artifacts, non-diagnostic study). Transient severe motion (TSM) was defined as a pre-contrast score of <=2, arterial score of >=4 and a portal and late venous score of <=3. Statistical tests included intraclass correlation coefficient (ICC), Kendall coefficient of concordance (W), normality test, and paired t-test.

RESULTS

ICC for interrater agreement and reliability were 0.983 (CI 0.973 - 0.990) and 0.985 (CI 0.978 - 0.991), respectively (both p<0.001), indicating excellent agreement and reliability. 874 (48.6%), 453 (25.2%), 346 (19.2%), 91 (5.1%), and 25 (1.4%) of all arterial phases were rated with a score of 1-5, respectively. Transient severe motion was detected in 51 of 1789 (2.9%) examinations. Mean motion scores for the pre-contrast scan, arterial phase, portal venous phase, late venous phase were 1.37 ± 0.68 , 1.85 ± 0.99 , 1.51 ± 0.80 , 1.38 ± 0.66 , respectively. Arterial phase motion scores were rated significantly worse than all other phases (p<0.001, respectively).

CONCLUSION

Although arterial phase imaging is significantly more often affected by motion artifacts than all other phases, the frequency of transient severe motion in gadoxetate enhanced dynamic liver MRI is only 2.9%.

CLINICAL RELEVANCE/APPLICATION

With only 2.9% the rate of transient severe motion in gadoxetate enhanced liver MRI is substantially lower than reported in previous single and dual center studies.

SST03-09 Role of Quantitative Parameters from Dynamic Contrast-Enhanced MRI in Evaluating Regional Lymph Nodes with Short-Axis Diameter Less Than 5 Millimeters in Rectal Cancer

Friday, Nov. 30 11:50AM - 12:00PM Room: E352

Participants

Xiaojuan Xiao, BMedSc, MMedSc, Shenzhen, China (*Abstract Co-Author*) Nothing to Disclose Xinyue Yang, Guangzhou, China (*Presenter*) Nothing to Disclose Shen Ping Yu, Guangzhou, China (*Abstract Co-Author*) Nothing to Disclose Bao Lan Lu, Guangzhou, China (*Abstract Co-Author*) Nothing to Disclose Yan Chen, Guangzhou, China (*Abstract Co-Author*) Nothing to Disclose Guanxun Cheng, Shenzhen, China (*Abstract Co-Author*) Nothing to Disclose

For information about this presentation, contact:

xiaoxj90@126.com

PURPOSE

It is still a challenge for radiologists to evaluate lymph nodes (LNs) metastatic status in rectal cancer with morphology when LNs are too small. However, there are about 50% metastatic LNs in rectal cancer which are less than 5 millimeters in size. The aim of this study was to investigate whether it was feasible to differentiate metastatic from non-metastatic LNs with short-axis diameter less than 5mm in rectal cancer using quantitative parameters derived from dynamic contrast-enhanced (DCE)-MRI.

METHOD AND MATERIALS

Sixty-five LNs with short-axis diameter less than 5mm from 122 patients were evaluated, including malignant LNs (n=27) and benign LNs (n=38). DCE-MR examinations were performed on a 3.0 Tesla MRI system (Magnetom Verio, Siemens, Germany). The following parameters were assessed: volume transfer constant (Ktrans), rate constant (kep), fractional extravascular extracellular space (EES) volume (ve), short-axis diameter (S), long-axis diameter (L) and short-to-long-axis diameter ratio (S/L). Receiver operating characteristic (ROC) curves were applied for analyzing significant parameters.

RESULTS

The metastatic LNs exhibited lower Ktrans than the non-metastatic LNs (P<0.001), but other parameters had no statistical differences in two groups. The AUC of Ktrans was 0.732 with the 95% CI being 0.610-0.854, and the diagnostic cutoff value was 0.088 min-1 (sensitivity, 60.5%; specificity, 81.5%).

CONCLUSION

Ktrans had moderate diagnostic performance in assessing small regional LNs in rectal cancer, making it a supplementary predictor when it is hard to distinguish malignant LNs from benign ones only by morphology.

CLINICAL RELEVANCE/APPLICATION

LN status plays a pivotal role in the treatment strategy of rectal cancer and has an influence on the prognosis of the colorectal cancer patients. Therefore, accurate LN evaluation is a necessary before treatment.



SST04

Genitourinary (Imaging of Pregnancy)

Friday, Nov. 30 10:30AM - 12:00PM Room: E260









AMA PRA Category 1 Credits ™: 1.50 ARRT Category A+ Credit: 1.75

FDA

Discussions may include off-label uses.

Participants

Dean A. Nakamoto, MD, Beachwood, OH (*Moderator*) Researcher, Canon Medical Systems Corporation; Researcher, General Electric Company

Mariam Moshiri, MD, Bellevue, WA (*Moderator*) Grant, Koninklijke Philips NV; Author with royalties, Reed Elsevier Priyanka Jha, MBBS, San Francisco, CA (*Moderator*) Nothing to Disclose

Sub-Events

SST04-01 Placenta Accreta Spectrum: Diagnosing Myometrial Invasion with Presence of Placental Bulge Sign

Friday, Nov. 30 10:30AM - 10:40AM Room: E260

Participants

Priyanka Jha, MBBS, San Francisco, CA (*Presenter*) Nothing to Disclose Ruth B. Goldstein, MD, San Francisco, CA (*Abstract Co-Author*) Nothing to Disclose Lee-may Chen, MD, San Francisco, CA (*Abstract Co-Author*) Nothing to Disclose Joseph Rabban, San Francisco, CA (*Abstract Co-Author*) Nothing to Disclose Ben Li, MD, San Francisco, CA (*Abstract Co-Author*) Nothing to Disclose Liina Poder, MD, Mill Valley, CA (*Abstract Co-Author*) Nothing to Disclose

For information about this presentation, contact:

priyanka.jha@ucsf.edu

PURPOSE

To evaluate the correlation of "placental bulge sign" with the depth of invasion in patients with placenta accreta spectrum. Placental bulge sign is defined as deviation of uterine serosa from expected plane caused by abnormal outward bulge of placental tissue. Uterine serosa may appear intact but outline shape is distorted.

METHOD AND MATERIALS

In this HIPAA- compliant, IRB-approved, retrospective study, patients undergoing MR Imaging for evaluation of placenta accreta spectrum between March 2015 to 2018 were included. Patients who delivered elsewhere were excluded. Evaluation for placental bulge was performed by 2 independent readers and its presence or absence was recorded. Surgical pathology from cesarean hysterectomy or pathology of the delivered placenta was used as a reference standard. Statistical significance was calculated using Chi square test and inter-reader agreement was evaluated with kappa analysis.

RESULTS

61 patients underwent MRI for invasive placenta over 3 years. 2 patients delivered elsewhere and were excluded. 17 cases were normal placenta. At surgical pathology from cesarean hysterectomy, there were 8 cases of placenta accreta, 29 increta & 4 percreta. Placental bulge was present in 32 of 33 increta & percreta cases (True positive= 96.9%). Placental bulge was absent in 25 of 26 cases of normal placenta or placenta accreta without myometrial invasion(True negative=96.2%). Positive & negative predictive values were 96.9% and 96.2%,respectively. The results were statistically significant(p<0.01). Estimated Kappa of 0.87 signified excellent inter reader concordance. In 1 false positive, placenta itself was normal but the bulge was present. On surgical pathology, this patient has markedly thinned, fibrotic myometrium without accreta. 1 false negative case was imaged at 16 weeks and may have been too early to diagnose the placental bulge sign.

CONCLUSION

Presence of uterine bulge can be confidently used to diagnose myometrial invasion and signifies at least placenta increta. In conjunction with other findings of invasive placenta, placental bulge was 100% predicitve of myometrial invasion. Using the bulge alone without other signs can be fraught with pitfalls and false positive results.

CLINICAL RELEVANCE/APPLICATION

Till date, no diagnostic finding for placenta increta is recognized. This diagnosis has surgical implications i.e. increased hemorrhage. Adjunct measures to control post-partum bleeding become necessary

SST04-02 ADC and IVIM: The New Perspective to Diagnose Placenta Accreta by MRI

Friday, Nov. 30 10:40AM - 10:50AM Room: E260

Yuwei Bao, Wuhan, China (*Presenter*) Nothing to Disclose Ying Pang, MBBS, Wuhan, China (*Abstract Co-Author*) Nothing to Disclose Ziyan Sun, Wuhan, China (*Abstract Co-Author*) Nothing to Disclose Qian Li, MSc, Wuhan, China (*Abstract Co-Author*) Nothing to Disclose Liming Xia, Wuhan, China (*Abstract Co-Author*) Nothing to Disclose

For information about this presentation, contact:

byw2271564204@163.com

PURPOSE

To investigate the diagnostic value of single b value (ADC) and multiple b value (IVIM) model for placenta accreta in pregnant women by MRI in functional perspective. We evaluate the differences of tissue characters between placenta accreta and normal placenta quantitatively, aimed to provide the basis for the functional diagnosis of placenta accreta by MRI.

METHOD AND MATERIALS

61 pregnant women were enrolled in our retrospective study. Among them, 24 cases were confirmed for placenta accreta by operation or pathology. The remaining 37 cases were normal placenta. Gestational weeks were 23 weeks to 36 weeks. All patients underwent DWI scanning which including 7 b values (0, 50, 100, 150, 400, 700, 1000s / mm²) and the 2 b values (0, 800 mm²). The perfusion percentage (f%), diffusion coefficient (D), pseudo-diffusion coefficient (D*) and apparent diffusion coefficient (ADC) were measured by DKI tool and Siemens workstation respectively. The enrolled cases were divided into accreta group and control group. The accreta group were divided into two groups according to implanted part and non-implanted part. And the differences between the groups were tested by the Kruskal-Wallis test.

RESULTS

The average values of f%, D * and D in normal group were $(29.66\pm7.0)\%$, (11.02 ± 3.5) and (1.45 ± 0.27) respectively, and those in the implanted part of accreta group were $(52.18\pm7.8)\%$, (12.99 ± 2.99) and (1.41 ± 0.3) respectively. Those in non-implanted part of accreta group were $(38.18\pm7.29)\%$, (11.04 ± 3.23) and (1.40 ± 0.17) respectively. ADC was (1.87 ± 0.15) mm2 / s in the normal group, (2.32 ± 0.17) mm2 / s in implanted part and (1.99 ± 0.12) mm2 / s in non-implanted part of accreta group. The above comparison groups were statistically significant except for the D value.

CONCLUSION

f% and D * ADC provide information about perfusion and diffusion of placental tissue. Placenta accreta is significantly higher than the normal one. Implanted part is also higher than the non-implanted part in the accreta cases. IVIM and DWI (ADC) can be used as a potentially functional technique for placenta accreta's diagnosis by Magnetic Resonance Imaging.

CLINICAL RELEVANCE/APPLICATION

IVIM and ADC are recommended as new fMRI sequences which provide the perfusion and diffusion imformation to diagnosis the placenta accreta

SST04-03 Predictive Parameters of the Morbidly Adherent Placenta on MRI

Friday, Nov. 30 10:50AM - 11:00AM Room: E260

Participants

Timothy W. Ng, MD, Dallas, TX (*Presenter*) Nothing to Disclose Ambereen A. Khan, MD, Dallas, TX (*Abstract Co-Author*) Nothing to Disclose Yin Xi, PhD, Dallas, TX (*Abstract Co-Author*) Nothing to Disclose Christine M. Dang, BA,BS, Dallas, TX (*Abstract Co-Author*) Nothing to Disclose Diane M. Twickler, MD, Dallas, TX (*Abstract Co-Author*) Nothing to Disclose

PURPOSE

To assess predictive indicators of morbidly adherent placenta in 2nd and 3rd trimester MRI.

METHOD AND MATERIALS

This is a retrospective study of 2nd and 3rd trimester pregnancies assessed by MR from 2007 to present. Women were included if there was suspicion for placental invasion based on surgical history and suspicion of placenta previa on ultrasound. MR was performed on 1.5 T Signa (GE Healthcare) or Magnetom (Siemens) magnet. Studies were anonymized on OsiriX (Pixmeo SARL). The MRIs were then reviewed by an experienced radiologist, specialized in OBGYN imaging, who was blinded to clinical outcomes. Twenty qualitative and quantitative parameters were assessed and compared to four clinical outcome measurements: need for cesarean hysterectomy, pathology report, impression at time of surgery, and intraoperative blood transfusions. Univariate logistic regression analysis was performed. P-values less than 0.05 were considered significant. Analyses were performed using SAS (SAS Institute Inc).

RESULTS

Of 41 women, 29 required a cesarean hysterectomy, 11 had cesarean delivery, and 1 delivered vaginally. Twenty-five of 41 required blood transfusion. On pathological assessment, 22 had evidence of invasion. Twenty-five of 41 women were deemed clinically invaded by the surgeon during delivery. Eleven out of the twenty MRI parameters assessed demonstrated statistical significance (see table). Of particular note, the greatest linear dimension of invasion, inhomogeneity, fibrin deposition, radiologist impression and assessment of degree of invasion had the greatest predictive value.

CONCLUSION

Multiple MR parameters can predict placental invasion and correlate with the need for cesarean hysterectomy, as well as pathological and surgical impressions of invasion. These defined MRI parameters provide a systematic method for assessing placental invasion. Future work should combine these and clinical variables in a larger series with multiparameteric analysis to design a standardized index.

Quantitative outcomes based assessment of MR parameters can be used to predict placental invasion and reduce diagnostic uncertainty.

SST04-04 Feasibility and Reliability of a Novel Low Cost 3D Ultrasound System in 2nd Trimester Fetal Imaging

Friday, Nov. 30 11:00AM - 11:10AM Room: E260

Awards

Student Travel Stipend Award

Participants

Julia Salinaro, BA, Durham, NC (*Presenter*) Stockholder, Incyte Corporation
Joao Ricardo Nickenig Vissoci, Durham, NC (*Abstract Co-Author*) Nothing to Disclose
Sarah Ellestad, MD, Durham, NC (*Abstract Co-Author*) Nothing to Disclose
Patricia J. Mcnally, BS, Durham, NC (*Abstract Co-Author*) Nothing to Disclose
Brian Nelson, MD, Durham, NC (*Abstract Co-Author*) Nothing to Disclose
Joshua Broder, MD, Durham, NC (*Abstract Co-Author*) President, OmniSono, Inc; Stockholder, OmniSono, Inc

For information about this presentation, contact:

julia.salinaro@duke.edu

PURPOSE

The clinical utility of ultrasound (US) is limited by operator dependence and restricted planar image capture. We have developed a novel, low cost technology to enable 3D volumetric image acquisition and automatic orientation using existing 2DUS platforms. We demonstrate its feasibility and reliability in 2nd trimester fetal imaging.

METHOD AND MATERIALS

The research device (orientation sensor, screen capture device, and computer) plus 2DUS machine (GE Voluson E8, 2D C1-5 probe) were used to capture 2 image volumes for each of 10 2nd trimester fetuses. Source images were obtained by a student with minimal US experience by sweeping the US transducer continuously across the region of interest. Acquisition and reconstruction times were automatically recorded. Volumes were reconstructed using a voxel-based algorithm designed by the research team. 3DSlicer was used for image analysis. Blinded measurements of biparietal diameter (BPD), femur, and humerus were made by the student during image review and compared to those reported by expert sonographers during routine anatomy scans performed on the same day. Inter-rater reliability was assessed using the intraclass correlation coefficient (ICC).

RESULTS

Gestational ages ranged from 16 to 23 weeks. BMI ranged from 23.2 to 30.9. Image acquisition (sweep time) and volume reconstruction required mean 29.9s and 72.9s, respectively. Fetal orientation, BPD, femur, and humerus could be identified in multiplanar and volumetric images. ICCs demonstrated strong inter-rater reliability between the student and expert report for each measurement (BPD ICC 0.88 CI95% 0.53-0.97; femur ICC 0.91 CI95% 0.63-0.98; humerus ICC 0.81 CI95% 0.22-0.95).

CONCLUSION

Comprehensive fetal image volumes were rapidly acquired by a novice and reconstructed for interactive visualization without restriction to planar images. Orientation, BPD, femur, and humerus could be identified for each fetus during image review despite no attempt at identification during scan acquisition. Measurements were highly reliable. This low cost technology could advance the clinical utility of US in obstetric imaging, especially in low resource settings.

CLINICAL RELEVANCE/APPLICATION

A novel, low cost device enabled capture of comprehensive, oriented fetal image volumes by a novice and may enhance the clinical utility of US in obstetrics, particularly in low resource settings.

SST04-05 Utility of High Resolution Images in MR Evaluation of Placenta Accreta Spectrum

Friday, Nov. 30 11:10AM - 11:20AM Room: E260

Participants

Priyanka Jha, MBBS, San Francisco, CA (*Presenter*) Nothing to Disclose Liina Poder, MD, Mill Valley, CA (*Abstract Co-Author*) Nothing to Disclose

For information about this presentation, contact:

priyanka.jha@ucsf.edu

PURPOSE

To assess the utility of high resolution (HR) images in management of placenta accreta spectrum (PAS).

METHOD AND MATERIALS

In this HIPAA- compliant, IRB-approved, retrospective study, patients undergoing 3T MR Imaging for evaluation of placenta accreta spectrum between March 2015 to 2018 were included. The images were analyzed by 2 independent readers with 5 and 15 years of experience and expertise in placental imaging. First, the large field of view (FOV) images, which include the entire uterus were analyzed for diagnostic quality and the presence or absence of findings of PAS. Additional pertinent observations included location of invasion, depth of invasion/myometrial thinning, presence of cervical invasion, bladder invasion and intra-placental hemorrhage. Next the HR, small FOV images were reviewed for diagnostic quality. These images were reviewed for any additional findings not previously identified on large FOV images. Intraoperative findings & surgical pathology were used as reference standard. Reader confidence for diagnosis was recorded on both large & small FOV images.

RESULTS

60 patients who underwent 3T MRI for invasive placenta were included in the study. Of these, HR images were found to be non-

diagnostic from respiratory motion artefact in 19 cases(32%). In remaining cases, HR images were not found to add any additional information to effect patient management in 37 cases(58%). In 2 cases, HR images were found to be helpful to exclude focal accreta. In additional 2 cases with placenta increta, HR images were helpful to exclude bladder invasion. However, when adequately performed, reader confidence for diagnosis of all accreta, increta and percreta was increased.

CONCLUSION

HR images are often degraded from artefact, probably related to their acquisition later in the protocol, reflecting increasing patient discomfort. Although HR images improve reader confidence, in most cases, no new findings or additional diagnostic information is acquired. If MRI is positive for invasive placenta, additional HR may rarely be necessary to evaluate for invasion of adjacent organs. In a negative examination, they may be helpful to exclude focal invasion. Live review of acquired images can guide need for HR aquisition.

CLINICAL RELEVANCE/APPLICATION

HR images can be omitted during MR for invasive placenta in many cases, reducing imaging time, associated cost and patient discomfort. Rarely, they are useful to assess focal invasion.

SST04-06 Estimation of Fetal Weight by Measurement of Fetal Thigh Soft-Tissue Thickness (STT) in the Late Third Trimester: Its Correlation with Hadlock's Method and Actual Birth Weight

Friday, Nov. 30 11:20AM - 11:30AM Room: E260

Participants

Chetankumar M. Mehta, MBBS,MD, Vadodara, India (*Presenter*) Nothing to Disclose Ayaz J. Dabivala, MBBS, Vadodara, India (*Abstract Co-Author*) Nothing to Disclose Arpita D. Fernandez, MD, Vadodara, India (*Abstract Co-Author*) Nothing to Disclose

For information about this presentation, contact:

drchetan_mehta@yahoo.com

PURPOSE

The purpose of this study is To assess the reliability of the linear measurement of mid-thigh soft-tissue thickness (STT). To prospectively evaluate the Formula derived by Scioscia et al using Fetal STT for estimating fetal EFW. To assess its correlation with established method of Hadlock and finally compare the results with actual birth weight post delivery.

METHOD AND MATERIALS

This was a prospective study involving 325 singleton uncomplicated pregnancies presenting to emergency department. 300 of these, who delivered within 48 hours of measurement were considered for the analysis. Scioscia et al developed the equation for Estimated Fetal Weight using multiple stepwise regression analysis (EFW = $-1687.47 + (54.1 \times \text{femur length}) + (76.68 \times \text{STT})$). This equation was utilised in following three consecutive phases: (1) Evaluation of the novel formula derived by Scioscia et al for EFW using femur length and STT , (2) Comparing the resulting EFW with existing Hadlock's equation and (3) To test the accuracy of the formula by comparison with actual birth weight.

RESULTS

The STT was significantly correlated with both abdominal circumference and birth weight (r2=0.64 and 0.34, respectively; P < 0.001). The correlation matrix of FL and STT with actual birth weight was higher (r2=0.86 and 0.80, respectively) as compared to their mutual correlation. However, among the studied estimates, the model using STT proposed herein was apparently more accurate compared with the hadlock's method owing to lower standard error and better stronger correlation with actual birth weight. Moreover, the differences between EFW and actual birth weight were more spread out using the estimates of Hadlock et al. than they were using ours.

CONCLUSION

Our findings confirm the potential of linear measurement of mid-thigh STT as a valuable parameter for the sonographic assessment of fetal growth and EFW. Scioscia's equation is apparently at least as reliable as the most widely used formulae for EFW, is easily reproducible and has a better correlation with actual birth weight.

CLINICAL RELEVANCE/APPLICATION

Accuracy of STT in estimating the estimatedd fetal weight (EFW) outperforms the routinely used formulas, so STT shall be measured in all obstetric sonograms in third trimester.

SST04-07 Predictive Accuracy of Trans-Cerebellar Diameter in the Determination of Gestational Age in Third Trimester of Pregnancy

Friday, Nov. 30 11:30AM - 11:40AM Room: E260

Participants

Omolola Akinwunmi, MBBS, Ibadan, Nigeria (*Abstract Co-Author*) Nothing to Disclose Babatunde Akinwunmi, MD,MMedSc, Boston, MA (*Presenter*) Nothing to Disclose Janet Akinmoladun, Ibadan, Nigeria (*Abstract Co-Author*) Nothing to Disclose Omolola M. Atalabi, MBBS, Ibadan, Nigeria (*Abstract Co-Author*) Nothing to Disclose

For information about this presentation, contact:

omololakinwunmi@gmail.com

PURPOSE

To determine the accuracy of trans-cerebellar diameter (TCD) measurement in sonographic assessment of gestational age in third trimester of pregnancy and its correlation with other conventional fetal biometric parameters

METHOD AND MATERIALS

A cross-sectional study was conducted on 500 pregnant women who fulfilled the inclusion criteria and were attending the hospital's antenatal clinic from January to October, 2015. Each participant underwent a transabdominal obstetric ultrasound examination for the measurement of trans-cerebellar diameter and other fetal biometric parameters using an Ultrasonix touch ultrasound machine version 5.6.4 with a 3,5MHz curvilinear probe

RESULTS

The average age of participants was 32 years. The average gestational age was 34 weeks and the mean trans-cerebellar diameter (TCD) estimation was 46.1 ± 6.1 mm (corresponding to 34.7 ± 2.6 weeks). We observed a statistically significant correlation between gestational age and TCD at third trimester with correlation co-efficient of 0.97 and R2 of 0.931 (p< 0.001). From regression analysis, a strong significant association was observed between fetal TCD at third trimester and actual gestational age. The observed sensitivity of TCD in predicting gestational age was 95.6% with a positive predictive value of 98.3%. TCD was also significantly correlated with other fetal biometeric parameters including bipareital diameter (BPD), head circumference (HC), abdominal circumference (AC) and femur length (FL) with correlation co-efficient of 0.76, 0.90, 0.79 and 0.75 respectively.

CONCLUSION

The findings of this study have suggested trans-cerebellar diameter as a reliable sonographic tool in the estimation of gestational age in normal third trimester pregnancy.

CLINICAL RELEVANCE/APPLICATION

Tran-cerebellar diameter measurement can be reliably used to estimate gestatinal age for optimal obstetric management especially for pregnant women who are not sure of their last menstrual period, those who have had no antenatal records or those who present with obstetric emergency. It is therefore recommended as part of the baseline sonographic parameter in estimating gestational age



SST05

Musculoskeletal (Spine)

Friday, Nov. 30 10:30AM - 12:00PM Room: E351

MR

мк

NR NR

AMA PRA Category 1 Credits ™: 1.50 ARRT Category A+ Credit: 1.75

FDA

Discussions may include off-label uses.

Participants

Corrie M. Yablon, MD, Ann Arbor, MI (*Moderator*) Nothing to Disclose Marcelo Bordalo-Rodrigues, MD,PhD, Sao Paulo, Brazil (*Moderator*) Nothing to Disclose

Sub-Events

SST05-01 Location of First Radiographic Spinal Fracture as Determinant of Future Vertebral Fracture Risk

Friday, Nov. 30 10:30AM - 10:40AM Room: E351

Participants

Fjorda Koromani, MD, MSc, Rotterdam, Netherlands (*Presenter*) Nothing to Disclose
Ling Oei, MD, MA, Rotterdam, Netherlands (*Abstract Co-Author*) Nothing to Disclose
Stephan J. Breda, MD, Rotterdam, Netherlands (*Abstract Co-Author*) Institutional research collaboration, General Electric Company
Enisa Shevroja, MD, MSc, Lausanne, Switzerland (*Abstract Co-Author*) Nothing to Disclose
Mohammad A. Ikram, Rotterdam, Netherlands (*Abstract Co-Author*) Nothing to Disclose
Gabriel P. Krestin, MD, PhD, Rotterdam, Netherlands (*Abstract Co-Author*) Nothing to Disclose
Fernando Rivadeneira, MD, PhD, Rotterdam, Netherlands (*Abstract Co-Author*) Nothing to Disclose
Edwin H. Oei, MD, PhD, Palo Alto, CA (*Abstract Co-Author*) Nothing to Disclose

For information about this presentation, contact:

f.koromani@erasmusmc.nl

PURPOSE

We aimed to examine if the location of a first radiographic vertebral fracture (VF) determines the risk of future incident radiographic VFs.

METHOD AND MATERIALS

Prevalent radiographic VFs were scored in 3882 subjects aged 55 years or older at baseline and after a mean follow-up of four years, using two methods: SpineAnalyzer® Quantitative Morphology (QMSA) and Algorithm Based Qualitative (ABQ). We defined the location by a) three regions: T4-T8; T9-T12 and L1-L4, b) exact vertebral level from T4 to L4. The association between the location of first prevalent VF and occurrence of future incident VFs was examined using logistic regression models adjusted for age, sex, BMI, and FN- BMD.

RESULTS

At least one incident VF was observed in 3.9 % (QMSA) and 2.0% (ABQ) of the participants. As compared to participants without VFs, individuals with multiple fractures at baseline had three (OR= 2.7; 95%CI 1.7-4.2 for QM) to 12 (OR= 12.4; 95%CI 4.8-31.9 for ABQ) times increased likelihood of suffering incident VFs. A first QMSA VF at T4-T8 was associated with increased risk of incident VF (OR= 7.7; 95%CI 4.3; 13.8), at T9-T12 (OR=2.5; 95% CI 1.0; 6.1) and L1-L4 (OR= 3.5; 95% CI 1.2; 10.5). A first ABQ VF at T4-T8 was associated with increased risk of incident VF (OR= 17.2; 95%CI 4.8; 61.4), at T9-T12 (OR=4.2; 95% CI 1.3; 12.7) but not at L1-L4 (OR= 1.9; 95% CI 0.5; 6.5). Of all vertebral levels, subjects with VFs arising at T8 had (with both methods) the highest risk for incident VFs (OR= 16.0; 95%CI 2.5; 102.2) for ABQ and (OR=11.5; 95%CI 4.5; 29.1) for QMSA, as compared to participants without VFs. Fractures at T6 scored with QMSA (OR=16.8; 95%CI 5.3; 52.6), T7 (OR=5.5; 95%CI 1.9; 15.2), L1 (OR=7.3; 95%CI 2.3; 22.6) and at T12 scored with ABQ (OR=5.6; 95%CI 1.5-20.8) were also associated with incident VFs. No other vertebral body locations were significantly associated with future VFs risk.

CONCLUSION

A first radiographic VF located at the upper thoracic region (T4-T8) and specifically at T8, is strongly and robustly associated with increased risk for future VFs independent of age, sex and BMD according to two different scoring methods.

CLINICAL RELEVANCE/APPLICATION

Since VFs in the upper thoracic spine (T4-T8), and specifically at T8, are strongly associated with increased risk for future VFs, such fractures require special attention for radiologists and warrant referral for monitoring and appropriate treatment.

SST05-02 UTE MR Morphology of Disco Vertebral Junction: Correlation with Disc Grade and T2 Values

Friday, Nov. 30 10:40AM - 10:50AM Room: E351

Student Travel Stipend Award

Participants

Tim Finkenstaedt, MD, San Diego, CA (*Presenter*) Nothing to Disclose Karen C. Chen, MD, Providence, RI (*Abstract Co-Author*) Nothing to Disclose Palanan Siriwanarangsun, MD, Bankok, Thailand (*Abstract Co-Author*) Nothing to Disclose Michael Carl, Menlo Park, CA (*Abstract Co-Author*) Researcher, General Electric Company Nirusha Abeydeera, BS, La Jolla, CA (*Abstract Co-Author*) Nothing to Disclose Sheronda Statum, San Diego, CA (*Abstract Co-Author*) Nothing to Disclose Graeme M. Bydder, MBChB, San Diego, CA (*Abstract Co-Author*) Nothing to Disclose Christine B. Chung, MD, La Jolla, CA (*Abstract Co-Author*) Nothing to Disclose Won C. Bae, PhD, La Jolla, CA (*Abstract Co-Author*) Nothing to Disclose

For information about this presentation, contact:

wbae@ucsd.edu

PURPOSE

We have previously reported unique capability of ultrashort echo time (UTE) MRI to image the morphology of the discovertebral junction (DVJ) in human lumbar spines. In this cadaveric study, we sought to determine if DVJ morphology correlates with disc Pfirrmann grades and T2 values.

METHOD AND MATERIALS

Lumbar spines from 37 cadavers (30 males, 60 ± 10.1 yrs, mean \pm SD) were imaged at 3T using UTE (TR=300 ms, TEs=0.01 and 5.5 ms, FOV=16 cm, matrix=512x512) and spin echo T2 map (TR=2000 ms, 8 TEs=10 to 70 ms) sequences. UTE images were used to define morphology of the DVJ as being normal (distinct linear high signal intensity, Figure 1A, arrows) or abnormal with focal signal loss (Figure 1A, arrowhead) and/or irregularity (Figure 1A, curved arrow). Spin echo data was used to perform Pfirrmann grading of the disc (Figure 1B), and T2 mapping (Figure 1C). T2 values of nucleus pulposus was determined using an atlas-based automated region of interest. Using statistics, we compared proportion of disc grades (Figure 1D) and nucleus T2 values (Figure 1E) when the disc was adjacent to normal DVJs, 1 abnormal DVJ, or 2 opposing abnormal DVJs.

RESULTS

Out of 278 DVJs, 198 were normal, 45 had focal signal loss, and 35 were irregular. There was greater proportion of higher disc grades (Figure 1D; chi-square p=0.00004), as well as lower T2 values (Figure 1E; ANOVA p=0.18), in discs adjacent to 2 opposing abnormal DVJs, compared to discs adjacent to normal DVJs.

CONCLUSION

These results suggest that the prevalence of abnormal DVJs in human lumbar spines are quite high (\sim 25%), and given the association between DVJ and disc degeneration, altered DVJs could be important for the etiology of disc degeneration.

CLINICAL RELEVANCE/APPLICATION

By direct assessment of the DVJ with UTE MRI early detection of beginning disc pathology in a preclinical stage is feasible. DVJ may play a biomechanical/metabolic role in support of healthy discs.

SST05-03 Feasibility of Zero Echo Time Sequence of the Cervical Spine MRI: Emphasis on Evaluation of Osseous Structures and Calcification

Friday, Nov. 30 10:50AM - 11:00AM Room: E351

Participants

Hoseok Lee, Daegu, Korea, Republic Of (*Presenter*) Nothing to Disclose Young Hwan Lee, Daegu, Korea, Republic Of (*Abstract Co-Author*) Nothing to Disclose Seo Young Park, MD, Daegu, Korea, Republic Of (*Abstract Co-Author*) Nothing to Disclose Jae Hyuck Yi, MD, Daegu, Korea, Republic Of (*Abstract Co-Author*) Nothing to Disclose Jae-Kwang Lim, Daegu, Korea, Republic Of (*Abstract Co-Author*) Nothing to Disclose Sang Yub Lee, Daegu, Korea, Republic Of (*Abstract Co-Author*) Nothing to Disclose Jongmin J. Lee, MD, PhD, Daegu, Korea, Republic Of (*Abstract Co-Author*) Nothing to Disclose

For information about this presentation, contact:

firehs@naver.com

PURPOSE

To determine the availability of zero echo time (ZET) sequence for the evaluation of osseous foraminal stenosis (OFS) and presence of peridiscal osteophyte (PO), discal calcification (DC), and ossification of posterior longitudinal ligament (OPLL) by comparison with CT as reference standard.

METHOD AND MATERIALS

Twenty one patients (mean age, 67.7 years; 10 male, 11 female) who underwent cervical MRI including 3D ZET sequence and concomitant CT within 1 months (mean interval, 3.8 days; range, 0-27 days) were retrospectively enrolled from November 2017 to March 2018. Two independent musculoskeletal radiologists evaluated ZET images and CT in separate sessions for the followings at each level: 1) grading of OFS by a visual 4-point scale from 0-3 (0=none or minimal, 1=mild, 2=moderate, 3=severe) on oblique sagittal images from C2-3 to C7/T1 (total 252 foramina); 2) presence of PO and DC of central zone of central canal from C2-3 to C7/T1 (total 126 disc level); 3) presence of OPLL from C2 to C7 (total 126 vertebral body level). Intermodality agreement between ZET and CT, and intra- and interobserver agreements for ZET were measured with the kappa (κ) statistics.

RESULTS

Intermodality agreements for detecting PO, DC, and OPLL between ZET and CT were almost perfect by 2 readers (κ =0.943-1 by reader 1; κ =0.867-1 by reader 2, respectively). Substantial to almost perfect agreements (κ =0.826 by reader 1, κ =0.787 by reader

2) were found for grading of OFS between ZET and CT. Overall intra- and interobserver agreements were substantial to almost perfect for ZET (κ =0.788-1).

CONCLUSION

The results of our study shows strong intermodality agreement between ZET sequence of MRI and CT in the cervical spine for evaluation of osseous structures and calcification.

CLINICAL RELEVANCE/APPLICATION

ZET sequence of MRI can demonstrate 'CT-like' contrast for the evaluation of cervical spine.

SST05-04 Effect of Physical Activity on Thoracic and Lumbar Disc Degeneration - a MRI Based Analysis of 385 Healthy Controls from the KORA Cohort

Friday, Nov. 30 11:00AM - 11:10AM Room: E351

Participants

Sven S. Walter, MD, Tuebingen, Germany (Presenter) Nothing to Disclose

Elke Wintermeyer, Tuebingen, Germany (Abstract Co-Author) Nothing to Disclose

Roberto Lorbeer, Greifswald, Germany (Abstract Co-Author) Nothing to Disclose

Sergios Gatidis, MD, Tubingen, Germany (Abstract Co-Author) Nothing to Disclose

Fabian Bamberg, MD, Tuebingen, Germany (Abstract Co-Author) Speakers Bureau, Bayer AG; Speakers Bureau, Siemens AG; Research Grant, Siemens AG

Konstantin Nikolaou, MD, Tuebingen, Germany (Abstract Co-Author) Advisory Panel, Siemens AG; Speakers Bureau, Siemens AG; Speaker Bureau, Bayer AG

Mike Notohamiprodjo, Munich, Germany (Abstract Co-Author) Nothing to Disclose

PURPOSE

Depending on the type and extent of physical activity, there isn't always a health preventing and health promoting impact found. Less information is available on the impact of physical activity on vertebra disc degeneration. Therefore, the purpose was to evaluate the impact of physical activity on intervertebral disc degeneration of the thoracic and lumbar spine.

METHOD AND MATERIALS

A total of 385 patients of the KORA study (Cooperative Health Research in the Augsburg Region) were included in this study. All subjects underwent full body dual-echo Dixon and T2 Haste sequence MR scan performed on a 3T scanner (Magnetom Skyra, Siemens Healthcare). Furthermore, they were tested on the basis of a standardized assessment tool inter alia on anthropometric data such as age, weight and heights as well as on physical activity/work, daily bike rides and daily walks. In order to quantify thoracic and lumbar disc degeneration, assessment was performed by two experienced radiologists according to the Pfirmann Score (Grade >2 = pathological). Statistical analysis was performed by univariate and multivariate analysis.

RESULTS

Age (BWS-Pfirrmann score:0.15; p<0.001, LWS Pfirrmann score:0.06; p<0.001 and Overall-Pfirrmann score:0.21, p<0.001), BMI (BWS-Pfirrmann score:0.11; p<0.05, LWS Pfirrmann score:0.05; p<0.01 and Overall-Pfirrmann score:0.16, p<0.01) as well as no physical activity (BWS-Pfirrmann score:1.96; p<0.01, LWS Pfirrmann score:0.99; p<0.001 and Overall-Pfirrmann score:2.95, p<0.001) lead to significant thoracic and lumbar disc degeneration when testing for univariate correlation. When testing on interdependency, we showed that age (BWS-Pfirrmann score:0.15; p<0.001, LWS Pfirrmann score:0.06; p<0.001 and Overall-Pfirrmann score:0.21, p<0.001) and no physical activity (BWS-Pfirrmann score:1.85; p<0.01, LWS Pfirrmann score:0.97; p<0.001 and Overall-Pfirrmann score: 2.82, p<0.001) still correlate with disc degeneration in multivariate analysis. On the other hand, we found that much physical activity also leads to a thoracic and lumbar disc degeneration.

CONCLUSION

No or less physical activity as well as age and BMI correlate with thoracic and lumbar disc degeneration.

CLINICAL RELEVANCE/APPLICATION

According to the literature, high physical activity increases degeneration. In contrast research for no to little physical activity and degeneration is limited. We were able to show that no or less activity results in a similar outcome.

SST05-05 The Assessment of Disco-Ligamentous Complex Injury on Magnetic Resonance Imaging (MRI) and CT Scan After Acute Cervical Spine Trauma

Friday, Nov. 30 11:10AM - 11:20AM Room: E351

Participants

You Seon Song, Busan, Korea, Republic Of (*Presenter*) Nothing to Disclose Insook Lee, Busan, Korea, Republic Of (*Abstract Co-Author*) Nothing to Disclose Jong Woon Song, Busan, Korea, Republic Of (*Abstract Co-Author*) Nothing to Disclose

For information about this presentation, contact:

shangkmii@hanmail.net

PURPOSE

to investigate useful imaging findings to assess disco-ligamentous injury after acute cervical spine trauma

METHOD AND MATERIALS

Between January 2015 and December 2017, 96 patients (11women, 85 men, age range 20-83 years, mean age 58 years) performed cervical spine MRIs and CT scans after acute trauma. We evaluated pre-vertebral hematoma, edema of cervical back muscles, high signal intensity (SI) within the spinal cord (contusion), instability, discontinuity of anterior longitudinal ligament (ALL), abnormal high SI of disc, ossification of ALL or anterior spur formation, and fracture of posterior elements. The presence or absence of disco-

ligamentous complex injury confirmed by surgery were compared with imaging findings.

RESULTS

Disco-ligamentous complex injuries were identified in 58 patients (60%) at surgery. The instability of the bony structure associated with fracture was seen only 27 patients (28%). Prevertebral hematoma (mild;26, moderate;27, severe;34) were presented in 87 (91%), edema of cervical back muscles in 75 (78%), spinal cord contusion in 86 (90%), high SI of disc in 67 (70%), and OALL or spur formation in 44 (46%). The agreement between the imaging assessment of ALL discontinuity and the disco-ligamentous injury identified in surgery was very low (kappa value; 0.25). There was a high correlation between disco-ligamentous complex injuries identified in surgery and cord contusion, abnormal high SI of disc and fractures of posterior elements on the images.

CONCLUSION

The imaging findings of cord contusion, abnormal high SI of disc and fractures of posterior elements might be useful for assessment of disco-ligamentous complex injury while the imaging assessment of ALL discontinuity is less accurate.

CLINICAL RELEVANCE/APPLICATION

If instabilities or fractures are not well seen on the images, it is difficult to directly recognize ALL rupture including disc. Therefore these secdonary imaging findings might be useful to recognize disco-ligamentous complex injury before surgery and scoring subaxial cervical spine injury.

SST05-06 Prediction of Abnormal Bone Density and Osteoporosis from Lumbar Spine MR Using Modified Dixon Quant in 257 Subjects with QCT as Reference

Friday, Nov. 30 11:20AM - 11:30AM Room: E351

Participants

Yinxia Zhao, MD, New York, NY (*Presenter*) Nothing to Disclose Mingqian Huang, MD, Syosset, NY (*Abstract Co-Author*) Nothing to Disclose Jie Ding, MS, Stony Brook, NY (*Abstract Co-Author*) Nothing to Disclose Xintao Zhang, Guangzhou, China (*Abstract Co-Author*) Nothing to Disclose Xiaodong Zhang, Guangzhou, China (*Abstract Co-Author*) Nothing to Disclose Quan Zhou, Guangzhou, China (*Abstract Co-Author*) Nothing to Disclose Chuan Huang, PhD, Stony Brook, NY (*Abstract Co-Author*) Nothing to Disclose

PURPOSE

To investigate the predictive value of using vertebral bone marrow fat fraction (BMFF) obtained from lumbar spine MRI to assess abnormal bone density and osteoporosis

METHOD AND MATERIALS

257 participants (181 females, and 76 males; age: 48.9+-14.7 years old; BMI: 22.9+-3.04 kg/m2) were recruited for the study with written consent and approved by local institutional review board (IRB). Exclusion criteria: history of known spinal tumor, trauma, dysplasia, spinal surgery and hormone therapy. All subjects underwent lumbar MRI (Ingenia 3.0T, Philips) including modified Dixon(mDixon) Quant for assessment of BMFF at L1, L2 and L3 by manually drawing ROI (region of interest) on the fat fraction map (InterlliSpace TM Portal, Philips). Quantitative computed tomography (QCT) was performed on all subjects for determination of bone mineral density (BMD). Partial correlation analysis between vertebral BMFF and BMD was first performed. Logistic regression analysis using independent training and validation data sets were performed to evaluate the performance of predicting abnormal BMD (osteopenia [80 to 120 mg/cm3] and osteoporosis [<80mg/cm3]) or osteoporosis using BMFF.

RESULTS

All participants were divided into three groups based on their BMD from QCT: normal bone density (>120mg/cm3, 135 subjects), osteopenia (82 subjects) and osteoporosis (40 subjects). Moderate inverse correlation was found between vertebral BMFF and BMD after controlling age, gender and BMI (r = -0.529, p < 0.001). The logistic regressions were trained using 2/3 of the cases and the performance was evaluated using the independent validation set comprised of the rest 1/3 cases. The area under the curve, sensitivity, specificity of predicting abnormal bone density were 0.940, 0.902, and 0.867, respectively and 0.906, 0.929 and 0.764, respectively for predicting osteoporosis. Its positive predictive value was found to be 0.907, making it an excellent screening tool.

CONCLUSION

Our study demonstrates statistically significant moderate correlation between vertebral BMFF and BMD. mDixon Quant as a fast, simple, non-invasive and non-ionizing imaging method to access vertebral BMFF has a high predictive power for identifying abnormal bone density and osteoporosis.

CLINICAL RELEVANCE/APPLICATION

Lumbar spine MRI is one of the most commonly performed study in clinical practice, added value of prediction of abnormal BMD using mDixon Quant would greatly benefit the patients.

SST05-07 Quantitative Assessment of Fat Infiltration in Lumbar Multifidus Muscle using T2-Weighted Multipoint Dixon in Patients with Low Back Pain: Correlation with Herniated Nucleus Pulposus

Friday, Nov. 30 11:30AM - 11:40AM Room: E351

Participants

Yeo Ryang Kang, MD, Goyang, Korea, Republic Of (*Presenter*) Nothing to Disclose
Seul Ki Lee, MD, Gyeonggi, Korea, Republic Of (*Abstract Co-Author*) Research Grant, Dongkook Life Science Co, Ltd
Joon-Yong Jung, MD, Seoul, Korea, Republic Of (*Abstract Co-Author*) Nothing to Disclose
Jin-Hee Jung, Gyeonggi-do, Korea, Republic Of (*Abstract Co-Author*) Nothing to Disclose
Jae Jun Yang, Goyang, Korea, Republic Of (*Abstract Co-Author*) Nothing to Disclose

For information about this presentation, contact:

PURPOSE

This study is to quantitatively assess fat infiltration in lumbar multifidus muscle using T2-weighted multipoint Dixon (T2 Dixon) and to reveal the relationship with herniated nucleus pulposus (HNP) in patients with low back pain (LBP).

METHOD AND MATERIALS

......

Among 241 patients who performed MRI of lumbar spines (L-spine) for LBP on 1.5T scanner, 114 patients (age, $42.7\pm1.4y$; 58 females) were enrolled, excluding patients with prior spine surgery, malignancy, compression fracture, spondylolisthesis, spondylitis, and advanced spinal stenosis. The presence and level of HNP were recorded. Two readers independently measured multifidus sectional area from T2 Dixon of axial L3 level and coronal L-spine. Volumetric multifidus measurement was performed using Syngo.via. Fat fraction (Ff) of multifidus was calculated from signal intensity (SI) of in-phase (IP) and out-of-phase (OP) images by using the formula: '(SIIP-SIOP)/2SIIP x 100(%)'.

RESULTS

Inter-reader agreement of Ff for each method and inter-method agreement of Ff were excellent (ICCs: 0.81 to 0.98). 20 patients had no HNP (age, $39.3\pm15.7y$; 9 females; BMI, 22.4 ± 2.4) and 94 patients had HNP (age, $43.7\pm14.6y$; 49 females; BMI, 25.3 ± 3.4). Among positive HNP, 76 patients had HNP less than 3 levels (age, $40.8\pm13.9y$; 38 females; BMI, 25.3 ± 3.4) and 18 patients had multi-level (>=3 levels) HNP (age, $56.0\pm10.3y$; 11 females; BMI, 25.4 ± 3.7). In positive HNP, coronal Ff ($20.1\pm2.8\%$) and volumetric Ff ($19.8\pm2.6\%$) were significantly higher than those of negative HNP ($18.0\pm3.8\%$, $17.6\pm3.2\%$; P=.005, .002, respectively). In multi-level HNP, axial-L3 Ff ($22.1\pm2.9\%$) and coronal Ff ($22.2\pm2.0\%$) were significantly higher than those of HNP less than 3 levels ($19.0\pm3.3\%$, $19.6\pm2.7\%$; P<.001 for each). Multivariate logistic regression analysis adjusted for age, sex, and BMI showed that BMI is significantly associated with HNP (odds ratio [OR]: 1.376, P=.004), while age and coronal Ff are significantly associated with multi-level HNP (OR: 1.075, 1.524, P=.021, 0.15, respectively).

CONCLUSION

Coronal Ff from T2 Dixon of L-spine has the best discriminating power to quantify the fatty infiltration of lumbar multifidus in patients of HNP. Increased coronal Ff was significantly associated with multilevel HNP.

CLINICAL RELEVANCE/APPLICATION

The fat fraction of lumbar multifidus using coronal T2 Dixon is recommended method for patient of LBP to discriminate multi-level HNP from one or two level HNP.

SST05-08 Epidural Fibrosis and Nerve Root Changes on Magnetic Resonance Imaging (MRI) After Lumbar Disc Surgery: Correlation with Clinical Symptoms

Friday, Nov. 30 11:40AM - 11:50AM Room: E351

Participants

Hie Bum Suh, MD, Pusan, Korea, Republic Of (*Presenter*) Nothing to Disclose Insook Lee, Busan, Korea, Republic Of (*Abstract Co-Author*) Nothing to Disclose You Seon Song, Busan, Korea, Republic Of (*Abstract Co-Author*) Nothing to Disclose Jong Woon Song, Busan, Korea, Republic Of (*Abstract Co-Author*) Nothing to Disclose

For information about this presentation, contact:

shangkmii@hanmail.net

PURPOSE

To investigate correlation between epidural fibrosis and nerve root changes on Magnetic resonance image (MRI) and clinical symptoms after lumbar disc surgery

METHOD AND MATERIALS

Between January 2010 and May 2017, 75 patients (32 women, 43 men, age range 30-87 years, mean age 60 years) who performed lumbar disc surgery at unilateral side of only one level examined follow-up lumbar spine MRI due to back pain or variable neurologic symptoms. We investigated size change, abnormally increased signal intensity, distinction in the epidural space, displacement and compression of nerve root and epidural fibrosis at operative site on mainly axial sequences. Also, the presence or absence of arachnoiditis was evaluated. The clinical symptoms were compared with MR imaging findings using statistical analysis.

RESULTS

Symptoms related with lumbar disc surgery were found in 31 patients (41.3%). The size change of nerve root was seen in 43 patients and high SI of nerve root in 44. The displacement of nerve root was presented in 11 patients and there were no patients showing definite nerve root compression. 51 patients showed epidural fibrosis and definite distinction of nerve root in the epidural space was seen in 45 patients. Arachnoiditis was seen in only 22 patients. The size change of nerve root at surgery site was the only significant MR finding correlating with symptom (p < 0.05).

CONCLUSION

The size change of nerve root at surgery site was significantly correlated with new or persistent symptoms after lumbar disc surgery.

CLINICAL RELEVANCE/APPLICATION

MR imaging findings of size change and abnormally high SI of nerve root, indistinction of nerve root in the epidural space and epidural fibrosis are common after lumbar disc surgery. However, these findings except size change of nerve root were post-operative changes unrelated to new or persistent symptoms.

SST05-09 Assessment of Osseous Cervical Foraminal Stenosis in Spinal Radiculopathy Using Susceptibility-Weighted MRI

Participants

Guenther Engel, MD, Berlin, Germany (*Presenter*) Nothing to Disclose Yvonne Y. Bender, Berlin, Germany (*Abstract Co-Author*) Nothing to Disclose Lisa C. Adams, MD, Berlin, Germany (*Abstract Co-Author*) Nothing to Disclose Sarah M. Boker, Berlin, Germany (*Abstract Co-Author*) Nothing to Disclose Moritz Wagner, MD, Berlin, Germany (*Abstract Co-Author*) Nothing to Disclose Ute L. Fahlenkamp, MD, Berlin, Germany (*Abstract Co-Author*) Nothing to Disclose Gerd Diederichs, MD, Berlin, Germany (*Abstract Co-Author*) Nothing to Disclose

Bernd K. Hamm III, MD, Berlin, Germany (Abstract Co-Author) Research Consultant, Canon Medical Systems Corporation; Stockholder, Siemens AG; Stockholder, General Electric Company; Research Grant, Canon Medical Systems Corporation; Research Grant, Koninklijke Philips NV; Research Grant, Siemens AG; Research Grant, General Electric Company; Research Grant, Elbit Imaging Ltd; Research Grant, Bayer AG; Research Grant, Guerbet SA; Research Grant, Bracco Group; Research Grant, B. Braun Melsungen AG; Research Grant, KRAUTH medical KG; Research Grant, Boston Scientific Corporation; Equipment support, Elbit Imaging Ltd; Investigator, CMC Contrast AB

Marcus R. Makowski, Berlin, Germany (Abstract Co-Author) Nothing to Disclose

For information about this presentation, contact:

quenther.engel@charite.de

PURPOSE

The aim of this study was to evaluate the diagnostic performance of susceptibility-weighted MRI for the evaluation of osseous foraminal stenosis of the cervical spine compared to conventional MR sequences, using CT as a reference standard.

METHOD AND MATERIALS

Twenty-one patients with suspected radiculopathy of the cervical spine were prospectively included. As standard of reference, 280 neuroforamen of the cervical spine, including 58 foraminal stenosis, were identified on sagittal CT images. T1, T2 and SW-MRI of the cervical spine were performed. For this study, the presence of foraminal stenosis was assessed on sagittal views on T1, T2 and SW-MR images. Sensitivity / specificity were calculated and differences in detection rate, severity scoring and sagittal diameter of spinal foraminal stenosis between the different sequences were tested. CT was used as reference standard for all analysis.

RESULTS

56 of 58 osseous foraminal stenosis could be correctly identified on SW-MR magnitude images. SW-MR imaging achieved a sensitivity of 96.6% and specificity of 99.5% for the identification of foraminal stenosis of the cervical spine. In comparison, conventional T1 spine MR sequences achieved a sensitivity and specificity of 43.1% and 100% respectively. Conventional T2 spine MR sequences achieved a sensitivity and specificity of 65.5% and 99.1%, respectively. The overall detection rate was significantly (p0.05) higher on SW-MR imaging and there was no significant difference (p>0.05) in severity scoring compared to CT imaging. T1/T2-weighted MR underestimated the degree of foraminal stenosis. Intermodality and interobserver agreement were highest for SW-MR sequences.

CONCLUSION

Susceptibility-weighted MRI enables the reliable detection of osseous foraminal stenosis of the cervical spine in patients with spinal radiculopathy with a higher sensitivity and specificity compared to conventional T1/T2 MR sequences, with CT as a reference standard.

CLINICAL RELEVANCE/APPLICATION

The main limitation of MRI, compared to CT, is limited value for the detection of osteophytic changes as a cause of foraminal stenosis. Standard MR T1 and T2-weighted sequences often do not allow a differentiation these changes. Therefore, CT or conventional radiographs are often required to detect and quantify these changes. SW-MRI may therefore replace additional tests and prevent radiation exposure for patients as well as speed up diagnostic work up.



SST06

Nuclear Medicine (Abdomen and Pelvis Nuclear Imaging)

Friday, Nov. 30 10:30AM - 12:00PM Room: E261







NM

AMA PRA Category 1 Credits ™: 1.50 ARRT Category A+ Credit: 1.75

Participants

Michael V. Knopp, MD, PhD, Columbus, OH (Moderator) Nothing to Disclose

Ephraim E. Parent, MD, PhD, Ponta Vedra Beach, FL (Moderator) Research support, Blue Earth Diagnostics Ltd; Research support,

Advanced Accelerator Applications SA

Andrew C. Homb, MD, Rochester, MN (Moderator) Nothing to Disclose

Sub-Events

SST06-01 Liver/Spleen Scintigraphy: An Old Technique with a current Application

Friday, Nov. 30 10:30AM - 10:40AM Room: E261

Participants

Maxwell P. Cocco, Ann Arbor, MI (Presenter) Nothing to Disclose

Daniel J. Wale, DO, Ann Arbor, MI (Abstract Co-Author) Nothing to Disclose

Timothy Frankel, Ann Arbor, MI (Abstract Co-Author) Nothing to Disclose

Richard K. Brown, MD, Ann Arbor, MI (Abstract Co-Author) Nothing to Disclose

James H. Ellis, MD, Ann Arbor, MI (Abstract Co-Author) Research Consultant, General Electric Company; Medical Advisory Board, Nuance Communications, Inc

William J. Weadock, MD, Ann Arbor, MI (Abstract Co-Author) Owner, Weadock Software, LLC

Benjamin L. Viglianti, MD, PhD, Ann Arbor, MI (Abstract Co-Author) Nothing to Disclose

For information about this presentation, contact:

bviglia@med.umich.edu

PURPOSE

Cross sectional imaging of the abdomen on occasion can demonstrate incidental pancreatic/peri-pancreatic lesions of unknown etiology. Although these lesions sometimes have the appearance of splenic tissue, situation arise were metastasis and/or primary pancreatic etiology are also on the differential. Scintigraphy with Tc99m Sulfur colloid or heat damaged RBC can be a useful diagnostic tool in identifying the presence of splenic tissue, suggesting a benign etiology for these lesions although the accuracy is uncertain.

METHOD AND MATERIALS

Retrospective review of all non-PET nuclear medicine studies in which a lesion in the upper abdomen were the cause of imaging from 1/2000 to 7/2017. Studies performed for hepatic artery perfusion or liver parenchyma lesion were excluded. Patients charts were reviewed, the date/results of the index study, subsequent imaging, clinical management, along with the last recorded encounter in our electronic medical record to establish benignity in the absence of pathology.

RESULTS

Initial review obtained 623 studies performed, a majority (74%) for hepatic artery perfusion. Liver lesion evaluation was performed in 7% of the cases (hemangioma or FNH). The remainder of the cases were done for evaluating splenic tissue in ITP (\sim 5% of cases), ectopic splenic tissue (\sim 9% after trauma or splenectomy) or to evaluate incidental pancreatic/peri-pancreatic lesions with potential neoplastic etiology (\sim 5% cases, 34 cases total). Of these 34 cases, pathology was obtained in 12/34 patients. Imaging was correct in identifying nonsplenic tissue in 11/12 cases (92%). One case was splenic tissue on path, but was not identified on imaging. For the patients that had imaging indicating splenic tissue without subsequent pathology (12/22), follow up of the patient occurred > 3-years.

CONCLUSION

Pancreatic/peri-pancreatic lesions of unknown etiology can present a diagnostic challenge with causes ranging from benign splenic tissue to a neoplastic process. Scintigraphy offers a unique ability to identify ectopic splenic tissue with a high degree of diagnostic accuracy, >90%, yielding a benign diagnosis and limiting the need of further workup.

CLINICAL RELEVANCE/APPLICATION

Liver/Spleen imaging with Tc99m Sulfur colloid or damaged RBC can accurately identify incidental pancreatic/peri-pancreatic lesions as ectopic splenic tissue not requiring further workup.

The Diagnostic Accuracy of Brain-Lung Uptake and Whole-Body Uptake Derived from Technetium-99m-Labeled Macroaggregated Albumin (MAA) Lung Perfusion Scan for the Diagnosis of Hepatopulmonary Syndrome

Participants

He Zhao, Beijing, China (*Abstract Co-Author*) Nothing to Disclose Jiaywei Tsauo, Beijing, China (*Presenter*) Nothing to Disclose Xiaowu Zhang, Beijing, China (*Abstract Co-Author*) Nothing to Disclose Tao Gong, Beijing, China (*Abstract Co-Author*) Nothing to Disclose Jingui Li, Beijing, China (*Abstract Co-Author*) Nothing to Disclose Xiao Li, PhD, Chengdu, China (*Abstract Co-Author*) Nothing to Disclose

For information about this presentation, contact:

hezhaoo@gmail.com

PURPOSE

Technetium-99m-labeled macroaggregated albumin (MAA) lung perfusion scan is considered as a complementary tool for detecting intrapulmonary vascular dilations (IPVD), which is an essential criterion for diagnosing hepatopulmonary syndrome (HPS). The purpose of this study was to compare the diagnostic accuracy of brain-lung uptake and whole-body uptake for detecting IPVD.

METHOD AND MATERIALS

From December 2014 to October 2015, all patients with chronic liver disease and/or portal hypertension, undergoing interventional radiological procedures at our institution were eligible for inclusion in this prospective study. The brain-lung uptake was calculated using the geometric mean (GMT) of technetium counts around the brain and lung in the following formula: (GMTbrain / 0.13) / (GMTbrain / 0.13 + GMTlung). The brain-lung uptake was regarded as positive when the MAA shunt fraction was > 6%. The whole-body uptake was calculated using the GMT of technetium counts around the lung and whole body in the following formula: (1 - GMTlung / GMTwhole-body)

RESULTS

A total of 69 patients were included, IPVD was detected in 32 (46%) patients by contrast-enhanced echocardiography. Of these patients, 26 (38%) patients with elevated AaO2 were diagnosed as HPS. The brain-lung uptake was similar between those with or without IPVD [median, 3.5 (interquartile range (IQR), 2.6-5.8) % vs. 3.1 (IQR, 2.5-4.9) %; P = 0.245]. However, the whole-body uptake was significantly higher in the patients with IPVD than those without IPVD (48.0 \pm 6.1 % vs. 40.1 \pm 8.1 %; P = 0.001). Multivariable logistic regression showed that whole-body uptake was the only independent predictor that associated with the presence of IPVD [odds ratio (OR), 1.29; 95% CI, 1.07-1.55; P = 0.008]. The AUC values of the whole-body uptake for detecting IPVD were 0.75 (95% CI, 0.60-0.86). The optimal cut-off values of whole-body uptake for detecting IPVD was 42.5%. The sensitivity, specificity, and accuracy for detecting IPVD were 100%, 52%, and 74%, respectively.

CONCLUSION

Whole-body uptake could be a useful alternative to CEE and brain-lung uptake for detecting IPVD, especially in patients with mild or moderate HPS.

CLINICAL RELEVANCE/APPLICATION

Whole-body uptake derived from MAA lung perfusion scan could be a useful alternative to contrast-enhanced echocardiography and brain-lung uptake for detecting intrapulmonary vascular dilations.

SST06-03 Diagnosing Hepatobiliary Disease during Myocardial Perfusion Imaging Using Tc99m Methoxy Isobutyl Isonitrile

Friday, Nov. 30 10:50AM - 11:00AM Room: E261

Participants

Haitham M. Elsamaloty, MD, Holland, OH (*Abstract Co-Author*) Nothing to Disclose Mohamad F. Bazerbashi, MD, Ann Arbor, MI (*Presenter*) Nothing to Disclose Eslam Y. Youssef, MD, Toledo, OH (*Abstract Co-Author*) Nothing to Disclose Lina Elsamaloty, Toledo, OH (*Abstract Co-Author*) Nothing to Disclose Hassan B. Semaan, MD, Toledo, OH (*Abstract Co-Author*) Nothing to Disclose

For information about this presentation, contact:

haitham.elsamaloty@utoledo.edu

PURPOSE

Tc99m Methoxy Isobutyl Isonitrile (MIBI) has been used for myocardial perfusion imaging (MPI) for the detection of ischemia. This study aimed to investigate the feasibility of effectively evaluating cystic duct patency, during routine visual analysis of the raw MPI and/or with the 3-D reconstructed data.

METHOD AND MATERIALS

A retrospective study of 91 patients undergoing cardiac Sestamibi scan for acute chest pain, and HIDA scan (within no more than 3 months) for suspected gallbladder obstructive disease (GBD). Gallbladder visualization during either the rest or stress portion of the MIBI study was indicative of cystic duct patency. These results were compared to those by the HIDA studies.

RESULTS

Ten patients had the MIBI and HIDA studies 4 days apart, both studies agreed 100% with the diagnosis of cystic duct patency. Sixteen patients had both studies between 4 days and 3 weeks and had an agreement of 87.5% with cystic duct patency. Sixtyone patients had both studies 3 weeks to 3 months apart and had an agreement of 80% with cystic duct patency.

CONCLUSION

The initial results of this study indicate that MPI with Tc99m MIBI is useful in detecting a patent cystic duct and should help in eliminating unnecessary additional Gallbladder testing.

CLINICAL RELEVANCE/APPLICATION

If the interpreting physician was made aware of the benefits of being able to diagnose cystic duct obstruction and gallbladder disease when using the Tc-99m cardiac sestamibi to evaluate myocardial perfusion, it would lead to earlier diagnosis and more efficient patient care; thus, decreasing the amount of imaging that patients need to go through to reach a diagnosis of gallbladder obstruction, which will lead to decreased cost.

SST06-04 Qualitative and Quantitative Analysis of 68ga-DOTA-Peptide Uptake for Identifying Neuroendocrine Tumor in Uncinated Process of Pancreas

Friday, Nov. 30 11:00AM - 11:10AM Room: E261

Participants

Amrita Kasat, MBBS,MD, Mumbai, India (*Presenter*) Nothing to Disclose Sachin K. Gawde, MD, Mumbai, India (*Abstract Co-Author*) Nothing to Disclose

For information about this presentation, contact:

amrita.lahotinm@gmail.com

PURPOSE

68Ga-DOTA-peptide is a somatostatin analogue used for imaging neuroendocrine tumors (NET). Various organs demonstrate physiological distribution of which uncinate process of pancreas is a particular concern because uncinate is a common site for NET and great variability of tracer distribution at this location is making the interpretation difficult. Thus aim is to characterize 68Ga-DOTA-peptide distribution in uncinate process and useful hints for distinguishing pathology from physiological distribution.

METHOD AND MATERIALS

83 68Ga-DOTApeptide PET CT scans of 25 patients done between May 2009 and Oct 2014 were reviewed retrospectively. 66 scans from 20 subjects tumor involvement of uncinate process was excluded based on pathological, clinical, radiological evaluation and atleast 1 year follow-up. 17 scans from 5 subjects neuroendocrine tumor involvement of the uncinate process was confirmed by histology and/or multimodality imaging. Statistical analyses univariable Generalized Estimating Equations was carried out for normal uncinate uptake features. Comparison of normal vs tumor uptake was carried out using Mann Whitley test.

RESULTS

There are 3 types of normal distribution in uncinate process diffuse, focal and multifocal. Average SUVmax for normal uncinate process is 5.88 + /-3.34 with highest to be 21.07. The average SUVmax for uncinate neuroendocrine tumor is 76.28 + /-44.72 with lowest to be 27. Tumor/spleen ratio is significantly higher than uncinate/spleen ratio (8.98 + /-3.83 with lowest 3.67 + 0.36 + /-0.41 with highest 3.67 + 0.36 + 0.36 + 0.36 + 0.36 with highest 3.67 + 0.36 + 0.36 + 0.36 with highest 3.67 + 0.36 + 0.36 + 0.36 with highest 3.67 + 0.36 + 0.36 + 0.

CONCLUSION

Distribution pattern and uptake intensity in uncinate process vary greatly between patients and between scans. Pituitary and spleen uptake serve as references in judging the nature of uptake in uncinate. Low grade NET in uncinate process demonstrate significantly higher than normal uptake and greater than normal uncinate/spleen ratio.

CLINICAL RELEVANCE/APPLICATION

SUVmax and uncinate/spleen ratio is useful for differentiating normal versus tumor. SUVmax of 25 and uncinate/spleen ratio of 1.5 are recommended reasonable cutoff values for this purpose. But tumor involvement in uncinate process should be made by not only by presentation on PET scan but correlating with other imaging findings and/or biopsy result.

SST06-05 Hepatobiliary Scintigraphy versus Ultrasound in the Evaluation of Acute Cholecystitis: An Institutional Review

Friday, Nov. 30 11:10AM - 11:20AM Room: E261

Participants

Timur Kotlyar, MD, New Hyde Park, NY (*Presenter*) Nothing to Disclose Christopher Kyriakakos, MD, New Hyde Park, NY (*Abstract Co-Author*) Nothing to Disclose Vincent Lau, MD, New Hyde Park, NY (*Abstract Co-Author*) Nothing to Disclose Maria B. Tomas, MD, New Hyde Park, NY (*Abstract Co-Author*) Nothing to Disclose Christopher J. Palestro, MD, New Hyde Park, NY (*Abstract Co-Author*) Nothing to Disclose Meera Raghavan, MD, Tampa, FL (*Abstract Co-Author*) Nothing to Disclose

PURPOSE

Acute cholecystitis is a common entity. Hepatobiliary radionuclide scintigraphy (HIDA) is considered the gold standard for diagnosing cholecystitis, with sensitivity up to 97%. Ultrasound (US) is the preferred modality in the initial evaluation of acute cholecystitis, due to its availability, low cost, and short examination time, despite being less sensitive than HIDA. At our institution, US is the initial imaging study of choice, and a HIDA is subsequently obtained for equivocal studies. We aim to evaluate the concordance of US and HIDA, and to identify clinical and/or laboratory parameters which may correlate with equivocal US in order to better guide patient management.

METHOD AND MATERIALS

Following institutional IRB approval, MONTAGE was used to search our reporting database between October 2016 and October 2017. HIDA results were categorized as "positive" or "negative". US results were categorized as "negative", "positive", or "equivocal" for the assessment of acute cholecystitis. Clinical and laboratory data were also collected.

RESULTS

A total of 307 patients underwent both US and HIDA (n=307) with 43% (n=132) with an equivocal US. 35% (n=107) of these patients had discordant US and HIDA. Of the cases with an equivocal US, 43% (n=57) underwent cholecystectomy. At pathology,

51% (n=29) had acute cholecystitis with a positive HIDA and 4% (n=2) had acute cholecystitis with a negative HIDA. 14% (n=8) had chronic cholecystitis with a positive HIDA, and 32% (n=18) had chronic cholecystitis with a HIDA negative for acute cholecystitis. In patients with equivocal US, HIDA had a sensitivity of 93.6% and specificity of 69.2%.

CONCLUSION

Over one-third discordance between US and HIDA can have significant clinical implications. Given the high sensitivity of HIDA in patients with equivocal US, initial evaluation with HIDA may be more appropriate in patients in whom US is likely to be equivocal, possibly leading to decreased time to surgery and length of stay.

CLINICAL RELEVANCE/APPLICATION

Our results may elucidate factors influencing HIDA/US concordance, and whether US or HIDA is a more appropriate initial test. Imaging utilization may influence length of stay and time to surgery.

SST06-06 Identification and Characterization of Myocardial Metastases in Neuroendocrine Tumor Patients Using 68Ga-DOTATATE PET-CT

Friday, Nov. 30 11:20AM - 11:30AM Room: E261

Participants

Wolfgang G. Kunz, MD, Munich, Germany (Presenter) Grant, Medtronic plc

Ralf S. Eschbach, Munich, Germany (Abstract Co-Author) Nothing to Disclose

Robert Stahl, MD, Munich, Germany (Abstract Co-Author) Nothing to Disclose

Philipp M. Kazmierczak, MD, Munich, Germany (Abstract Co-Author) Nothing to Disclose

Peter Bartenstein, Munich, Germany (Abstract Co-Author) Nothing to Disclose

Axel Rominger, Munich, Germany (Abstract Co-Author) Nothing to Disclose

Christoph Auernhammer, MD, PhD, Munich, Germany (Abstract Co-Author) Research Grant, Novartis AG Speaker, Novartis AG Research Grant, Ipsen SA Speaker, Ipsen SA Advisory Board, Novartis AG

Christine Spitzweg, Munich, Germany (Abstract Co-Author) Advisory Board, Swedish Orphan Biovitrum AB; Advisory Board, Bayer AG; Advisory Board, Eisai Co, Ltd; Advisory Board, AstraZeneca PLC; Speaker, Swedish Orphan Biovitrum AB; Speaker, Bayer AG; Speaker, Eisai Co, Ltd; Speaker, AstraZeneca PLC

Jens Ricke, MD,PhD, Munich, Germany (Abstract Co-Author) Research Grant, Sirtex Medical Ltd Research Grant, Bayer AG Clemens C. Cyran, MD, Munich, Germany (Abstract Co-Author) Research Grant, iThera Medical GmbH Speakers Bureau, Siemens AG

For information about this presentation, contact:

wolfgang.kunz@med.lmu.de

PURPOSE

Focal 68Ga-DOTATATE PET lesions within the myocardium of neuroendocrine tumor (NET) patients are observed in clinical practice. We determined the frequency and characteristics of lesions that are consistent with cardiac metastasis and assessed the lesion detection rate of conventional imaging.

METHOD AND MATERIALS

629 patients who underwent 68Ga-DOTATATE PET-CT at a supraregional comprehensive cancer center on NET were included from a consecutive registry. Inclusion criteria were: (1) focal 68Ga-DOTATATE tracer uptake within the myocardium in more than two sequential PET exams, and (2) contrast-enhanced CT. To determine the diagnostic accuracy of conventional CT imaging, a case-control cohort with a ratio of 1:3 was used. PET and CT were independently analyzed by two blinded readers. Cohen's k was assessed for interreader agreement. Descriptive statistics were applied for frequencies and characteristics and group comparisons were analyzed using the Fisher's exact test.

RESULTS

The prevalence of myocardial metastases related to the registry was 2.4% with 15/629 NET patients fulfilling the inclusion criteria and a total of 21 focal myocardial 68Ga-DOTATATE tracer uptakes detected. Myocardial lesions were most frequently located in the left ventricle (43%) and the septum (43%). No patient demonstrated a pericardial effusion. Patients with myocardial metastases did not differ in demographics, tumor grading, disease stage or circulating tumor markers compared to the overall registry (all p>0.05). The patient characteristics are shown in Table 1. Higher Ki67-Indices were observed (p=0.049) for patients with myocardial metastases. Interreader agreement for PET assessment was excellent (Cohen's =1.0). CT reading showed a sensitivity of 19% (95% confidence interval: 6%-43%) at a specificity of 100% (95% confidence interval: 90%-100%). A patient example with a CT-detected cardiac metastasis is provided in Figure 1.

CONCLUSION

68Ga-DOTATATE PET enables detection of myocardial metastatic lesions in NET patients. In contrast, standard morphologic CT imaging provides very limited sensitivity.

CLINICAL RELEVANCE/APPLICATION

68Ga-DOTATATE PET imaging provides added diagnostic value in the initial staging of NET patients with cardiac metastasis and may provide further guidance during patient follow-up.

SST06-07 Evaluation of [18F]-FDG PET/MR Enterography in the Assessment of Ileocolonic Inflammation in Crohn's Disease - Which Surrogate Marker is Better? MaRIA, Clermont, PET, or PET-MR index?

Friday, Nov. 30 11:30AM - 11:40AM Room: E261

Participants

Lale Umutlu, MD, Essen, Germany (*Abstract Co-Author*) Consultant, Bayer AG
Benedikt M. Schaarschmidt, MD, Essen, Germany (*Presenter*) Stockholder, Bayer AG; Stockholder, General Electric Company;
Stockholder, Siemens AG; Stockholder, Teva Pharmaceutical Industries Ltd
Jost Langhorst, Essen, Germany (*Abstract Co-Author*) Nothing to Disclose
Johannes Grueneisen, Essen, Germany (*Abstract Co-Author*) Nothing to Disclose

Verena Ruhlmann, Essen, Germany (*Abstract Co-Author*) Nothing to Disclose Karsten J. Beiderwellen, MD, Essen, Germany (*Abstract Co-Author*) Nothing to Disclose Julian Kirchner, Dusseldorf, Germany (*Abstract Co-Author*) Nothing to Disclose Aydin Demircioglu, Essen, Germany (*Abstract Co-Author*) Nothing to Disclose

Felix Nensa, MD, Essen, Germany (Abstract Co-Author) Nothing to Disclose

Ken Herrmann, Essen, Germany (Abstract Co-Author) Co-founder, SurgicEye GmbH; Stockholder, SurgicEye GmbH; Consultant, Sofie Biosciences; Consultant, Ipsen SA; Consultant, Siemens AG; Research Grant, Advanced Accelerator Applications SA; Research Grant, Ipsen SA

Yan Li, Essen, Germany (Abstract Co-Author) Nothing to Disclose

For information about this presentation, contact:

Lale.Umutlu@uk-essen.de

PURPOSE

To define a PET-MR index as hybrid surrogate marker and evaluate the diagnostic performance of validated MR indices, PET and PET-MR index in detecting ileocolonic inflammation in Crohn's disease (CD) with an integrated whole-body PET/MR.

METHOD AND MATERIALS

53 CD patients with recurrent symptoms underwent ileocolonoscopy with biopsy (reference standard) and PET/MR enterography. 7 ileocolonic segments were divided. The endoscopic activity of inflammation was determined by Simplified Endoscopic Activity Score for CD (SES-CD) and categorized in absent, mild to moderate and severe. Receiver Operating Characteristic (ROC) curves were performed and tested against each other with DeLong' test. Correlations between surrogate markers and SES-CD were tested with Spearmann's rank correlation test.

RESULTS

303 ileocolonic segments were analyzed. A simplified PET-MR index was defined as 0.87*wall thickness + 1.97*edema + 0.83*ulceration + 0.55*SUVmax ratio + 1.14. In detecting active disease (defined as SES-CD >= 2), MaRIA, Clermont score and PET-MR Index as multiparametric indicies performed significantly better than monoparametric SUVmax ratio (areas under ROC: 0.916, 0.914, 0.924 and 0.857, p < 0.05). In predicting severe inflammation with ulcerations, among all the surrogate makers (areas under ROC fo MaRIA, Clermont, PET-MR index and PET: 0.962, 0.970, 0.971 and 0.935) only a slightly significant difference could be observed between MaRIA and Clermont score (p = 0.02) in their operating characteristics. All surrogate markers correlated moderately with SES-CD both on segmental basis and gobal level (0.4 , all <math>p < 0.001).

CONCLUSION

As hybrid surrogate marker comprised of MR parameters and PET component, PET-MR index yielded a significantly increased diagnostic performance compared to PET alone. However, neither in predicting active disease nor in detecting severe ulcerative inflammation, PET-MR index could outperform MaRIA or Clermont significantly. Nevertheless, PET-MR index showed the best operating characteristics among all the surrogate markers.

CLINICAL RELEVANCE/APPLICATION

PET/MR enterography provides valuable surrogate markers for assessment of active disease in Crohn's disease.

SST06-08 Dynamic Study by PET/CT: Phantom Study and Clinical Trial on Sequential 26 Cases of Malignant Lesions of Uterus

Friday, Nov. 30 11:40AM - 11:50AM Room: E261

Participants

Eri O'Uchi, MD, Kamogawa City, Japan (*Presenter*) Nothing to Disclose Toshihiro O'uchi, MD,PhD, Kamogawa, Japan (*Abstract Co-Author*) Nothing to Disclose

PURPOSE

Dynamic study of PET/CT with 18F-FDG has not been reported up to now. The purpose of this study was to check the reliability of SUVmax on GE IQ PET/CT by phantom study, and to compare tumor 18F-FDG uptake between two phases of 30-second acquisition of dynamic deep-inspiration breath-hold PET/CT (BHPC) before and after 5 to 7 steps of 150-sec free-breathing PET/CT(FBPC). These sequence was named 'Dynamic study by PET/CT'.

METHOD AND MATERIALS

The PET/CT scanner was GE IQ with 26cm BGO crystal and PET images were reconstructed by patented new method of successive approximation (25-times). Before the clinical study, a phantom study was performed using an International Electrotechnical Commission body phantom set corresponding to the NU 2-2001 standard. The phantom set was consisted of a torso cavity and two spheres (inner diameters: 10, 13, 17, 22, 28, and 37 mm). The torso cavity was filled with water, and the 6 spheres were filled with 18F-FDG solutions of the same radioactivity concentration (25 kBq/mL). We studied sequential 26 patients, from 40 to 84 years old, with uterine malignant tumor including 11 cases of corpus carcinomas, 13 cases of cervical carcinomas, and 2 cases of uterus origin malignant lymphomas. On the basis of the phantom study, patients with uterine malignant tumors smaller than 13mm were excluded. Maximum tumor 18F-FDG SUV (SUVmax) was measured in FBPC and the two phases of BHPC.

RESULTS

Our phantom study revealed that BHPC was also reliable when the size of lesion was bigger than 13mm with the accuracy of one SD which was smaller than 2% of SUVmax. This reliability was markedly improved by one tenth in comparison with that of 10 years ago. On clinical study, the mean SUVmax was 18.56 with FBPC, 15.51 with the early phase of BHPC, whereas 18.15 with the delayed phase of BHPC. In dynamic study, 19.2% increase in SUVmax in delayed scan.

CONCLUSION

SUVmax obtained in the early and delayed phase of BHPC which had 15 minutes discrepancy showed a significant difference. BHPC before and after FBPC may contribute to distinguish benign lesions from malignant tumors, and this technique is feasible in the clinical setting with minimum increase in examination time.

CLINICAL RELEVANCE/APPLICATION

The new technique 'Dynamic study of PET/CT' may contribute to distinguish benign lesions from malignant tumors, and this technique is feasible in the clinical setting with minimum increase in examination time.

SST06-09 Multiparametric Evaluation by 18F-Fluorocholine PET-CT and MRI Examinations in Patients with Prostate Cancer

Friday, Nov. 30 11:50AM - 12:00PM Room: E261

Participants

Xavier Palard-Novello, 35000, France (*Presenter*) Nothing to Disclose Anne-Lise Blin, Rennes, France (*Abstract Co-Author*) Nothing to Disclose Luc Beuzit, Rennes, France (*Abstract Co-Author*) Nothing to Disclose Pierre Salaun, MD, PhD, Brest, France (*Abstract Co-Author*) Nothing to Disclose Anne Devillers, Rennes, France (*Abstract Co-Author*) Nothing to Disclose Etienne Garin, MD, Rennes, France (*Abstract Co-Author*) Nothing to Disclose Solene Querellou, Brest, France (*Abstract Co-Author*) Nothing to Disclose Patrick Bourguet, Rennes, France (*Abstract Co-Author*) Nothing to Disclose Florence Le Jeune, MD, PhD, Rennes, France (*Abstract Co-Author*) Nothing to Disclose Herve Saint-Jalmes, PhD, Rennes, France (*Abstract Co-Author*) Nothing to Disclose

PURPOSE

To evaluate the relationship between metabolic 18F-fluorocholine (FCH) PET-CT and functional parameters derived by Magnetic Resonance Imaging (MRI) in patients with prostate cancer (PC).

METHOD AND MATERIALS

Patients with proven PC who underwent FCH PET/CT and 1.5 T multiparametric MRI were included. FCH PET/CT consisted in a dual phase: early and late whole-body acquisition. A 12x5' - 3x30' time sampling was reconstructed from the first 150 seconds of the early acquisition. A freehand FCH PET/CT volume-of-interest (VOI) with a threshold of 40% of the maximum signal intensity was drawn on the late acquisition and projected onto the early static frame of 10 min and each frame of the dynamic reconstruction. For the kinetic analysis, an imaging-derived plasma input function was estimated from VOI placed within the largest arterial blood-pool structures available on the early PET image. The pharmacokinetic modeling was the reversible one-tissue compartment model. Kinetic parameter (K1 as influx) and static parameters (early SUVmean, late SUVmean and SUVmean retention index) were extracted. Concerning multiparametric MRI, axial diffusion-weighted imaging was obtained using three b values: 0, 50 and 1300 s/mm2. Dynamic contrast-enhanced studies were obtained with intravenous administration of gadolinium-based contrast agent with a 11x13' dynamic time sampling. Using co-registration of diffusion-weighting MRI with late whole-body FCH PET/CT, a freehand VOI was drawn to obtain the mean Apparent Diffusion Coefficient (ADC). VOI was projected onto the perfusion parametric maps to extract the mean transfer constant (ktrans) and the mean volume of the extracellular space (Ve) using the Tofts pharmakinetic model. Spearman's correlation coefficients were calculated to compare imaging findings.

RESULTS

Thirteen patients were analysed. The median time interval between PET and MRI was 39 days. Concerning correlation analysis between PET and MRI parameters, K1 was significantly correlated with ktrans (r=0.59, p=0.035) and early SUVmean was significantly correlated with ADC (r=-0.58, p=0.04).

CONCLUSION

FCH influx using the reversible one-tissue compartment model is significantly correlated with the transfer constant of gadolinium-based contrast agent in prostate cancer.

CLINICAL RELEVANCE/APPLICATION

These results might be useful in the design of future clinical trials involving FCHOLINE-PET/DCE-MR for the assessment of prostate cancer.



SST07

Neuroradiology/Head and Neck (Head and Neck Imaging: Back to the Future)

Friday, Nov. 30 10:30AM - 12:00PM Room: E353A







AMA PRA Category 1 Credits ™: 1.50 ARRT Category A+ Credit: 1.75

Participants

Brent D. Griffith, MD, Troy, MI (*Moderator*) Nothing to Disclose Asim Z. Mian, MD, Cambridge, MA (*Moderator*) Stockholder, Boston Imaging Core Lab, LLC; Consultant, Median Technologies

Sub-Events

SST07-01 Radiogenomic Analysis Identifies Multiple Therapeutically Relevant Subtypes for Head and Neck Squamous Cell Carcinoma

Friday, Nov. 30 10:30AM - 10:40AM Room: E353A

Participants

Chao Huang, PhD, Hangzhou, China (*Presenter*) Nothing to Disclose Murilo B. Cintra, Ribeirao Preto, Brazil (*Abstract Co-Author*) Nothing to Disclose Kevin Brennan, Stanford, CA (*Abstract Co-Author*) Nothing to Disclose Mu Zhou, PhD, Mountain View, CA (*Abstract Co-Author*) Nothing to Disclose A D. Colevas, MD, Stanford, CA (*Abstract Co-Author*) Nothing to Disclose Nancy J. Fischbein, MD, Stanford, CA (*Abstract Co-Author*) Nothing to Disclose Kuan S. Zhu, Hangzhou, China (*Abstract Co-Author*) Nothing to Disclose Olivier Gevaert, PhD, Stanford, CA (*Abstract Co-Author*) Nothing to Disclose

For information about this presentation, contact:

huangchao09@zju.edu.cn

PURPOSE

To investigate whether radiogenomics can identify therapeutically relevant molecular phenotypes defined by genomics, epigenomics, and/or transcriptomics for head and neck squamous cell carcinoma (HNSCC).

METHOD AND MATERIALS

We included 113 HNSCC patients from The Cancer Genome Atlas Head-Neck Squamous Cell Carcinoma (TCGA-HNSC) project. Molecular phenotypes investigated were RNA-defined HPV infection, 5 epigenomic subtypes discovered by MethylMix, 4 mRNA subtypes by TCGA group, and 5 common somatic gene mutations. In total, 2,131 quantitative image features were extracted from pre-treatment CT scans. Discriminative features were selected using the Minimum Redundancy Maximum Relevance (mRMR) algorithm. Afterwards, we applied logistic regression model with the least absolute shrinkage and selection operator (LASSO) to build binary classifiers for predicting each molecular subtype. All classifiers were trained using nested stratified 10-fold cross-validation repeated 10 times and the performance metric was the average area under the Receiver Operator Characteristic (ROC) curve (AUC) of the outer loop of the nested cross-validation. Additionally, an HPV prediction model was developed using the entire TCGA-HNSC cohort, and was validated by an independent validation cohort (N = 53).

RESULTS

Our results showed that CT-based features were capable of distinguishing multiple molecular phenotypes in HNSCC. We obtained significant predictive performance for RNA-defined HPV+ vs. HPV- (AUC = 0.82), MethylMix HPV+ vs. other MethylMix subtypes (AUC = 0.85), CIMP-Atypical vs. other MethylMix subtypes (AUC = 0.73), atypical vs. other mRNA subtypes (AUC = 0.83), basal vs. other mRNA subtypes (AUC = 0.75). Furthermore, the HPV prediction model was successfully validated in the validation cohort (AUC = 0.84).

CONCLUSION

Our study demonstrates that CT-based radiogenomic analysis has the potential to predict multiple HNSCC subtypes defined by molecular biological characteristics.

CLINICAL RELEVANCE/APPLICATION

Radiogenomic analysis of CT images can enable automated non-invasive assessment of therapeutically relevant HNSCC molecular subtypes across diverse clinical settings.

Performance Analysis and Optimization of ACR-TIRADS Using a Genetic Algorithm: An Opportunity for Improvement?

Friday, Nov. 30 10:40AM - 10:50AM Room: E353A

Participants

Benjamin Wildman-Tobriner, MD, Durham, NC (*Presenter*) Nothing to Disclose
Mateusz Buda, MSc, Durham, NC (*Abstract Co-Author*) Nothing to Disclose
Maciej A. Mazurowski, MS, PhD, Durham, NC (*Abstract Co-Author*) Nothing to Disclose
Ryan G. Short, MD, Durham, NC (*Abstract Co-Author*) Co-founder, Scanslated, Inc; Officer, Scanslated, Inc
David A. Thayer, MD, PhD, Saint Louis, MO (*Abstract Co-Author*) Nothing to Disclose
William D. Middleton, MD, Saint Louis, MO (*Abstract Co-Author*) Nothing to Disclose
Jenny K. Hoang, MBBS, Durham, NC (*Abstract Co-Author*) Nothing to Disclose

For information about this presentation, contact:

benjamin.wildman-tobriner@duke.edu

PURPOSE

To use the computer science technique of genetic algorithm to create an optimized version of the American College of Radiology Thyroid Imaging and Reporting Data System (ACR TI-RADS), and to compare the performance of the optimized system to the current version.

METHOD AND MATERIALS

1425 thyroid nodules from 1264 consecutive patients were retrospectively reviewed in this IRB-approved, HIPAA compliant study. Each nodule had either fine needle aspiration (FNA) or surgical histologic correlation. An expert reader assigned ACR TI-RADS features to each nodule. A genetic algorithm then used the TI-RADS assignments and the histologic 'ground truth' as input for a training set of 1325 nodules to create new TI-RADS feature points, numbers optimized using area under the receiver operating characteristic (ROC) curves. The algorithm-derived, optimized TI-RADS risk categories were then calculated and compared to ACR TI-RADS using a test set of 100 nodules not yet used in the algorithm.

RESULTS

The genetic algorithm created a new set of point assignments for 21 different TI-RADS features. The algorithm assigned the same number of points (as ACR TI-RADS) for 13 of the features and ascribed a new point value for 8 features (Figure). Some of the features that had point values that differed from the ACR version included mixed solid and cystic nodules, solid nodules, macrocalcifications, and taller-than-wide shape. Using the test set, sensitivity and specificity for biopsy of malignant nodules were 93% and 47%, respectively, for ACR TI-RADS and 93% and 65%, respectively, for the genetic algorithm optimized TI-RADS.

CONCLUSION

An optimized version of ACR TI-RADS derived from a genetic algorithm has similar point allocation to ACR TI-RADS, which validates many of the ACR's designated point values. The genetic algorithm version has improved specificity while maintaining sensitivity. In addition, newly proposed point values of 0 for some features may simplify the model and eliminate the need to scrutinize potentially confusing features.

CLINICAL RELEVANCE/APPLICATION

Further refinement of ACR TI-RADS points allocation by a genetic algorithm can both improve performance and simplify its clinical application.

SST07-03 MRI Texture Analysis (MTA) in the Optic Nerve During Acute Optic Neuritis (ON): Can Be Considered an Indicator of Optic Nerve Pathology or a Predictor of Visual Recovery?

Friday, Nov. 30 10:50AM - 11:00AM Room: E353A

Participants

Michaela I. Cellina, Milan, Italy (*Presenter*) Nothing to Disclose
Marta Maria Panzeri, MD, Milan, Italy (*Abstract Co-Author*) Nothing to Disclose
Daniele Gibelli, Milan, Italy (*Abstract Co-Author*) Nothing to Disclose
Paolo Mirani, Mialn, Italy (*Abstract Co-Author*) Nothing to Disclose
Marta Pirovano, Milan, Italy (*Abstract Co-Author*) Nothing to Disclose
Vincenza Fetoni, Milan, Italy (*Abstract Co-Author*) Nothing to Disclose
Matteo Ciocca, Milan, Italy (*Abstract Co-Author*) Nothing to Disclose
Giancarlo Oliva, Milan, Italy (*Abstract Co-Author*) Nothing to Disclose

For information about this presentation, contact:

michaela.cellina@asst-fbf-sacco.it

PURPOSE

Retinal nerve fiber layer (RNFL) thickness at Optical Coherence Tomography (OCT) is a biomarker of neuroaxonal loss and a reliable index of visual function in multiple sclerosis (MS). Our aim was to assess the correlation between MTA and RNFL thickness and between MTA and visual outcome (VO).

METHOD AND MATERIALS

We enrolled clinical 27 consecutive patients, who presented to our Emergency Department with a first episode of acute ON (15 female, 12 male; age range: 21-50 years; mean age: 34; 32 eyes: 5 bilateral ON; 10 left ON; 12 right ON) from January 2015 to January 2017. At their arrival all patients underwent a complete ophthalmological evaluation, including assessment of visual acuity and of RNFL thickness at OCT, blood tests to exclude infective or autoimmune ON, and neurological evaluation. Orbit MRI was executed within 7 days from ON onset (mean time: 3.5±3 days) including the following sequence: an axial T1 TSE performed 1 minute after contrast medium injection (gadobutrol, 1ml/10kg), slice thickness:3 mm, gap: 0.5 mm; SPIR fat saturation, FOV 18 cm, from occlusal plane to above orbits. Segmentation of the whole affected optic nerves was executed by the same experienced neuroradiologist through 3D slicer open software version 4.9.0-2017 to get texture analysis. All patients underwent a complete neuro-ophthalmological follow-up at 6 months to assess the VO, classified as: complete recovery, partial recovery, or deficit persistence/relapse.

RESULTS

At Kruskal-Wallis test, we observed a statistically significant correlation between RNFL and the following radiomics features: uniformity (p=.02), energy (p=.01), median (p=.002), 90°percentile (p=.003), 10°percentile (p=.003), gray level variance (p=.005). Analyzing the correlation between radiomics features and VO, we observed a statistically significant correlation only with kurtosis (p=.002).

CONCLUSION

Analysis of the texture in orbit MRI during the acute phase of a first episode of ON may be a potential measure of visual function in ON patients. Kurtosis proved to be correlated with VO.

CLINICAL RELEVANCE/APPLICATION

In patients affected by acute ON, radiomics features can be considered indicators of visual function and kurtosis can be used to predict VO.

SST07-04 3D-FLAIR Sequence with Delayed Acquisition After Intravenous Administration of Gadolinium Can Detect Intralabyrinthine Abnormalities in Patients Referred with Typical Vestibular Neuritis

Friday, Nov. 30 11:00AM - 11:10AM Room: E353A

Participants

Michael Eliezer, Paris, France (*Presenter*) Nothing to Disclose Julien Horion, 76000, France (*Abstract Co-Author*) Nothing to Disclose Guillaume Poillon, Rouen, France (*Abstract Co-Author*) Nothing to Disclose Arnaud Attye, MEd, Grenoble, France (*Abstract Co-Author*) Nothing to Disclose

PURPOSE

The origin of vestibular neuritis (also known as acute vestibular syndrome) remains unkown. The blood labyrinth barrier is similar to the blood-brain barrier yet requiring at least 4 hours after an intravenous administration of contrast media to be evaulated on 3D-FLAIR sequences. We assessed the enhancement of the vestibular nerve and of the semi circular canals on 3D FLAIR sequences in patients with typical acute vestibular syndrome.

METHOD AND MATERIALS

In this multicentric study, 28 patients with an acute vestibular syndrome diagnosed on the basis of typical clinical findings were included. We performed 3D T2 free-precession and 3D-FLAIR sequences 4 hours after contrast media administration. Two radiologists, blinded to the clinical data, independently performed a visual assessment in order to evaluate the perilymph enhancement.

RESULTS

We found a delayed enhancement of the semi circular canals in 24 out of 28 patients (84%). The superior and lateral semi circular canals were involved in 14/24 patients (58%) while the posterior semi circular canal was involved in 4/24 patients (16%). By contrast, an enhancement of the vestibular nerve was never displayed. We found a signal loss on T2 sequences in 11/24 patients (39%). The utricle was involved in 7 patients and the posterior semi circular canal in 4 patients.

CONCLUSION

We demonstrated a significant enhancement of the semi-circular canals on 3D FLAIR sequences performed 4 hours after administration of gadolinium.

CLINICAL RELEVANCE/APPLICATION

Intratympanic therapies such as corticosteroids could be performed depending on the results of imaging in order to reduce chronic dizziness.

SST07-05 Hyperintensity of the Optic Nerve on 3D-FLAIR Imaging is Effective for Identifying Clinically Significant Papilledema in Patients with Idiopathic Intracranial Hypertension

Friday, Nov. 30 11:10AM - 11:20AM Room: E353A

Participants

Edwarda Golden, BA, Madison, WI (*Presenter*) Nothing to Disclose Roman Krivochenitser, MD, Madison, WI (*Abstract Co-Author*) Nothing to Disclose Nathan Mathews, MD, Madison, WI (*Abstract Co-Author*) Nothing to Disclose Colin Longhurst, Madison, WI (*Abstract Co-Author*) Nothing to Disclose Yanjun Chen, MD, PhD, Madison, WI (*Abstract Co-Author*) Nothing to Disclose John-Paul J. Yu, MD, PhD, Madison, WI (*Abstract Co-Author*) Nothing to Disclose Tabassum A. Kennedy, MD, Saint Louis, MO (*Abstract Co-Author*) Nothing to Disclose

PURPOSE

Our group previously demonstrated the role of contrast-enhanced (CE) 3D-Fluid Attenuated Inversion Recovery (FLAIR) imaging in detecting papilledema in idiopathic intracranial hypertension (IIH). The purpose of this study is to determine if a correlation exists between the degree of hyperintensity of the optic nerve (ON) and optic nerve head (ONH) on CE 3D FLAIR imaging and the severity of papilledema on the ophthalmologic Frisén scale.

METHOD AND MATERIALS

In this IRB-approved study, a retrospective chart review was performed of consecutive patients with diagnosed IIH and concurrent magnetic resonance imaging (MRI) with CE 3D FLAIR sequences between 2012 and 2015; MRIs with CE 3D FLAIR sequences from age- and sex-matched control patients were also identified. Two blinded CAQ-neuroradiologists independently reviewed each MRI and graded each ON independently on a scale of 0-3: 0=normal;1=hyperintensity within the nerve without ONH involvement; 2=hyperintensity within the ON and mild inversion of the ONH; and 3=hyperintensity within the ON and significant inversion of the

ONH. To estimate the correlation between MR and Frisén scores, a non-parametric correlation coefficient (Kendall's T) with the associated 95% BCa-bootstrapped confidence intervals (4,000 iterations) were calculated for both eyes (OS and OD) using R (3.4.3).

RESULTS

49 patients (3 males, 45 females, mean age 29.2 \pm 10.99) with IIH and 62 controls (5 males, 57 females, mean age 30.89 \pm 11.74) with normal MRIs were included in this study. For both eyes, there was moderate correlation between the two scales (OD: τ =0.48, 95%CI=(0.32,0.48),OS: τ =0.38, 95%CI=(0.24,0.50)). Inter-reader reliability for MR scores was assessed using weighted Cohen's kappa (OD: κ =0.76 95%CI=(0.55,0.88), OS: κ =0.87 95%CI=(0.78,0.94)).

CONCLUSION

CE 3D FLAIR imaging correlates with the Frisén scale for moderate to severe papilledema and less so for mild papilledema. CE 3D FLAIR sequences also allow for consistent image interpretation with excellent inter-reader reliability. These findings suggest that MRI is effective for identifying clinically significant papilledema, in a setting where prompt diagnosis is crucial and where an ophthalmology evaluation may not be readily available.

CLINICAL RELEVANCE/APPLICATION

CE 3D FLAIR is a feasible imaging technique for the detection of papilledema. Herein, we demonstrate its utility for identifying clinically significant papilledema.

SST07-06 Lacrimal Passage Diseases: Clinical Application of 3.0T MR Dacryocystography of Whole Lacrimal Passages

Friday, Nov. 30 11:20AM - 11:30AM Room: E353A

Participants

Xuejun Guo, MD, Shenzhen, China (*Abstract Co-Author*) Nothing to Disclose Mingmei Li, MMed, Shenzhen, China (*Presenter*) Nothing to Disclose

For information about this presentation, contact:

marabout@139.com

PURPOSE

To analyze the causes of obstruction or stenosis of lacrimal passages, and to investigate the value of 3.0T MR dacryocystography of whole lacrimal passages in clinical application.

METHOD AND MATERIALS

Thirty-eight cases with lacrimal passage diseases underwent MR dacryocystography of whole lacrimal passages. Before the examination, the conjunctival sac was instilled into Sodium Hyaluronate Eye Drops after Racanisodamine Eye Drops was administrated, and 3D-SPC sequence of 2D-TSE sequence were used, which section thickness of 0.2-2.0mm, and Special Purpose Coil was employed. Each part of whole lacrimal passages included lacrimal canaliculitis was demonstrated clearly. The location and cause of obstruction and the degree of stenosis were determined in patients with lacrimal passage diseases.

RESULTS

Of 38 cases of lacrimal passage diseases, chronic inflammation of lacrimal passages(n=28 cases, 35 eyes) were found, included dacryocystitis(n=21 eyes), inflammation of nasolacrimal duct and dacryocyst(n=11 eyes) and lacrimal canaliculitis (n=2 eyes). One cases with lacrimal canaliculus and inner canthus ligament abruption was diagnosed, and congenital variation of defective lacrimal duct(n=6 cases) and stenosing lacrimal sac(n=1 cases) was diaplayed. In addition, inflammation(n=5 cases, 5 eyes) and abscess(n=2 cases) around lacrimal passage were estimated, which closed to lacrimal passages. Paracrymal tumors or tumor- like lesions include steatocystoma (n=3 cases), epidermoid cyst with rupture infection (n=1 case), mucosa-associated lymphoid tissue lymphoma involving nasolacrimal duct(n=1 case) were found. MR dacryocystography of whole lacrimal passages can accurately identified the obstructive location of lacrimal passage, respectively in the lacrimal canaliculus(n=3 cases), in the dacryocyst (n=21 eyes), and in the distal nasolacrimal duct(n=11 eyes).

CONCLUSION

MR dacryocystography of whole lacrimal passages is a absolute noninvasive examination method with higher clinical value in diagnosis of lacrimal passage and its surrounding lesions. It must be recommended as a preferred examination method of lacrimal passage lesions.

CLINICAL RELEVANCE/APPLICATION

MR dacryocystography of whole lacrimal passages can completely replace the commonly used invasive methods such as lacrimal radiography, fluorescein imaging and radionuclide imaging.

SST07-07 MR-Based Quantitative Texture and Shape Analysis: Can It Differentiate Benign and Malignant Solid Epithelial Neoplasms of the Lacrimal Gland?

Friday, Nov. 30 11:30AM - 11:40AM Room: E353A

Participants

Jian Guo, PhD, Beijing, China (*Presenter*) Nothing to Disclose Xiaoxia Qu, Beijing, China (*Abstract Co-Author*) Nothing to Disclose Junfang Xian, MD, Beijing, China (*Abstract Co-Author*) Nothing to Disclose

For information about this presentation, contact:

jiangjoojle@163.com

To assess the performance of MR-based texture and shape features in the differentiation of benign and malignant solid epithelial neoplasms of the lacrimal gland.

METHOD AND MATERIALS

This retrospective study of consecutive patient data was approved by the institutional review board and informed consent was waived. 76 consecutive patients with histopathology-proven epithelial neoplasms of lacrimal gland were enrolled in the study. A total of 924 first-order histogram, grey-level co-occurrence matrix (GLCM) and gray level run-length matrix (GLRLM) textural features, as well as shape features, were extracted from T2-weighted images (T2WI) and fat-suppression post-enhanced T1-weighted images (FS post-enhanced T1WI) of these cases. The least absolute shrinkage and selection operator (LASSO) method and linear discriminant analysis were used to select imaging features and reduce data dimension to discriminate malignant lesions from benign ones. Diagnostic performance was assessed by receiver operating characteristic area under the curve (ROC-AUC) analysis and cross-validated with leave-one-out analysis. Combinations of features were also entered as classification model in logistic regression models and optimal threshold criteria were used to assess its diagnostic sensitivity, specificity and accuracy.

RESULTS

Thirty-five cases of malignant and forty-one cases of benign epithelial neoplasms were enrolled in this study. Four quantitative image features (gray level co-occurrence matrix-inverse difference moment normalized, first-order high-high mean deviation, mean radius and gray level run-length matrix high-high long run emphasis) were selected according to the LASSO logistic regression. AUC-ROC of these four features were 0.880, 0860, 0.882 and 0.857 respectively, with AUC-ROC of 0.930 for combination of all four features. Using optimum-threshold criteria, the combined features identified malignant lacrimal gland epithelial neoplasms from benign group with 92.7% sensitivity, 82.9% specificity and 88.2% accuracy.

CONCLUSION

MRI-based quantitative texture and shape analysis provided improved predictive ability in discriminating malignant epithelial neoplasms from benign ones of lacrimal gland.

CLINICAL RELEVANCE/APPLICATION

The quantitative texture and shape analysis can help lesion characterization of benign and malignant lacrimal gland tumors and allows an appropriate diagnosis and treatment strategy.

SST07-08 Deep Learning Model for Biopsy Recommendations of Thyroid Nodules on Ultrasound: Comparison of a Machine and Radiologists

Friday, Nov. 30 11:40AM - 11:50AM Room: E353A

Participants

Mateusz Buda, MSc, Durham, NC (*Abstract Co-Author*) Nothing to Disclose
Benjamin Wildman-Tobriner, MD, Durham, NC (*Abstract Co-Author*) Nothing to Disclose
David A. Thayer, MD, PhD, Saint Louis, MO (*Abstract Co-Author*) Nothing to Disclose
Ryan G. Short, MD, Durham, NC (*Abstract Co-Author*) Co-founder, Scanslated, Inc; Officer, Scanslated, Inc
William D. Middleton, MD, Saint Louis, MO (*Abstract Co-Author*) Nothing to Disclose
Jenny K. Hoang, MBBS, Durham, NC (*Abstract Co-Author*) Nothing to Disclose
Maciej A. Mazurowski, MS, PhD, Durham, NC (*Presenter*) Nothing to Disclose

For information about this presentation, contact:

mateusz.buda@duke.edu

PURPOSE

To develop a deep learning algorithm that uses thyroid ultrasound images to decide whether a thyroid nodule should undergo a biopsy, and to compare the performance of such algorithm to expert and non-expert radiologists based on ACR TI-RADS.

RESULTS

The proposed deep learning algorithm achieved 87% sensitivity, outperforming expert consensus using ACR TI-RADS (81%) as well as five non-expert radiologists. The specificity of the deep learning algorithm was 52% which was higher than expert consensus (51%) and six non-expert radiologists. The mean sensitivity and specificity for non-expert radiologists was 80% and 48%, respectively, both lower than for our deep learning algorithm.

CLINICAL RELEVANCE/APPLICATION

Deep learning may play a significant role in assisting less experienced radiologists in FNA recommendation of thyroid nodules and may improve their sensitivity and specificity.

SST07-09 Reducing Beam Hardening Artifacts in Thyroid CT Images with Model-Based Iterative Reconstruction

Friday, Nov. 30 11:50AM - 12:00PM Room: E353A

Participants

Zhian Pi, Ankang, China (*Abstract Co-Author*) Nothing to Disclose Yongjun Jia, MMed, Xianyang City, China (*Abstract Co-Author*) Nothing to Disclose Nan Yu, MD, Xian Yang, China (*Abstract Co-Author*) Nothing to Disclose Chuangbo Yang, MMed, Xianyang City, China (*Abstract Co-Author*) Nothing to Disclose Xirong Zhang, Xianyang, China (*Abstract Co-Author*) Nothing to Disclose Haifeng Duan, Xianyang City, China (*Abstract Co-Author*) Nothing to Disclose Yuhuan Chen, MD, Xianyang, China (*Presenter*) Nothing to Disclose Yanan Zhu, Ankang, China (*Abstract Co-Author*) Nothing to Disclose Taiping He, Xianyang, China (*Abstract Co-Author*) Nothing to Disclose

PURPOSE

Io investigate the ability of a new model-based iterative reconstruction algorithm with either spatial and density resolution balance (MBIRSTND) or low-density resolution preference (MBIRNR40) to reduce the beam hardening artifacts in thyroid images, in comparison with the adaptive statistical iterative reconstruction (ASIR) algorithm.

METHOD AND MATERIALS

Twenty patients with thoracic nodules and underwent chest CT scans were retrospectively reviewed. Images at the 0.625mm slice thickness were retrospectively reconstructed with 40%ASIR, MBIRSTND and MBIRNR40 algorithms. Coronal images with the most obvious beam hardening artifacts in the thyroid were selected for comparison. The CT value and standard deviation (SD) value of the left and right thyroid lobes affected by beam hardening artifacts and the surrounding normal tissue were measured and SD values were used to calculate the artifact index (AI) in the thyroid: AI=sqrt(SDthyroid2-SDnormal tissue2). Two radiologists used a 4-point scoring system (with 4 being the best) evaluate the subjective image quality in terms of artifacts in the image and the clarity of displaying thyroids on the coronal images. ANOVA and paired t-test were used to compare the CT value difference between the normal and affected thyroid tissues and AI values of different reconstructions. Subjective score differences were tested using the Wilcoxon symbol scale.

RESULTS

MBIRSTND and MBIRNR40 images significantly reduced the CT value difference between the normal and affected thyroid tissues and the beam hardening artifacts in the left and right thyroid lobes: AI values from 2.27 ± 0.52 and 2.52 ± 0.85 for the left and right lobe with 40%ASIR to 1.64 ± 0.79 and 1.75 ± 0.80 with MBIRNR40, respectively (P <0.05). MBIRSTND and MBIRNR40 had significantly higher subjective scores for thyroid and nodules than 40%ASIR, with MBIRNR40 being the highest (P <0.05).

CONCLUSION

MBIR, especially the one with low-density resolution preference, can significantly reduce the impact of the beam hardening artifacts caused by clavicle on the thyroid and its nodules during CT scans.

CLINICAL RELEVANCE/APPLICATION

Beam hardening artifacts caused by clavicle affect the image quality at the entrance of the thorax and are not conducive to the quality of CT images of the thyroid and other cervical structures. MBIR can reduce this effect.



SST08

Pediatrics (Neuroradiology)

Friday, Nov. 30 10:30AM - 12:00PM Room: E263

MR

NR

PD

AMA PRA Category 1 Credits ™: 1.50 ARRT Category A+ Credit: 1.75

FDA

Discussions may include off-label uses.

Participants

Stephen F. Kralik, MD, Indianapolis, IN (Moderator) Nothing to Disclose

Sub-Events

SST08-01 The Application Study on MRI Segmentation of Brain and T2MAP Sequence in Neonatal Intracranial Hypertension

Friday, Nov. 30 10:30AM - 10:40AM Room: E263

Participants

Yan Qin, Changsha, China (*Presenter*) Nothing to Disclose
Xie Jing, Changsha, China (*Abstract Co-Author*) Nothing to Disclose
Yang Liu, Changsha, China (*Abstract Co-Author*) Nothing to Disclose
Ge Yang, MD, Changsha, China (*Abstract Co-Author*) Nothing to Disclose
Ouyang Lirong, Changsha, China (*Abstract Co-Author*) Nothing to Disclose
Gaofeng Zhou, Changsha, China (*Abstract Co-Author*) Nothing to Disclose
Zhengchang Liao, Changsha, China (*Abstract Co-Author*) Nothing to Disclose
Zhengchang Liao, Changsha, China (*Abstract Co-Author*) Nothing to Disclose
Ying Ding, Changsha, China (*Abstract Co-Author*) Nothing to Disclose
Ping Hu, Changsha, China (*Abstract Co-Author*) Nothing to Disclose
Chuanding Cao, Changsha, China (*Abstract Co-Author*) Nothing to Disclose
Dongcui Wang, Changsha, China (*Abstract Co-Author*) Nothing to Disclose
Shaojie Yue, Changsha, China (*Abstract Co-Author*) Nothing to Disclose
Weihua Liao, MD, Changsha, China (*Abstract Co-Author*) Nothing to Disclose

For information about this presentation, contact:

yanqin1607@163.com

PURPOSE

To find the MRI appearance of neonatal intracranial hypertension and study the relationship between intracranial volume (including cerebral white matter, grey matter and cerebrospinal fluid) of neonatal and intracranial hypertension, and consequently offer help for the diagnosis and treatment.

METHOD AND MATERIALS

A total of 51 suspicious intracranial hypertensive patients from the neonatology department in our hospital were included. All patients had undergone MRI examination and all of them had the result of cerebrospinal fluid pressure measured by lumbar puncture. All of the data were collected by Siemens 3.0T PRISMA. The scanning sequences included conventional T1WI, T2WI, T2FLAIR, T1MP2RAGE and T2MAP. The SMP12 software was used to do the volumetric segmentation . As for T2MAP, we counted the T2 value of bilateral frontal lobes, temporal lobes, occipital lobes and basal ganglia regions. Statistical analysis was performed using Pearson correlation analysis and independent sample T-test.

RESULTS

Our study found that there was no significant correlation between the volume of white matter or grey matter and intracranial pressure. The proportion of CSF to intracranial volume was significantly negatively correlated with intracranial pressure at 0.01 level (bilateral). The proportion of CSF to intracranial volume in the intracranial pressure normal group is significantly different from that in intracranial hypertension group. There was a significant difference in basal ganglia T2 value between the two groups. No significant difference in the T2 value of white matter of bilateral temporal lobe, frontal lobe and occipital lobe was found.

CONCLUSION

We found that CSF can provide a certain compensative capacity, while the compensative capacity of brain tissue is relatively weaker. We also found out that T2 value of basal ganglia region significantly increased in intracranial hypertensive patients, suggesting that basal ganglia region may be most common involved in encephaledemia caused by intracranial hypertension. Our study proves that MRI T1MP2RAGE and T2MAP are noninvasive and convenient and can offer a strong help for the diagnosis and treatment of neonatal intracranial hypertension.

CLINICAL RELEVANCE/APPLICATION

Our study proves that MRI T1MP2RAGE and T2MAP are noninvasive and convenient and can offer a strong help for the diagnosis and treatment of neonatal intracranial hypertension.

SST08-03 Clinical Implications of the Punctate White Matter Lesion on Brain MRI in Preterm Infants

Friday, Nov. 30 10:50AM - 11:00AM Room: E263

Participants

Young Jin Ryu, MD, Seongnam, Korea, Republic Of (*Presenter*) Nothing to Disclose Ji Young Kim, MD, Seongnam-Si, Korea, Republic Of (*Abstract Co-Author*) Nothing to Disclose

PURPOSE

To investigate the association between punctate white matter lesions (PWML) on term-equivalent age brain MRI and neurodevelopment outcome in preterm infants.

METHOD AND MATERIALS

From March 2013 to March 2017, brain MRI performed around term-equivalent age in preterm infants (gestational age < 32 weeks) were retrospectively reviewed with focused on the presence of isolated PWML without other brain pathology such as cavitary white matter lesion (CWML). An analysis of the MR findings of PWML included evaluation of the number, pattern, laterality, presence of diffusion restriction and signal intensity on SWI, T2WI of PWML. The presence of combined abnormal MR findings including intraventricular hemorrhage (IVH), intraparenchymal hemorrhage (IPH), cerebellar hemorrhage, extra-axial hemorrhage and hydrocephalus were also analyzed. Clinical follow-up was performed and neurodevelopmental outcome was assessed by Bayley Scales of Infant Development scores.

RESULTS

213 infants were included in the study. Among them, 41(19.2%) of 348 have isolated PWML. Of 137 infants with neurodevelopmental outcome, 23(16.7%) infants have isolated PWML. The presence of CWML, grade III/IV IVH, IPH, and hydrocephalus were significantly associated with mental and psychomotor developmental delay (all p-values <.05). There was no significant difference of psychomotor developmental index(PDI) and mental developmental index(MDI) between infants with normal MR findings (n=71) and infants with isolated PWML (n=23) (PDI, 95.1±14.2 vs. 98.0±10.3, P=.372; MDI, 99.4±9.5 vs. 98.9±11.2, P=.604). Mental and psychomotor developmental delay was found in 8.7% and 8.7% of infants who had isolated PWML, respectively, while 4.2% and 18.3% of infants with normal MR findings showed mental and psychomotor developmental delay, without statistically significant difference between two groups (all p-values>.05). Developmental delay in infants with isolated PWML was not statistical association with number, pattern, and signal intensity on SWI, T2WI and DWI, and laterality of PWML lesions.

CONCLUSION

Isolated PWML were detected with high incidence (16.7-19.7%) on term-equivalent age MRI in preterm infants. Isolated PWML have no statistically significant association with neurodevelopmental outcome.

CLINICAL RELEVANCE/APPLICATION

Isolated punctate white matter lesion without other brain pathology in preterm infants around term-equivalent age is not correlated with an adverse neurologic outcome.

SST08-04 Abnormal Spontaneous Low-Frequency Brain Activity in Children with Repaired Tetralogy of Fallot: Resting-State Functional Magnetic Resonance Imaging Study

Friday, Nov. 30 11:00AM - 11:10AM Room: E263

Participants

Yuting Liu SR, MD, Nanjing, China (*Presenter*) Nothing to Disclose Ming Yang, MD, Nanjing, China (*Abstract Co-Author*) Nothing to Disclose Huijun Li, MS, Nanjing, China (*Abstract Co-Author*) Nothing to Disclose Ying Wang, Nanjing, China (*Abstract Co-Author*) Nothing to Disclose Yaping Li, Nanjing, China (*Abstract Co-Author*) Nothing to Disclose

For information about this presentation, contact:

liuytmonkey@sina.com

PURPOSE

The majority of previous neuroimaging studies have demonstrated both structural and functional abnormalities in children with congenital heart disease (CHD). However, few studies have focused on the regional intensity of spontaneous fluctuations during the resting state and the relationship between the abnormal properties clinical variables and the neurocognitive performances. We use the amplitude of low-frequency fluctuation (ALFF) method to explore the changes in spontaneous low-frequency brain activity in children with repaired Tetralogy of Fallot(TOF) relative to controls.

METHOD AND MATERIALS

In this study, ten repaired Tetralogy of Fallot (TOF) children and thirteen normal controls were recruited. The ALFF method was used to assess the local features of spontaneous brain activity in children with repaired TOF. The ALFF difference between repaired TOF children and normal controls was analyzed and the observed mean ALFF values of the different areas were correlated with clinical neurological assement.

RESULTS

Compared with normal controls, children with repaired TOF showed significantly lower ALFF in bilateral cerebellum, left occipital lobe, and higher ALFF in right parahippocampal cortex, left medial prefrontal cortex (MPFC), left posterior cingulate(PCC). In addition, significant, positive correlations were found between the Wechsler scale scores and the ALFF change coefficients in left occipital lobe (r = .728, P = .017; r = .818, P = .004; r = .719, P = .019; r = -.751, P = .012;), between the Wechsler scale scores and the ALFF change coefficients in left MPFC (r = .636, P = .048), and negative correlations were found between the Wechsler scale scores and the ALFF change coefficients in left cerebellum (r = -.636, P = -.048).

CONCLUSION

The significant regional spontaneous activity deficits was found in repaired TOF children, and the relation between clinical neurological assement and the ALFF change coefficients, which might offer new insights into the neural pathophysiology underlying TOF-related neurodevelopment impairments.

CLINICAL RELEVANCE/APPLICATION

Children with CHD after repaired surgery often along with neurodevelopment impairments ,including cognitive, verbal, behavioral and excution control dysfunction. This study showed correlations between the Wechsler scale scores and the ALFF change coefficients, which might provide powerful new insights into neurodevelopment impairments.

SST08-05 Classification of Seizure Onset Zones in Children with Focal Epilepsy

Friday, Nov. 30 11:10AM - 11:20AM Room: E263

Participants

Michael J. Paldino, MD, Houston, TX (*Abstract Co-Author*) Nothing to Disclose Rasoul Hekmat, Houston, TX (*Abstract Co-Author*) Nothing to Disclose Wei Zhang, PhD, Houston, TX (*Presenter*) Nothing to Disclose Zili David Chu, PhD, Houston, TX (*Abstract Co-Author*) Nothing to Disclose Farahnaz Golriz, MD, Houston, TX (*Abstract Co-Author*) Nothing to Disclose Robert Azencott, PhD, Houston, TX (*Abstract Co-Author*) Nothing to Disclose

PURPOSE

In refractory epilepsy, surgical resection of epileptogenic tissue can significantly improve seizure control. Accurate identification of seizure onset zones is crucial for surgical planning as well as post-operative prognosis. iEEG, the current gold standard for seizure onset zone localization is invasive and can only provide a local assessment. Resting-state fMRI has been used to provide a systematic evaluation of whole brain network architecture. We therefore aimed to identify features of the cerebral network constructed from resting-state fMRI that are useful for seizure onset localization.

METHOD AND MATERIALS

Patients were retrospectively identified with: 1. Focal epilepsy; 2. Resting-state fMRI; 3. A single seizure onset zone identified in a multidisciplinary epilepsy conference. Brain network nodes were defined by cortical parcellation, resulting in networks containing 148 anatomic regions. We then sub-divided each region into network nodes of size 350 mm2. Edges (connections) between each pair of nodes were defined as the mutual information between BOLD time courses. Intra-region connections were summarized by the 75% quantiles of edges within a region. A machine learning algorithm, Multi-layer Perceptron, was then used to predict seizure onset lobes of each individual based on their intra-region connectivity. Classification accuracy was assessed with the leave-one-out algorithm. Each anatomic region was analyzed according to its discrimination power with respect to seizure onset localization.

RESULTS

Fifteen patients met criteria (age: 4-18 years), of which seizure onsets were identified as 5 right frontal, 3 left frontal, 3 right temporal and 4 left temporal lobes. Leave-one-out classification accuracy was 14/15 (93%). The anatomic regions with the maximum discrimination power are distributed throughout the brain consistent with the idea that focal epilepsy is associated with global network abnormalities (Figure 1).

CONCLUSION

Intra-region connectivity obtained from resting-state fMRI had a strong association to clinical diagnosis of seizure onset zone.

CLINICAL RELEVANCE/APPLICATION

Whole brain network approaches can detect features of the epileptogenic network; more complete mapping of this network could improve surgical outcomes.

SST08-06 Comparison of CT and 'Black Bone' MRI for Detection of Skull Fractures in Children with Suspected Abusive Head Trauma

Friday, Nov. 30 11:20AM - 11:30AM Room: E263

Participants

Stephen F. Kralik, MD, Indianapolis, IN (*Presenter*) Nothing to Disclose Karen A. Eley, FRCR,DPhil, Cambridge, United Kingdom (*Abstract Co-Author*) Nothing to Disclose Nucharin Supakul, MD, Indianapolis, IN (*Abstract Co-Author*) Nothing to Disclose Isaac Wu, Indianapolis, IN (*Abstract Co-Author*) Nothing to Disclose Rupa Radhakrishnan, MD, Cincinnati, OH (*Abstract Co-Author*) Nothing to Disclose Chang Y. Ho, MD, Indianapolis, IN (*Abstract Co-Author*) Nothing to Disclose Gaspar Delso, PhD, Cambridge, United Kingdom (*Abstract Co-Author*) Employee, General Electric Company;

For information about this presentation, contact:

steve.kralik@gmail.com

PURPOSE

The purpose of this research was to determine the accuracy of "black bone" MRI for detection of skull fractures in children with potential abusive head trauma.

METHOD AND MATERIALS

A prospective study was performed in 35 pediatric patients who were evaluated for potential abusive head trauma. All patients had both a noncontrast Head CT (HCT) with multiplanar reformats and/or 3D volumetric reformatted images and "Black Bone" MRI of the brain with multiplanar reformatted images and 3D volumetric images. "Black Bone" MRI was performed using an ultrashort TE pointwise encoding time reduction with radial acquisition (PETRA) sequence at 1.5 T or 3T. "Black Bone" MRI datasets were post-

processed and 3D images created using Fovia's High Definition Volume Rendering software. A board certified pediatric neuroradiologist independently reviewed the HCTs and MRIs blinded to the findings from the other modality. The interpretation of the "Black Bone" MRI was compared to gold standard HCT diagnosis for skull fracture. The sensitivity, specificity, and accuracy for "Black Bone" MRI was calculated.

RESULTS

Median patient age was 4 months (range 1.2-18 months). The incidence of skull fracture was 20%. MRI demonstrated 86% sensitivity, 100% specificity, 97% accuracy, positive predictive value 100%, negative predictive value 97% for identifying skull fracture.

CONCLUSION

A "Black Bone" MRI sequence provides high sensitivity and specificity for detection of skull fractures in pediatric patients with abusive head trauma.

CLINICAL RELEVANCE/APPLICATION

"Black Bone" MRI detection of skull fractures may result in decreased utilization of CT and reduce exposure to ionizing radiation.

SST08-08 A Deep Learning System for Predicting Pediatric Brain Age Using Multi-Parametric MRI

Friday, Nov. 30 11:40AM - 11:50AM Room: E263

Participants

Katie Shpanskaya, BS, Menlo Park, CA (*Abstract Co-Author*) Nothing to Disclose Edward H. Lee, MS,BS, Stanford, CA (*Presenter*) Nothing to Disclose Mu Zhou, PhD, Stanford, CA (*Abstract Co-Author*) Nothing to Disclose Emily McKenna, BA, Palo Alto, CA (*Abstract Co-Author*) Nothing to Disclose Jason N. Wright, MD, Seattle, WA (*Abstract Co-Author*) Nothing to Disclose Zichen Wang, Hangzhou, China (*Abstract Co-Author*) Nothing to Disclose Matthew P. Lungren, MD, Palo Alto, CA (*Abstract Co-Author*) Nothing to Disclose Olivier Gevaert, PhD, Stanford, CA (*Abstract Co-Author*) Nothing to Disclose Simon Wong, PhD, Stanford, CA (*Abstract Co-Author*) Nothing to Disclose Kristen W. Yeom, MD, Palo Alto, CA (*Abstract Co-Author*) Nothing to Disclose

For information about this presentation, contact:

edhlee@stanford.edu

PURPOSE

The dynamically evolving architecture of the developing brain in early childhood through adolescence poses diagnostic challenges for pediatric brain MRI. We propose to develop and validate an accurate deep learning model predictive of pediatric age using MRI in a multi-institutional cohort.

METHOD AND MATERIALS

In this retrospective study, we examined a dataset of 1034 pediatric brain MRIs reviewed by expert pediatric neuroradiologists and determined diagnostically normal and within the normal range of neural development. For external validation cohort, we studied 111 pediatric patients from an independent institution, which were also confirmed to be normal based on signal intensity, morphology, and absence of pathologic lesions. Patient ages ranged from 0.1 to 200 months. For biological age prediction, we developed a deep learning model (PageNet) that incorporates 2D and 3D convolutional networks using multi-parametric T1-weighted, T2-weighted, and diffusion-weighted imaging (DWI) MRI sequences. We tested our model using 5-fold cross-validation on our internal cohort and, separately, on the independent external validation cohort. Pearson's r correlation between predicted and actual age and mean-average-error (MAE) were used to evaluate model predictive performance.

RESULTS

Using multi-parametric MRI, PageNet accurately predicted pediatric age (r = 0.95) in our internal cohort with a MAE of 15.8 months. Similar strong predictive performance was demonstrated on external cohort validation (r = 0.92; MAE = 20 months). Model performance using single MRI sequences was r = 0.93 for T1-weighted, r = 0.93 for T2-weighted, and r = 0.94 for DWI.

CONCLUSION

Deep learning can accurately map brain development captured by MRI to pediatric chronological age. This may serve as a useful clinical tool in assessing age-appropriate brain development and identifying developmental deviations.

CLINICAL RELEVANCE/APPLICATION

A reliable tool predictive of brain maturation can aid clinical assessment of healthy brain development and help gauge deviations of development and associated disorders in children.

SST08-09 Thrombectomy in Childhood Strokes

Friday, Nov. 30 11:50AM - 12:00PM Room: E263

Participants

Moritz Wildgruber, MD, PhD, Munster, Germany (Abstract Co-Author) Nothing to Disclose Peter Sporns, MD, Munster, Germany (Abstract Co-Author) Nothing to Disclose Uta Hanning, MD, Muenster, Germany (Abstract Co-Author) Nothing to Disclose Thomas Niederstadt, MD, Munster, Germany (Abstract Co-Author) Nothing to Disclose Walter L. Heindel, MD, Muenster, Germany (Abstract Co-Author) Nothing to Disclose Andre Kemmling, MD, Luebeck, Germany (Abstract Co-Author) Nothing to Disclose Max Masthoff, MD, Muenster, Germany (Presenter) Nothing to Disclose

For information about this presentation, contact:

moritz.wildgruber@ukmuenster.de

PURPOSE

As ischemic stroke is a rare but potentially severe event in children we aimed to evaluate endovascular treatment by mechanical thrombectomy for acute ischemic stroke in a pediatric patient population.

METHOD AND MATERIALS

In this retrospective trial, approved by the local institutional review board, we analyzed all patients < 18 years who were admitted to three large tertiary care centers for thrombectomy of thromboembolic intracranial vessel occlusion (Carotid-T, MCA- main stem M1 to M2- segment) within the last 5 years. Criteria to perform thrombectomy we similar compared to adult patients with acute ischemic stroke: symptoms (NIH score), time frame (onset of symptoms <6h) and imaging criteria (no infarct signs on native CT scan, mismatch in CT perfusion study and M1 vessel occlusion on CT angiography guided the decision for invasive treatment. Endovascular thrombectomy was performed using stent-retrievers alone, or in combination with thrombus aspiration. Clinical and Imaging data were extracted from electronic patient records and the picture archiving and communication system.

RESULTS

Thrombectomy was performed in a total of 12 children with a median age of 14 years (Interquartile Range IQR 7.8 to 16 years). Children presented with a median ASPECT Score of 8.0 (IQR 7.0 to 8.8) and a median pediatric NIHSS of 12.5 (IQR 8.0 to 21.5). Endovascular thrombectomy was successful in all children with acute ischemic stroke, with a TICI 2b stage in n=6 and TICI III in n=6 patients. Median pediatric NIHSS 7 days post thrombectomy was 3.5 (IQR 1 to 8), Modified Ranking Scale Score at 3 months was 1.0 (IRQ 0 to 2.0). No major complications such as arterial dissection, vessel rupture or bleeding were observed.

CONCLUSION

Our data adds to the growing evidence that thrombectomy is effective and safe not only in adults but also in children. Hence, it can be a valuable therapeutic option in childhood stroke.

CLINICAL RELEVANCE/APPLICATION

Our study adds that thrombectomy should be evaluated as a valuable option in pediatric patients presenting with acute ischemic stroke.



SST09

Physics (Nuclear Medicine, Quantitative Image Analysis in Imaging and Radiation Therapy)

Friday, Nov. 30 10:30AM - 12:00PM Room: E264

BQ

СТ

MI

NM PH

AMA PRA Category 1 Credits ™: 1.50 ARRT Category A+ Credit: 1.75

FDA

Discussions may include off-label uses

Participants

Chin-Tu Chen, PhD, Chicago, IL (*Moderator*) Board Member, BioMed Global; Board Member, EVO Worldwide, Inc; Board Member, AEPX; Board Member, EnDepth Vision Systems, LLC; Research Grant, DxRay, Inc; Advisor, Reflexion Medical Inc; Shareholder, EDDA Technology, Inc

Robert Miyaoka, PhD, Seattle, WA (*Moderator*) Research Consultant, MIM Software Inc; Research Grant, Koninklijke Philips NV; Research Grant, General Electric Company

Sub-Events

SST09-01 Performance Evaluation of inSPira HD: A High Resolution SPECT System for Neuroimaging

Friday, Nov. 30 10:30AM - 10:40AM Room: E264

Participants

Rameshwar Prasad, PHD, Chicago, IL (*Presenter*) Nothing to Disclose Volodymyr Pylypyuk, Chicago, IL (*Abstract Co-Author*) Nothing to Disclose Joseph Ringelstein, Hines, IL (*Abstract Co-Author*) Nothing to Disclose Sumeet Virmani, MD, Chicago, IL (*Abstract Co-Author*) Nothing to Disclose

CONCLUSION

The measured performances demonstrated that the inSPira HD SPECT scanner has high sensitivity, high resolution, and acceptable image quality and, hence, is well suited for high resolution static and dynamic SPECT neuroimaging studies.

Background

High-resolution SPECT imaging is of great interest for studying neurological pathologies. The objective of this study is to characterize the performances of high resolution inSPira HD SPECT scanner for neuroimaging applications.

Evaluation

inSPira HD is a dedicated high resolution SPECT scanner based on a rotating dual clamshell design that acquires data in dual-spiral geometry. The performance characteristics were evaluated in terms of spatial resolution, sensitivity, uniformity, and contrast. The spatial resolution was measured from images of a line source. System volume sensitivity (SVS) was calculated using large flood phantom filled with Tc-99m. ACR Small SPECT Phantom was used to evaluate the image quality in terms of uniformity and contrast. Brain phantom and patients images were acquired to access the system more realistically.

Discussion

Spatial resolution in terms of FWHM was 4.1 mm, 4.2 mm, and 4.3 mm for X, Y, and, Z plane respectively. SVS was 9914.6 cts/sec/uci/ml. Integral uniformity for UFOV and CFOV were 4.8 % and 2.1 % respectively. Percent contrast for the five visible spheres with attenuation correction was 26%, 58%, 76%, 93%, and 99%. Brain phantom and patients images show fine details of brain regions.

SST09-02 A Novel Approach for Dosimetry of 90Y Radioembolization Based on Quantitative 99mTc-MAA SPECT/CT Imaging

Friday, Nov. 30 10:40AM - 10:50AM Room: E264

Participants

Sara Ungania, Rome, Italy (*Presenter*) Nothing to Disclose
Antonino G. Guerrisi, MD, Rome, Italy (*Abstract Co-Author*) Nothing to Disclose
Marco D'Arienzo, Rome, Italy (*Abstract Co-Author*) Nothing to Disclose
Marco D'Andrea, Rome, Italy (*Abstract Co-Author*) Nothing to Disclose
Vicente Bruzzaniti, Rome, Italy (*Abstract Co-Author*) Nothing to Disclose
Aldo Morrone, Rome, Italy (*Abstract Co-Author*) Nothing to Disclose
Lidia Strigari, Rome, Italy (*Abstract Co-Author*) Nothing to Disclose

For information about this presentation, contact:

sara.ungania@gmail.com

PURPOSE

Radioembolization (RE) with 90Y-microspheres is a well-established treatment modality for treating liver malignancies. At a time of

increasing evidence for dose-effect relationships in RE with 90Y microspheres, the general consensus is that there is an urgent need for accurate dosimetry in patients undergoing RE treatment. This work aimed at estimating absorbed doses to lesions and normal liver in a novel anthropomorphic set-up.

CONCLUSION

In RE treatment planning the dose-kernel method proved to be more accurate with respect to deposition method based on full 3D dose distributions.

CLINICAL RELEVANCE/APPLICATION

Treatment planning in molecular radiotherapy is mandatory to obtain the most appropriate and effective treatment of patient. It is mandatory to validate dose quantification obtained by SPECT/CT imaging.

SST09-03 An Investigation Study of Deep Learning Convolutional Neural Network for Whole-Body PET Denoising

Friday, Nov. 30 10:50AM - 11:00AM Room: E264

Participants

Chung Chan, PhD, Vernon Hills, IL (*Presenter*) Nothing to Disclose
Jian Zhou, PhD, Vernon Hills, IL (*Abstract Co-Author*) Principal Scientist, Canon Medical Systems Corporation;
Wenyuan Qi, Chicago, IL (*Abstract Co-Author*) Nothing to Disclose
Jeffrey A. Kolthammer, MS, Cleveland Heights, OH (*Abstract Co-Author*) Nothing to Disclose
Evren Asma, Vernon Hills, IL (*Abstract Co-Author*) Nothing to Disclose
Li Yang, Vernon Hills, IL (*Abstract Co-Author*) Nothing to Disclose

For information about this presentation, contact:

cchan@MRU.MEDICAL.CANON

PURPOSE

The goal of this study is to investigate the quantitative impact of deep residual convolutional neural network (DCNN) configurations for PET image denoising.

METHOD AND MATERIALS

We first compared deep residual networks constructed with different numbers of layers (5 vs 8 vs 10 layers). For the 8 layers network, we also compared two versions such that one has half the number of filters of the other. We trained our networks using 64 clinical datasets representing a range of acquisition and reconstruction protocols. We evaluated the performance of different networks on 4 different human 18F-FDG studies acquired for 4 minutes per bed position. Synthetic lung and liver lesions were generated using GATE simulation and inserted into the listmode data. The listmode data were further rebinned into 2-minute and 3-minute lists in order to test the robustness of networks against different noise levels. All images were reconstructed using OSEM with 3 iterations, 10 ordered subsets and applied with a Gaussian filter (GF) at 6 mm FWHM. Quantifications were assessed by measuring the lesion contrast recovery versus variability of the background liver uptake.

RESULTS

The 10 layers and 8 layers networks with the full number of filters resulted in comparable quantitative and qualitative performance. However, the 10 layers network used 2-fold the training time than the 8 layers network did. Reducing the layers to 5 resulted in reduced lesion contrast recovery and robustness to the noise levels in the input images. Reducing the number of filters in the 8 layers network also reduced quantitative performance compared to the full 8 layers network.

CONCLUSION

The network architecture plays an important role in the denoising performance of a DCNN network. While fewer layers fail to capture the full complexity of the noise distributions, too many layers result in over-parameterization and difficulties in training without substantial performance gain.

CLINICAL RELEVANCE/APPLICATION

A properly chosen denoising neural network architecture can significantly improve noise levels over alternative architectures and help improve clinical decisions made based on resulting images.

SST09-04 Large Scale Assessment of Detectability and Estimability Indices from ACR CT Accreditation Database: Report of an ACR-RSNA Collaboration

Friday, Nov. 30 11:00AM - 11:10AM Room: E264

Participants

Ehsan Samei, PhD, Durham, NC (*Abstract Co-Author*) Research Grant, General Electric Company; Research Grant, Siemens AG; Advisory Board, medInt Holdings, LLC; License agreement, 12 Sigma Technologies; License agreement, Gammex, Inc Yakun Zhang, MS, Durham, NC (*Abstract Co-Author*) Nothing to Disclose Laura P. Coombs, PhD, Reston, VA (*Abstract Co-Author*) Nothing to Disclose Taylor Smith, Durham, NC (*Presenter*) Nothing to Disclose

For information about this presentation, contact:

yakun.zhang@duke.edu

PURPOSE

To assess the variability in a subset of image quality attributes of clinical CT systems using advanced task-based metrics, detectability and estimability, across the US through a collaboration between the ACR and the RSNA (QIBA).

METHOD AND MATERIALS

The ACR CT accreditation program requires institutions to submit images using the Gammex 464 phantom. Through a collaboration between the RSNA QIBA and ACR, a set of 804 randomly-selected de-identified phantom data sets were analyzed using an automated image quality estimator. These data were not filtered with regard to ACR phantom pass/fail outcome. Basic image quality metrics, including HU numbers, CNR, and noise magnitude, were automatically extracted, as well as task-specific resolution (TTF) and noise power spectra. Two advanced task-based metrics that incorporate all the aforementioned metrics were also computed: detectability index (d') and estimability index (e') for CT volumetry, both with demonstrated correlation with human and machine performance. Results from each image set were binned into specific protocols. The data were analyzed in terms of variability across protocols.

RESULTS

For task-specific resolution, despite the wide spread of the frequencies for 0.5 TTF (f50) within each protocol, the median value was largely consistent across protocols (0.40-0.41 1/mm). Noise magnitude and CNR values, related to radiation dose, were highly dependent on the protocol. The d' median values and distribution changed considerably with the task definition. Similar trends were also observed for e'. The d' and e' median values for polyethylene were 142.3, 168.1, 85.8, and 129.1; and 0.026, 0.035, 0.017, and 0.024 for adult abdomen, adult head, pediatric abdomen, and pediatric head, respectively.

CONCLUSION

Assessment of detectability and estimatiblity indices from the ACR CT accreditation database was feasible. Phantom images can be used as a surrogate to ascertain variability across clinical operations. Such data could eventually be used in the development of future conformance assessment procedures.

CLINICAL RELEVANCE/APPLICATION

Analysis of reference phantom datasets across systems and institutions through the ACR Accreditation process enables granular assessment of multi-parameter variability across our national healthcare system enabling the development of key performance indicators, qualification of quantitative performance, and potential nation-wide image quality registries.

SST09-05 A Comprehensive Platform for Automated Analysis and Reporting of QC of Medical Imaging Modalities

Friday, Nov. 30 11:10AM - 11:20AM Room: E264

Participants

Arnold Schilham, PhD, Utrecht, Netherlands (*Presenter*) Nothing to Disclose Ralph Berendsen, Heerlen, Netherlands (*Abstract Co-Author*) Nothing to Disclose Dennis Dickerscheid, PhD, Nieuwegein, Netherlands (*Abstract Co-Author*) Nothing to Disclose Rob van Rooij, PhD, Utrecht, Netherlands (*Abstract Co-Author*) Nothing to Disclose Anne Talsma, MS, Groningen, Netherlands (*Abstract Co-Author*) Nothing to Disclose Tim C. De Wit, PhD, Amsterdam, Netherlands (*Abstract Co-Author*) Nothing to Disclose Joost P. Kuijer, PhD, Amsterdam, Netherlands (*Abstract Co-Author*) Nothing to Disclose

For information about this presentation, contact:

a.schilham@umcutrecht.nl

a.schilham@umcutrecht.nl

CONCLUSION

This QC platform provides a tested, comprehensive solution for analysis and reporting of QC for most medical imaging modalities.

Background

Periodic testing of image quality is part of Quality Control (QC) of medical imaging devices. Implementation of QC testing is modality and model specific. If vendor-supplied QC is available, the details are not disclosed and exporting QC results is rarely possible. Those results are needed to spot drifts in system performance and to inform all users about the time and outcome of the latest QC. To aid implementation of a department-wide multi-modality QC program, the Society for Medical Physics of the Netherlands (NVKF) devised a community-driven, open source platform for automated analysis of medical images for quality control. The platform comprises a PACS, analysis modules, a database, and web based front-ends for administration and reporting. Analysis modules are available for most modalities, including MR, CT, MG, US, DX, RF and NM. In a normal workflow a user performs a QC test and sends the images to the QC PACS. Based on DICOM metadata, the platform runs the appropriate analysis modules and stores the results in the database. The web-based interface allows immediate access to the QC results.

Evaluation

This platform has been used since 2013 in several Dutch hospitals, successfully analyzing tens of thousands of datasets. Easy access to recent reports and trend plots of QC metrics were found beneficial for successful implementation of a QC program. Due to the open-source nature of the project, analysis modules are reviewed and imporved continually.

Discussion

This platform is a community driven, open source project, with only open source third party software requirements. Its goal is a comprehensive solution for analysis and reporting of QC for all medical imaging modalities. Analysis modules were initially developed for specific models of modalities. Easy exchange of analysis modules and configurations between institutes resulted in a push from the user community towards generalizations to other models and brands. After extensive testing, the platform was publicly released.

SST09-06 An Embedded Pre-Screening Electrochemical Profile in Label-Free and Image-Free Quantified Tissue Behavioral Analysis

Friday, Nov. 30 11:20AM - 11:30AM Room: E264

Participants

Ali Zarafshani, Norman, OK (Presenter) Nothing to Disclose

Yunzhi Wang, Norman, OK (*Abstract Co-Author*) Nothing to Disclose
Faranak Aghaei, Norman, OK (*Abstract Co-Author*) Nothing to Disclose
Seyedehnafiseh Mirniaharikandehei, MS, Norman, OK (*Abstract Co-Author*) Nothing to Disclose
Liangzhong Xiang, PhD, Norman, OK (*Abstract Co-Author*) Nothing to Disclose
Bin Zheng, PhD, Pittsburgh, PA (*Abstract Co-Author*) Nothing to Disclose

For information about this presentation, contact:

a.zarafshani@ou.edubin.zheng-1@ou.edu

PURPOSE

To address the overcharging challenge of improving the efficiency of cancer screening programs, a label-free and image-free prescreening tool to detect a frequency-dependent electrochemical profile (or features) of body tissues is developed and tested.

METHOD AND MATERIALS

The study reports the integration of a unique pre-screening tool to non-invasively detect and analyse electrochemical tissue attributes. This pre-screening tool consists of a unique probe configuration including 8-sub-regional probes that are symmetrical distributed in a mirror reflection. The tool uses a 4-active-probe sensing (4-AP sensing) technique through which electrochemical profile of body tissues are measured with high-contrast bioelectrical properties. Therefore, information regarding the extraction of local tissue distinguishability and quantify of tissue behaviour in the frequency domain during asymmetric pathways in the electrochemical profile can be readily assessed without the use of other invasive techniques. The pre-screening tool is also unique in that it utilizes the delivery and sensing channels in a single-probe electrochemical analytical measurement attached directly to external layers of the body (e.g., breast) skin thereby preventing irreproducibility of results.

RESULTS

The performance of the pre-screening tool has been verified by analysis of electrochemical profile using several breast tissue and phantom studies with different simulated tissue density levels at different sub-regions. The results indicated that the tool enabled to sensitively detect, quantify and distinguish the simulated breast tissue and local asymmetrical distribution. The testing results are also quite reproducible and can be offer as a personalized measurement analysis.

CONCLUSTON

This research for the first time demonstrates a unique electrochemical sensing device coupled with a quantified behavioural analysis of breast tissue in an innovative pre-screening tool for label-free analysis of breast tissue bioelectrical features. In future human studies, it has potential to build a new low-cost and easy-to-use tool for pre-screening several types of cancers (i.e., breast cancer) to increase cancer detection yield and reduce false positive recalls in current screening methods.

CLINICAL RELEVANCE/APPLICATION

this is a pre-screening tool can be used to increase cancer detection yeild and reduce false-positive recalls (over-diagnosis) in current mammography screening

SST09-07 Development and Initial Evaluation of a DaTscan Digital Reference Object

Friday, Nov. 30 11:30AM - 11:40AM Room: E264

Participants

Robert Miyaoka, PhD, Seattle, WA (*Presenter*) Research Consultant, MIM Software Inc; Research Grant, Koninklijke Philips NV; Research Grant, General Electric Company

Larry Pierce, PhD, Seattle, WA (Abstract Co-Author) Nothing to Disclose

Robert L. Harrison, Ludwigsburg, Germany (Abstract Co-Author) Research Consultant, General Electric Company

For information about this presentation, contact:

rmiyaoka@uw.edu

PURPOSE

The goal of this work was to design and evaluate 123I-Ioflupane DaTscan digital reference objects (DROs) and to create realistic projection datasets from a DRO to allow testing of DaTscan image reconstruction methods.

METHOD AND MATERIALS

The initial striatal brain DRO was created from an MRI image of an age-appropriate patient. The MRI was segmented to delineate structures of interest. Each structure was assigned a value according to expected Ioflupane uptake: CSF: background: right putamen: left putamen: caudate $\Rightarrow 0.33:1:5.5:3.25:5.5$. This corresponds to a specific binding ratio (SBR) of 4.5 for the caudate and right putamen and an SBR of 2.25 for the left putamen. The initial, noise-free DRO was then smoothed using 6 mm and 10 mm Gaussian filters. The three versions were analyzed by four analysis packages. Next Monte Carlo simulation was used to model SPECT acquisition of the 123I-Ioflupane DRO. The simulation included multiple energy emissions and collimator/detector response modeling. After creation of a high count projection sinogram, Poisson-resampling was used to generate sinograms of different noise levels. Projection sinograms were reconstructed on a vendor workstation. Images were then analyzed using DaTquantTM software.

RESULTS

An Ioflupane DRO developed for assessing DaTscan analysis software was tested. The SBR for the striatum varied from 2.53-3.19 (right, healthy) to 1.81-2.05 (left, diseased putamen) for the non-blurred DRO for the different analysis packages. The caudate SBRs varied from 2.4-3.6 (right) to 2.33-3.05 (left). The putamen SBRs varied from 2.56-2.7 (right) to 1.7-2.14 (left, diseased). There was similar variability for the blurred DRO images. The SBRs for the Monte Carlo simulated DRO projection images reconstructed on a vendor workstation were similar to SBRs from experimentally collected phantom data.

CONCLUSION

DROs with known 123I-Ioflupane activity distributions have been created from a patient MRI. Results reveal the variability in the

calculated SBR for different analysis software. Monte Carlo simulation data sets have been created with full models of collimator detector response for testing DaTscan analysis packages and image reconstruction methodologies.

CLINICAL RELEVANCE/APPLICATION

DROs can be used to test/compare vendor analysis packages. Further, Monte Carlo simulations of DROs can be used to test/validate enhanced image reconstruction methods for 123I-Ioflupane brain imaging.

SST09-08 Quantitative Iodine Maps from Spectral Detector Computed Tomography in Daily Practice: A Real World Study in 60 Patients

Friday, Nov. 30 11:40AM - 11:50AM Room: E264

Participants

Nils Grosse Hokamp, MD, Cleveland, OH (*Presenter*) Nothing to Disclose
Leslie Ciancibello, RT, Cleveland, OH (*Abstract Co-Author*) Consultant, Cassling Group Consultant, Siemens AG
Omer Alabar, Cleveland, OH (*Abstract Co-Author*) Nothing to Disclose
David W. Jordan, PhD, Cleveland, OH (*Abstract Co-Author*) Nothing to Disclose
Karin A. Herrmann, MD, PhD, Cleveland, OH (*Abstract Co-Author*) Nothing to Disclose

For information about this presentation, contact:

nils.grosse-hokamp@uk-koeln.de

PURPOSE

Iodine maps are available from spectral detector computed tomography (SDCT). They visualize the distribution of iodinated contrast media and allow for its quantification. While the accuracy of such maps has been investigated ex vivo in phantoms under optimized conditions, this study aimed to evaluate their accuracy in routine examinations.

METHOD AND MATERIALS

We designed a reference object consisting of 5 tubes filled with potassium iodide solutions of different concentrations (0.0, 0.8, 1.6, 3.2, 4.8 mg/ml). In 60 patients (31 male, mean age 65.2±11.4 years) who underwent routine SDCT of the abdomen, the reference object was positioned within the scan region at random positions/orientations. Iodine maps (IM) were reconstructed using the vendor provided algorithm. Two circular regions of interest were drawn in each tube, mean and standard deviation within each ROI were determined and averaged. Difference between IM and known iodine concentration was calculated. We performed a confounder analysis for BMI and radiation dose. In addition, we developed a software that allows for automatic measurement of the anterior-posterior and left-right diameter of each patient and further, computes a three-compartment model of the examined tissue (fat, bone, lean); all parameters were considered as possible confounders in statistic assessment.

RESULTS

Overall, iodine maps had a high accuracy as indicated by an offset of -0.01 ± 0.12 mg/ml despite their random placement. The offset was found greater in low concentrations (relative offset in 0.8 and 4.8 mg/ml tubes: +6.5% and +1%, respectively). While smaller BMI tended to overestimate iodine content, greater BMI tended to underestimate iodine concentrations. Besides BMI, volume of bone was found to be a strong confounder regarding iodine quantification accuracy.

CONCLUSION

Iodine quantification using iodine maps from SDCT is technically feasible in routine examinations. When considering estimated concentrations for clinical decision making, increased caution is recommended in low concentrations, in skinny and obese patients and in images with presence of large amount of bone.

CLINICAL RELEVANCE/APPLICATION

Iodine quantification in daily practice is feasible with high accuracy using iodine maps from SDCT.

SST09-09 Quantifying Liver Iron Content Using Photon-Counting Detector Based Computed Tomography

Friday, Nov. 30 11:50AM - 12:00PM Room: E264

Participants

Kishore Rajendran, PhD, Rochester, MN (*Presenter*) Nothing to Disclose Shengzhen Tao, Rochester, MN (*Abstract Co-Author*) Nothing to Disclose Gregory J. Michalak, PhD, Rochester, MN (*Abstract Co-Author*) Nothing to Disclose Shuai Leng, PHD, Rochester, MN (*Abstract Co-Author*) License agreement, Bayer AG Cynthia H. McCollough, PhD, Rochester, MN (*Abstract Co-Author*) Research Grant, Siemens AG

For information about this presentation, contact:

rajendran.kishore@mayo.edu

PURPOSE

In a phantom, to quantify liver iron content using multi-energy photon-counting detector (PCD) CT and an image-based material decomposition technique.

METHOD AND MATERIALS

A wet liver analog was synthesized using dry liver extract (1:7 dilution of dry liver in water) to yield a base CT number enhancement of 50 HU at 140 kV, similar as that of normal human liver. Iron concentrations (iron III nitrate) were prepared at 1.8, 2.8 and 5.6 mg/mL with either wet liver or water as a solvent. Cylindrical vials containing approximately 10 mL of pure liver, iron-liver and iron-water solutions were placed inside a 20 cm multi-energy CT phantom (Gammex, Sun Nuclear, WI), and scanned using a whole-body PCD-CT system (Siemens CounT, Forchheim, Germany) at 120 kV, 178 mAs (CTDIvol = 13 mGy) and energy thresholds of 25, 63 keV. Multi-energy PCD-CT images were reconstructed at [25, 120] keV, [63, 120] keV and [25, 63] keV energy ranges using a quantitative smooth kernel (D30). Quantitative iron maps were obtained using an in-house material decomposition

technique with the [25, 120] keV and [63-120] keV images assuming 3 base materials: liver, water and iron. The image domain material decomposition (MD) algorithm is based on spectral prior image constrained compressed sensing (MD-SPICCS) which combines material decomposition and denoising into a unified framework. The mean density (mg/mL) of iron content was estimated from the iron maps generated using MD-SPICCS. A linear regression analysis was performed to compare measured iron concentrations in liver background with known true concentrations.

RESULTS

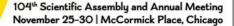
MD-SPICCS was able to successfully detect and quantify iron from liver background in the phantom images. Liver background from the iron-liver mixtures was assigned to the liver map, while water background from the iron-water mixtures was assigned to water map. Linear regression showed excellent correlation between measured and true iron concentrations in the iron-liver mixtures (slope = 1.1, R2 = 0.9997, RMSE =0.6 mg/mL).

CONCLUSION

We have demonstrated accurate iron quantification in a liver phantom scanned using the PCD-CT system and an image-based material decomposition technique. Measured iron concentrations showed excellent correlation with the ground truth.

CLINICAL RELEVANCE/APPLICATION

Diagnosing hemochromatosis characterized by liver iron overload using imaging methods requires accurate iron quantification to facilitate and monitor therapy.





SPFR61

Friday Imaging Symposium: Screening with Imaging in 2018: Who Benefits?

Friday, Nov. 30 12:30PM - 3:00PM Room: E350

BR

СН

GI

GU

OI

AMA PRA Category 1 Credits ™: 2.50 ARRT Category A+ Credits: 3.00

FDA

Discussions may include off-label uses.

Participants

Hebert Alberto Vargas, MD, Cambridge, United Kingdom (Moderator) Nothing to Disclose Dow-Mu Koh, MD,FRCR, Sutton, United Kingdom (Moderator) Nothing to Disclose

Sub-Events

SPFR61A Breast Cancer Screening: Lessons Learned from Where it all Started

Participants

Victoria L. Mango, MD, New York, NY (Presenter) Nothing to Disclose

For information about this presentation, contact:

mangov@mskcc.org

LEARNING OBJECTIVES

1) Discuss early mammography screening trials for breast cancer. 2) Analayze recent multi-modality breast cancer screening literature. 3) Apply lessons learned from breast cancer screening to future screening for other diseases.

ABSTRACT

N/A

URL

N/A

SPFR61B Emerging CRC Screening Options

Participants

Perry J. Pickhardt, MD, Madison, WI (*Presenter*) Stockholder, SHINE Medical Technologies, Inc; Stockholder, Elucent Medical; Advisor, Bracco Group;

LEARNING OBJECTIVES

1) To Understand the various CRC screening options, with emphasis on newer emerging strategies.

ABSTRACT

N/A

URL

N/A

Honored Educators

Presenters or authors on this event have been recognized as RSNA Honored Educators for participating in multiple qualifying educational activities. Honored Educators are invested in furthering the profession of radiology by delivering high-quality educational content in their field of study. Learn how you can become an honored educator by visiting the website at: https://www.rsna.org/Honored-Educator-Award/ Perry J. Pickhardt, MD - 2014 Honored EducatorPerry J. Pickhardt, MD - 2018 Honored Educator

SPFR61C Liver Cancer Screening: Who Benefits?

Participants

Bachir Taouli, MD, New York, NY (Presenter) Research Grant, Guerbet SA; Research Grant, Bayer AG

For information about this presentation, contact:

bachir.taouli@mountsinai.org

LEARNING OBJECTIVES

1) Review current guidelines for liver cancer screening, including target population and methods used. 2) Review the limitations of blood markers and ultrasound for liver cancer screening. 3) Review new methods such as abbreviated MRI for liver cancer

screening.

ABSTRACT

Hepatocellular carcinoma (HCC) is the 2nd leading cause of cancer-related death worldwide, and the fastest growing cause of cancer death in the USA. The most important risk factor for HCC is cirrhosis. In this presentation, we will discuss the rationale of HCC screening, the most recent AASLD guidelines for HCC screening and surveillance using ultrasound (US) with or without alphafetoprotein (AFP). We will review the current results and limitations of this strategy. We will also review recent developments in the use of abbreviated MRI protocols for HCC screening and surveillance.

SPFR61D Lung Cancer: Should We Be Screening Patients with Other Cancers?

Participants

Michelle S. Ginsberg, MD, New York, NY (Presenter) Nothing to Disclose

LEARNING OBJECTIVES

1) Review the approach to the inclusion of patients with a previous history of malignancy in lung cancer screening studies. 2) To discuss the need for lung cancer screening in survivors of other cancers.

SPFR61E Prostate Cancer Screening: Will it Ever Happen?

Participants

Harriet C. Thoeny, MD, Bern, Switzerland (Presenter) Advisory Board, Guerbet SA

LEARNING OBJECTIVES

1) To identify the disadvantages of the current gold standard of prostate cancer detection. 2) To differentiate significant form insignificant PCa and to understand its impact on management. 3) To assess the prerequisites of mpMRI as a screening tool of prostate cancer detection.

ABSTRACT

Prostate cancer (PCa) is the most frequent malignant tumor in men in Europe and the USA. Up to date systematic transrectal ultrasound guided- (TRUS) biopsy based on a rise in PSA and/or a suspicious digital rectal examinaition is the gold standard in PCa detection. However, this approach is unsatisfactory as it leads to over-and underdiagnosis of PCa. MpMRI is now an integrated part in the workup of PCa in many institutions and MR/TRUS-fuion guided instead of systematic blind biospies are more frequently used leading to a higher detection rate of significant PCa on one hand and a lower detection rate of insignificant PCa on the other hand. The NPV of mpMRI to detect significant PCa is reported between 63-98% depening on patient selection. mpMRI improves PCa detection and might therefore be a valuable tool for PCa screening however, the prerequisities include excellent image quality, a dedicated and experienced radiologist, availability of MRI and a short imaging protocol without contrast medium administration to make the healthcare authoritites considering mpMRI as a cost effective screening tool. Furthermore, an improved NPV might reduce the number of unnecessary biopsies in a high number of men and therefore decrease costs for the healthcare system.

SPFR61F Ovarian Cancer Screening: Have We Given Up Yet?

Participants

Andrea G. Rockall, FRCR, MRCP, London, United Kingdom (Presenter) Speaker, Guerbet SA

LEARNING OBJECTIVES

1) To know about the results of ovarian cancer screening studies. 2) To understand the possible reasons for failure. 3) To be aware of screening studies in high risk patients.

Honored Educators

Presenters or authors on this event have been recognized as RSNA Honored Educators for participating in multiple qualifying educational activities. Honored Educators are invested in furthering the profession of radiology by delivering high-quality educational content in their field of study. Learn how you can become an honored educator by visiting the website at: https://www.rsna.org/Honored-Educator-Award/ Andrea G. Rockall, FRCR,MRCP - 2017 Honored Educator

SPFR61G Non-cancer Screening: Should We Screen for Cardiovascular Diseases with Imaging?

Participants

Mathias Prokop, PhD, Nijmegen, Netherlands (*Presenter*) Speakers Bureau, Bracco Group; Speakers Bureau, Bayer AG; Research Grant, Canon Medical Systems Corporation; Speakers Bureau, Canon Medical Systems Corporation; Research Grant, Siemens AG; Speakers Bureau, Siemens AG; Departmental spinoff, Thirona; Departmental licence agreement, Varian Medical Systems, Inc; ;

SPFR61H Whole-body Screening for Multiple Cancers: Is a One-Stop-Shop Approach Feasible?

Participants

Giuseppe Petralia, MD, Milan, Italy (Presenter) Nothing to Disclose

LEARNING OBJECTIVES

1) Identify the most appropriate imaging technique for whole-body cancer screening. 2) Arrange a whole-body MRI scanning protocol in their home Institutions. 3) Describe findings observed in a whole-body MRI performed for cancer screening in a Likert scale. 4) Recommend the whole-body MRI for cancer screening to the appropriate population.